Fishery Data Series No. 13-58

Estimates of Chinook Salmon Passage in the Kenai River Using Split-Beam and Dual-Frequency Identification Sonars, 2010

by

James D. Miller

Debby L. Burwen

and

Steve J. Fleischman

December 2013

Alaska Department of Fish and Game Divisions of Sport Fish and Commercial Fisheries

Symbols and Abbreviations

The following symbols and abbreviations, and others approved for the Système International d'Unités (SI), are used without definition in the following reports by the Divisions of Sport Fish and of Commercial Fisheries: Fishery Manuscripts, Fishery Data Series Reports, Fishery Management Reports, and Special Publications. All others, including deviations from definitions listed below, are noted in the text at first mention, as well as in the titles or footnotes of tables, and in figure or figure captions.

Weights and measures (metric)

centimeter	cm
deciliter	dL
gram	g
hectare	ha
kilogram	kg
kilometer	km
liter	L
meter	m
milliliter	mL
millimeter	mm

Weights and measures (English)

cubic feet per second	ft^3/s
foot	ft
gallon	gal
inch	in
mile	mi
nautical mile	nmi
ounce	oz
pound	lb
quart	qt
yard	yd

Time and temperature

day	d
degrees Celsius	°C
degrees Fahrenheit	°F
degrees kelvin	K
hour	h
minute	min
second	s

Physics and chemistry

all atomic symbols	
alternating current	AC
ampere	A
calorie	cal
direct current	DC
hertz	Hz
horsepower	hp
hydrogen ion activity (negative log of)	pH
parts per million	ppm
parts per thousand	ppt, ‰
volts	V
watts	W

General

Alaska Administrative Code	AAC
all commonly accepted abbreviations	e.g., Mr., Mrs., AM, PM, etc.
all commonly accepted professional titles	e.g., Dr., Ph.D., R.N., etc.
at	@
compass directions:	
east	E
north	N
south	S
west	W
copyright	©
corporate suffixes:	
Company	Co.
Corporation	Corp.
Incorporated	Inc.
Limited	Ltd.
District of Columbia	D.C.
et alii (and others)	et al.
et cetera (and so forth)	etc.
exempli gratia (for example)	e.g.
Federal Information Code	FIC
id est (that is)	i.e.
latitude or longitude	lat or long
monetary symbols (U.S.)	$, ¢
months (tables and figures): first three letters	Jan,...,Dec
registered trademark	®
trademark	™
United States (adjective)	U.S.
United States of America (noun)	USA
U.S.C.	United States Code
U.S. state	use two-letter abbreviations (e.g., AK, WA)

Mathematics, statistics

all standard mathematical signs, symbols and abbreviations	
alternate hypothesis	H_A
base of natural logarithm	*e*
catch per unit effort	CPUE
coefficient of variation	CV
common test statistics	(F, t, χ^2, etc.)
confidence interval	CI
correlation coefficient (multiple)	R
correlation coefficient (simple)	r
covariance	cov
degree (angular)	°
degrees of freedom	df
expected value	*E*
greater than	>
greater than or equal to	≥
harvest per unit effort	HPUE
less than	<
less than or equal to	≤
logarithm (natural)	ln
logarithm (base 10)	log
logarithm (specify base)	log_2, etc.
minute (angular)	'
not significant	NS
null hypothesis	H_O
percent	%
probability	P
probability of a type I error (rejection of the null hypothesis when true)	α
probability of a type II error (acceptance of the null hypothesis when false)	β
second (angular)	"
standard deviation	SD
standard error	SE
variance	
population	Var
sample	var

FISHERY DATA SERIES NO. 13-58

ESTIMATES OF CHINOOK SALMON PASSAGE IN THE KENAI RIVER USING SPLIT-BEAM AND DUAL-FREQUENCY IDENTIFICATION SONARS, 2010

by

James D. Miller
Debby L. Burwen
Division of Sport Fish, Anchorage
and
Steve J. Fleischman
Division of Sport Fish, Research and Technical Services, Anchorage

Alaska Department of Fish and Game
Division of Sport Fish, Research and Technical Services
333 Raspberry Road, Anchorage, Alaska, 99518-1565

December 2013

This investigation was partially financed by the Federal Aid in Sport Fish Restoration Act (16 U.S.C. 777-777K) under Grant F10AF00553 (Project F-10-26) Job S-2-28.

ADF&G Fishery Data Series was established in 1987 for the publication of Division of Sport Fish technically oriented results for a single project or group of closely related projects, and in 2004 became a joint divisional series with the Division of Commercial Fisheries. Fishery Data Series reports are intended for fishery and other technical professionals and are available through the Alaska State Library and on the Internet: http://www.adfg.alaska.gov/sf/publications/. This publication has undergone editorial and peer review.

James D. Miller, Debby L. Burwen,
Alaska Department of Fish and Game, Division of Sport Fish
333 Raspberry Road, Anchorage, Alaska 99518-1599, USA
and
Steve J. Fleischman
Alaska Department of Fish and Game, Division of Sport Fish,
Research and Technical Services
333 Raspberry Road, Anchorage, Alaska 99518-1599, USA

This document should be cited as:
Miller, J. D., D. L. Burwen, and S. J. Fleischman. 2013. Estimates of Chinook salmon passage in the Kenai River using split-beam and dual-frequency identification sonars, 2010. Alaska Department of Fish and Game, Fishery Data Series No. 13-58, Anchorage.

TABLE OF CONTENTS

TABLE OF CONTENTS (Continued)

LIST OF TABLES

Table **Page**

LIST OF FIGURES

Figure **Page**

LIST OF FIGURES (Continued)

LIST OF APPENDICES

LIST OF APPENDICES (Continued)

ABSTRACT

Kenai River Chinook salmon (*Oncorhynchus tshawytscha*) passage was estimated in 2010 using split-beam sonar and experimental dual-frequency identification sonar (DIDSON). The split-beam sonar operated continuously from 16 May to 4 August, when operations were curtailed due to milling salmon that prevented accurate counting. The DIDSON was successfully deployed on both banks of the river and operated successfully on 48 days between 11 June and 10 August. Based on split-beam sonar target strength and range thresholds, total upstream passage of Chinook salmon was estimated to be 13,248 (SE 235) fish during the early run (16 May–30 June) and 48,343 (SE 726) fish during the late run (1 July–4 August only). Based on DIDSON length measurements and inriver netting catch rates, estimates of Chinook salmon passage were 5,874 (SE 645) fish for the early run (16 May–30 June) and 18,401 (SE 698) fish for the late run (1 July–10 August). Detailed comparisons of split-beam and DIDSON data indicated that the assumptions underpinning split-beam target-strength-based estimates are not valid. It is recommended that target-strength-based split-beam sonar estimates be discontinued in favor of DIDSON-based estimates in 2011.

Key words: split-beam sonar, DIDSON, Chinook salmon, *Oncorhynchus tshawytscha*, acoustic assessment, Kenai River, riverine sonar

INTRODUCTION

Chinook salmon (*Oncorhynchus tshawytscha*) returning to the Kenai River (Figure 1) support one of the largest and most intensively managed recreational fisheries in Alaska (Gamblin et al. 2004). Kenai River Chinook salmon are among the largest in the world and have sustained in excess of 100,000 angler-days of fishing effort annually (Howe et al. 1995-1996, 2001a-d; Mills 1979-1980, 1981a-b, 1982-1994; Walker et al. 2003; Jennings et al. 2004, 2006a-b, 2007, 2009a-b, 2010a-b, 2011). The Kenai River Chinook salmon fishery has been a source of contention because of competition for a fully allocated resource among sport, commercial, subsistence, and personal use fisheries.

Chinook salmon returning to the Kenai River are managed as two distinct runs (Burger et al. 1985): early (16 May–30 June) and late (1 July–10 August). Early-run Chinook salmon are harvested primarily by sport anglers, and late-run Chinook salmon by commercial, sport, subsistence, and personal use fisheries. These fisheries may be restricted if the projected escapement falls below goals adopted by the Alaska Board of Fisheries. These goals are defined by Alaska Administrative Codes 5 AAC 56.070 (Kenai River and Kasilof River Early-Run King Salmon Conservation Management Plan) and 5 AAC 21.359 (Kenai River Late-Run King Salmon Management Plan) and are intended to provide a stable fishing season without compromising sustainability. Escapement goals have evolved over the years as stock assessment and our understanding of stock dynamics have improved (McBride et al. 1989; Hammarstrom and Hasbrouck 1998-1999; Bosch and Burwen 1999). During the 2010 season, goals of 5,300–9,000 early-run and 17,800–35,700 late-run Chinook salmon were in effect, as assessed by target-strength-based split-beam sonar. Sonar estimates of inriver Chinook salmon passage provide the basis for estimating spawning escapement and implementing management plans that regulate harvest in the competing sport and commercial fisheries for this stock. Implementation of these management plans has been contentious and attracts public scrutiny. Restrictions were imposed on the sport fishery to meet escapement goals during the early run in 1990 through 1992, 1997, 1998, 2000, 2002, and 2010, and during the late run in 1990, 1992, and 1998.

PROJECT HISTORY

Mark–recapture

The first estimates of Kenai River Chinook salmon abundance were generated in 1984 for the late run using a mark–recapture project (Hammarstrom et al. 1985). From 1985 through 1990, the mark–recapture project produced estimates for both early- and late-run riverine abundance (Hammarstrom and Larson 1986; Conrad and Larson 1987; Conrad 1988; Carlon and Alexandersdottir 1989; Alexandersdottir and Marsh 1990). These estimates had low precision and appeared to be positively biased, particularly during the late run (Bernard and Hansen 1992).

Dual-beam Sonar

The Alaska Department of Fish and Game (ADF&G) initiated studies in 1984 to determine whether an acoustic assessment program could provide timely and accurate daily estimates of Chinook salmon passage in the Kenai River (Eggers et al. 1995). Acoustic assessment of Chinook salmon in the Kenai River is complicated by the presence of more abundant sockeye salmon (*O. nerka*), which migrate concurrently with Chinook salmon. From 1987 to 2009, sockeye salmon escapement estimates generated by the river mile–19 sockeye salmon sonar project ranged from 625,000 to 1,600,000 fish (Westerman and Willette 2011) while late-run Chinook salmon passage estimates generated by the Chinook salmon sonar project at river mile (RM) 8.5 ranged from 29,000 to 56,000 fish. Dual-beam sonar was initially chosen for the Chinook salmon sonar project because of its ability to estimate acoustic size (target strength), which was to serve as the discriminatory variable to systematically identify and count only Chinook salmon. Because of the considerable size difference between Chinook salmon and other fish species in the Kenai River, it was postulated that dual-beam sonar could be used to distinguish Chinook salmon from smaller fish (primarily sockeye salmon) and to estimate their numbers returning to the river.

Early Kenai River sonar and gillnetting studies indicated that Chinook salmon could be distinguished from sockeye salmon based on target strength and spatial separation in the river (Eggers et al. 1995). Target strength (TS) is a measure of the loudness of the echo returning from a fish, corrected for position of the fish in the beam. Sockeye salmon are smaller, on average, than Chinook salmon, and were assumed to have smaller target strength. A target strength threshold was established to censor small fish. Sockeye salmon also were thought to migrate primarily near the bank, therefore a range or distance threshold was also imposed. Since 1987, "TS-based estimates" based on these two criteria have been the primary basis for monitoring the number of Chinook salmon returning to the Kenai River for comparison with established escapement goals.

TS-based estimates made with dual-beam sonar were consistently lower than the 1987–1990 mark–recapture estimates (Eggers et al. 1995). The inconsistencies between sonar and mark–recapture estimates were greatest during the late run, presumably due to the mark–recapture biases mentioned above.

Split-beam Sonar

A more advanced acoustic technology, known as split-beam sonar, was used to test assumptions and design parameters of the dual-beam configuration in 1994 (Burwen et al. 1995). The split-beam system provided advantages over the dual-beam system in its ability to determine the 3-

dimensional position of an acoustic target in the sonar beam. Consequently, the direction of travel for each target and the 3-dimensional spatial distribution of fish in the acoustic beam could be determined for the first time. The split-beam system also operated at a lower frequency than the dual-beam system, providing a higher (improved) signal-to-noise ratio (SNR; Simmonds and MacLennan 2005). It also interfaced with improved fish-tracking software, which reduced the interference from boat wake, and improved fish-tracking capabilities (Burwen and Bosch 1996). The split-beam system was deployed side-by-side with the dual-beam system and was run concurrently for much of the 1994 season (Burwen et al. 1995). Both systems detected comparable numbers of fish. The split-beam data confirmed earlier studies (Eggers et al. 1995) showing that most fish targets were strongly oriented to the river bottom. However, experiments conducted with the split-beam system could not confirm that Chinook salmon could be discriminated from sockeye salmon based on target strength. Modeling exercises performed by Eggers (1994) also questioned the feasibility of discriminating between Chinook and sockeye salmon using target strength. It was hypothesized that discrimination between the two species was primarily accomplished using range thresholds on the acoustic data that exploited the known spatial segregation of the species (sockeye salmon migrate near shore and Chinook salmon migrate midriver; Burwen et al. 1995; Eggers et al. 1995). In 1995, the dual-beam system was replaced with the split-beam system to take advantage of the additional information on direction of travel and spatial position of targets. TS-based estimates continued to be produced with the split-beam sonar.

Ancillary drift gillnetting and sonar studies conducted in 1995 (Burwen et al. 1998) were directed at providing definitive answers to remaining questions regarding 1) the degree to which sockeye and Chinook salmon are spatially separated at the RM-8.5 Chinook salmon sonar site and 2) the utility of using target strength and other acoustic parameters for species separation. These studies confirmed the potential for misclassifying sockeye salmon as Chinook salmon. The drift gillnetting study found that sockeye salmon were present in the middle insonified portion of the river. In the concurrent sonar experiment using live fish tethered in front of the split-beam sonar, most sockeye salmon had mean target strengths exceeding the target strength threshold.

Concurrent Studies to Verify and Improve Sonar Passage Estimates

Radiotelemetry projects were implemented in 1996 and 1997 to estimate the magnitude of bias introduced into the Chinook salmon passage estimates during periods of high sockeye salmon passage (Hammarstrom and Hasbrouck 1998-1999). The radiotelemetry studies were designed to provide an independent and accurate estimate of inriver Chinook salmon passage during the late run when the potential to misclassify sockeye salmon using sonar is greatest. Although the precision of radiotelemetry estimates and previous mark–recapture estimates was similar, the use of radiotelemetry avoided certain biases associated with the earlier mark–recapture studies. Sonar estimates of late-run Chinook salmon abundance were 26% greater in 1996 and 28% greater in 1997 than the corresponding telemetry estimates.

An investigation in 1999 (Burwen et al. 2000) attempted to identify alternative sites above tidal influence with stronger bank orientation of sockeye salmon, where range thresholds would be more effective. The investigation concentrated on a site located at RM 13.2 that was upstream of tidal influence, but downstream of major spawning areas. Gillnetting data indicated that there were fewer sockeye salmon in the offshore area at the alternative site than at the current site. However, there were still relatively large numbers of sockeye salmon present in the offshore area of the alternative site during peak migration periods as well as high numbers of Chinook salmon present in the nearshore area. The alternate sonar site also had several disadvantages over the current site including more boat traffic, less acoustically favorable bottom topography, and higher background noise resulting in difficult fish tracking conditions.

The inriver drift gillnetting program, originally designed to collect age, sex, and length samples (Marsh 2000), was modified in 1998 to produce standardized estimates of Chinook salmon catch per unit effort (CPUE) for use as an index of Chinook salmon passage (Reimer et al. 2002). A drift zone was established just downstream from the sonar site and crews fished relative to the tide cycles because gillnets could not be fished effectively during parts of the rising and high tide stages due to lack of river current. In addition, the schedule was intensified so that CPUE estimates could be generated daily. During subsequent years, inriver gillnet CPUE was used as a comparison with sonar passage estimates to detect periods when Chinook salmon passage estimates were potentially high because of inclusion of sockeye salmon or other species (Bosch and Burwen 2000; Miller and Burwen 2002; Miller et al. 2002-2005, 2007a-b, 2010, 2011, 2012).

Analysis of the 1998–2000 standardized CPUE data suggested the gillnetting data were better suited for determining species apportionment of split-beam sonar counts than for passage estimates (Reimer et al. 2002). In 2002, the inriver gillnetting program was modified further. A 5-inch mesh gillnet was introduced, alternating with the existing 7.5-inch mesh to reduce size selectivity; nets were constructed of multi-monofilament (formerly cable-lay braided nylon); the color of the mesh was changed to more closely match that of the river; and drifts were shortened and constrained to more closely match the portion of the channel sampled by the sonar. These changes increased netting efficiency and decreased the effect of water clarity on gillnet catches (Reimer 2004).

In 2002, we refined the species discrimination algorithm for TS-based estimates, censoring selected hourly samples based on fish behavior. During samples when sockeye salmon were abundant, as evidenced by aggregation of migrating fish into groups, the data were censored, and Chinook salmon passage was estimated from the remaining hourly samples.

Also in 2002, two experimental methods of estimating Chinook salmon passage were initiated. The first alternative estimate, referred to as the net-apportioned estimate, used the product of Chinook salmon catch proportions from the netting program (Eskelin 2010) and sonar upstream midriver fish passage estimates (see Methods). Net-apportioned estimates have been published annually since 2002 (Miller et al. 2004-2005, 2007a-b, 2010, 2011, 2012), and have proven useful for tracking short term trends in Chinook salmon abundance.

The second alternative estimate was based on split-beam measures of echo envelope length, which is a better predictor of fish length than target strength (Burwen and Fleischman 1998; Burwen et al. 2003). Statistical methods were developed that enabled robust estimates of species composition even when species overlap in size (Fleischman and Burwen 2003). Echo length standard deviation (ELSD) information from the sonar was combined with fish length data from the netting program to estimate the species composition of fish passing the sonar site. The resulting estimated proportion of Chinook salmon was then multiplied by upstream fish passage estimates from the sonar. The resulting "ELSD-based" estimates, considered to be more accurate than the official TS-based estimates, were produced for the years 2002–2006. Because echo length measurements can be corrupted when 2 or more fish swim very close to one another, resulting in higher values of ELSD, only early-run estimates were published (Miller et al. 2004-2005, 2007a-b, 2010). The corresponding late-run estimates were suspected to be too high due to high sockeye salmon densities.

In 2007, the ELSD mixture model method was modified in an attempt to reduce the bias at high fish densities. Using split-beam measurements of 3-dimensional fish location, the distance between fish was calculated and fish within 1 meter of any other fish[1] were censored before fitting the mixture model. ELSD-based estimates published in the 2007 report (Miller et al. 2011) supplanted the previously published early-run estimates.

Dual-frequency Identification Sonar (DIDSON)

ADF&G began testing dual-frequency identification sonar (DIDSON[2]) in the Kenai River in 2002 (Burwen et al. 2007). DIDSON uses a lens system that provides high resolution images that approach the quality achieved with conventional optics (Simmonds and MacLennan 2005), with the advantage that images can be obtained in dark or turbid waters. Fish size was immediately evident from DIDSON footage[3] of migrating Kenai River salmon, suggesting that DIDSON had promise for improved discrimination of large Chinook salmon from smaller fish in the Kenai River. With ADF&G input, DIDSON developers designed custom software for manually measuring fish size directly from still images. Initial experiments using live tethered salmon showed that at ranges up to 12 m, precise estimates of fish length could be obtained by manually measuring fish images produced by a standard DIDSON unit (Burwen et al. 2007). Ranges to 30 m are required to adequately insonify the Kenai River at the current sonar location (RM 8.5), and subsequent advancements in DIDSON technology resulted in improved long-range image resolution. The development of a lower frequency DIDSON model (i.e., “long-range” DIDSON operating at 1.1 MHz) in 2004 extended the range of high-frequency operation to approximately 30 m, and a high resolution lens developed in 2007 improved the resolution by nearly a factor of two. Tethered-fish experiments conducted in 2007 with the new equipment established that DIDSON-estimated fish length was closely related to true length at ranges up to 22 m (Burwen et al. 2010; Miller et al. 2011). Additional experiments conducted with multiple observers on the left bank during 2009 confirmed the 2007 results at ranges up to 32 m (Miller et al. 2012).

In the years 2007–2009, the long-range high-resolution DIDSON sonar was deployed on the left bank to sample 10 m of river cross section that was simultaneously sampled by the split-beam transducer (Miller et al. 2011-2012). Methods and equipment were developed to minimize accumulation of silt in the lens, which could result in degraded image resolution. A pilot study concluded that automated tracking and measuring of free-swimming fish was feasible and potentially advantageous under some circumstances. DIDSON exhibited multiple advantages over split-beam sonar with respect to detection, tracking, and species classification of passing fish. Frequency distributions of DIDSON length measurements, along with paired netting data, lent themselves well to mixture modeling, which enabled estimation of species composition of passing fish. Such estimates agreed well with corresponding split-beam estimates from the ELSD mixture model in 2009.

---

1 Essentially, fish swimming close to other fish were assumed not to be Chinook salmon.
2 DIDSON was designed by the University of Washington Applied Physics Laboratory, originally for military applications.
3 DIDSON imagery resembles video footage taken from above the river’s surface.

A second DIDSON system was acquired in 2010, which made it possible to provide simultaneous coverage of both banks for the first time. In this report, we present daily and seasonal TS-based, net-apportioned, and ELSD-based estimates of Chinook salmon inriver abundance from the split-beam sonar and compare them with corresponding DIDSON-based estimates of abundance.

OBJECTIVES

The stated primary objective of this project was to produce daily and seasonal target-strength-based (TS-based) estimates of the inriver run of Chinook salmon to the Kenai River such that the upper and lower bounds of the 95% confidence interval were within 5% of the seasonal (early- and late-run) point estimate. This estimate was based on target strength and range thresholds, with hourly samples subject to censoring based on fish behavior. In keeping with previous practice, the precision criterion addressed only the sampling error of the estimates but not errors due to species classification, tracking, and detection.

A second objective was to produce weekly and seasonal ELSD-based estimates of the inriver run of Chinook salmon to the Kenai River such that the seasonal estimate was within 10% of the true value 95% of the time. This estimate was based on mixture modeling of ELSD measurements subject to censoring based on fish behavior. The precision criterion for ELSD-based estimates was intended to address sampling error and species classification, but not target tracking or detection.[4]

The third objective was to continue the experimental development of DIDSON for inseason assessment of Kenai River Chinook salmon. DIDSON was deployed from the left and right banks of the river at RM 8.5; protocols were tested and refined for measuring fish and processing data in real-time, and Chinook salmon abundance estimates were produced for comparison with those from split-beam sonar.

METHODS

STUDY AREA

The Kenai River drainage is approximately 2,150 square miles. It is glacially influenced, with discharge rates lowest during winter (<1,800 ft^3/s), increasing throughout the summer, and peaking in August (>14,000 ft^3/s; Benke and Cushing 2005). The Kenai River has 10 major tributaries, many of which provide important spawning and rearing habitat for salmon. Tributaries include the Russian River, Skilak River, Killey River, Moose River, and Funny River.

The Kenai River drainage is located in a transitional zone between a maritime climate and a continental climate (USDA 1992). The geographic position and local topography influence both rainfall and temperature throughout the drainage. Average annual (1971–2006) precipitation for the City of Kenai, located at the mouth of the Kenai River, is 48 cm (WRCC 2008). Average summer (June, July, and August) temperature for the City of Kenai is 12°C (WRCC 2008).

[4] In addition, daily ELSD-based estimates of Chinook salmon passage were produced inseason during 2010 based on adaptive ELSD threshold values. These estimates, described by Miller et al (2012: page 18), served as daily proxies for the weekly ELSD-based estimates. Adaptive ELSD threshold estimates are not reported here.

SITE DESCRIPTION

The sonar site was located 14 km (8.5 miles) from the mouth of the Kenai River (Figure 2). This site has been used since 1985 and was selected for its acoustic characteristics and its location downstream of the sport fishery and known Chinook salmon spawning habitat.

The river bottom in this area has remained stable for the past 25 years (Bosch and Burwen 1999). The slope from both banks is gradual and uniform, which allows a large proportion of the water column to be insonified without acoustic shadowing effects. On the right bank, the bottom is composed primarily of mud, providing an acoustically absorptive surface. This absorptive property improves the signal-to-noise ratio (SNR) when the beam is aimed along the river bottom. The left-bank bottom gradient is steeper and consists of more acoustically reflective small rounded cobble and gravel.

The sonar site is located downstream of the lowest suspected Chinook salmon spawning sites, yet far enough from the mouth that most of the fish counted are probably committed to the Kenai River (Alexandersdottir and Marsh 1990). Most sport fishing activity occurs upstream of the site.[5]

SPLIT-BEAM SONAR

Acoustic Sampling

A Hydroacoustic Technology Inc. (HTI[6]) split-beam sonar system was operated from 16 May to 4 August[7] in 2010. Components of the system are listed in Table 1 and are further described in HTI manuals (HTI 1996-1997). A brief explanation of the theory of split-beam sonar and its use in estimating target strength can be found in Appendix A1. A more detailed explanation can be found in Ehrenberg (1983).

Sonar System Configuration

Sonar sampling on both banks was controlled by electronics housed in a tent located on the right (north) bank of the river. Communication cables were connected to the sonar equipment on both banks. Cables leading to the left-bank equipment were suspended above the river at a height that would not impede boat traffic (Figure 3). Steel tripods were used to deploy the transducers offshore. One elliptical, split-beam transducer was mounted horizontally (side-looking) on each tripod. At the start of the season the transducer tripods were placed on each bank in a position close to shore but still submerged at low tide. Throughout the season, water levels at low tide increased approximately 1.3 m. Rising water level and heavy debris accumulation resulted in occasional relocation of transducer tripods. Total range insonified by both (right and left bank) sonar beams ranged from approximately 62.5 m to 68.0 m (Figure 4).

Vertical and horizontal aiming of each transducer was remotely controlled by a dual-axis electronic pan-and-tilt system. A digital readout from an angular measurement device (attitude sensor) attached to the transducer indicated the aiming angle in the vertical and horizontal

---

5 In 2005, approximately 98% of the early-run Chinook salmon sport fishing effort and 86% of the late-run effort occurred upstream of the Chinook salmon sonar site (Eskelin 2007).

6 Product names used in this publication are included for completeness but do not constitute product endorsement.

7 Sampling was terminated prior to 10 August due to numerous fish holding in the sonar beam, making it difficult to accurately track fish targets. Chinook salmon passage was estimated through 3 August.

planes. In the vertical plane, the transducer was aimed using an oscilloscope and chart recorder to verify that the sonar beam was aligned along the river bottom. In the horizontal plane, the transducer was aimed perpendicular to the river flow to maximize probability of insonifying fish from a lateral aspect. The range encompassed by each transducer was determined by the river bottom contour and the transducer placement. Transducers were placed to maximize the counting range and to fully insonify the cross section of the river between the right- and left-bank transducers.

River Profile Mapping and Coverage

A detailed profile of the river bottom and the area encompassed by the sonar beams was produced prior to acoustic sampling. Depth readings collected with a Lowrance X-16 were paired with range measurements taken from a Bushnell Laser Ranger (±1 m accuracy) aimed at a fixed target on shore. When bottom profile information is combined with information from the attitude sensor, a detailed visualization of how the acoustic beam insonifies the water column above the bottom substrate can be generated (Figure 5). Each time a transducer was moved, new measurements of the transducer height above the bottom substrate and its position relative to a fixed shore location were updated in an EXCEL worksheet so that beam coverage at the new location could be evaluated.

Before 2001, the right- and left-bank transducers were deployed directly across the river from each other, and complete beam coverage for the entire middle portion of the river was accomplished by extending the counting range for both banks to the thalweg (the line delimiting the lowest points along the length of the river bed). Under these conditions, we could be relatively certain that the entire middle portion of the river was insonified. In 2001, river bottom profiles indicated improved beam coverage (in the vertical plane) could be attained on the left bank by moving the transducer approximately 35 m downstream of its original location (Miller et al. 2003). The left-bank transducer has been deployed at this location since 2001. Because of the offset deployment of the right- and left- bank transducers (Figure 3), it is difficult to determine if there is complete beam coverage[8] (Miller et al. 2004).

Split Beam Sonar System Calibration

Prior to the field season, HTI performed reciprocity calibrations with a naval standard transducer to verify target strength measurements of a 38.1-mm tungsten carbide standard sphere (Foote and MacLennan 1984). The right bank transducer measured the sphere at a target strength of –38.6 dB, and the left bank transducer measured the sphere at –38.8 dB (HTI 2009; Table 2). The theoretical value for the sphere is −39.5 dB (MacLennan and Simmonds 1992). During a subsequent *in situ* calibration check using the same sphere, mean target strength measured –38.7 dB on the right bank and –38.8 dB on the left bank (Table 2). Small fluctuations in target strength are expected during *in situ* calibration checks due to changes in signal to noise ratio, water temperature, depth, conductivity, and other factors.

Sampling Procedure

A systematic sample design (Cochran 1977) was used to estimate fish passage from each bank for 20 minutes each hour. Although the sonar system is capable of sampling both banks continuously, data collection was restricted to 20-min samples per hour to limit the data

---

8 For this reason it is possible that some fish migrating near the thalweg (comprising a small fraction of the inriver run) are double-counted or missed entirely.

processing time and personnel required to estimate daily fish passage. The equipment was automated to sample the right bank for 20 min starting at the top of each hour followed by a 20-min left-bank sample. The system was inactive for the third 20-min period unless ancillary sonar studies were being conducted. This routine was followed 24 hours per day and 7 days per week unless a transducer on one or both banks was inoperable. A test of this sample design in 1999 found no significant difference between estimates of Chinook salmon passage obtained using 1-hour counts and estimates obtained by extrapolating 20-min counts to 1 hour (Miller et al. 2002).

Because fish passage rates are related to tides (Eggers et al. 1995), tide stage was recorded at the top of each hour and at 20 min past each hour to coincide with the start of each 20-min sample. Tide stage was determined using water level measurements taken from depth sensors attached to the sonar transducers.

Data Collection Parameters

An HTI Model 244 digital echo sounder (DES) was used for data collection. Key data collection parameters (echo-sounder settings) are listed in Table 3 with complete summaries by bank in Appendices B1 and B2. Most echo-sounder settings were identical for each bank and remained consistent throughout the sample period. High power and low gain settings were used to maximize SNR. The transmitted pulse width was set relatively low to maximize resolution of individual fish and SNR.

Data Acquisition

The DES performed the initial filtering of returned echoes based on user-selected criteria (Table 4; Appendices B1 and B2) that are input via software stored on an external data processing computer (Table 1; Figure 6). The DES recorded the start time, date, and number of pings (acoustic pulses) processed for each sample.

Echoes that originated in the transducer near field (≤ 2.0 m) were excluded because fluctuating sound intensity near the face of the transducer results in unreliable data (Simmonds and MacLennan 2005). Echoes that exceeded maximum vertical and horizontal angles off axis were also excluded to prevent consideration of unreliable data near the edge of the sonar beam.

Voltage thresholds were used to exclude most background noise from spurious sources such as boat wake, the river bottom, and the water surface. Collection of data from unwanted noise causes data management problems and makes it difficult to distinguish echoes originating from valid fish targets. The level of background noise is determined largely by the dimensions of the sonar beam in relation to the depth of the river. Because the water level at the sonar site is strongly influenced by tidal stage (vertical fluctuations of more than 4 m), the background noise fluctuates periodically, with the lowest noise levels during high tide and the highest levels during falling and low tides. Voltage thresholds corresponding to a –35 dB target on axis were selected for each bank as the lowest thresholds that would exclude background noise at low tide when noise was at a maximum.

For each echo passing initial filtering criteria, the DES wrote information in ASCII file format (*.RAW files). This file provided a record of all raw echo data, which could then be used by other post-processing software. A uniquely-named file was produced for each sample hour. The file stored the following statistics for each tracked echo: 1) distance from the transducer, 2) sum channel voltage produced by the echo, 3) pulse widths measured at −6 dB, −12 dB, and −18 dB down from the peak voltage, 4) up-down (vertical) angle, left-right (horizontal) angle, and 5) multiplexer port.

The sum channel voltage from the DES was also output to a printer, to a Nicolet 310 digital storage oscilloscope, and to a Harp HC2 color chart monitor. Output to the printer was filtered only by a voltage threshold, which was set equal to the DES threshold. Real-time echograms were produced for each sample. The echograms were used for data backup and transducer aiming, and to aid in manual target tracking. Voltage output to the oscilloscope and color monitor was not filtered. Monitoring the unfiltered color echogram ensured that sub-threshold targets were not being unintentionally filtered. Advanced features on the digital oscilloscope aided in performing field calibrations with a standard target and in monitoring the background noise level relative to the voltage threshold level.

Fish Tracking and Echo Counting

Using HTI proprietary software called TRAKMAN 1400 (version 1.31), echoes (from the *.RAW files) were manually grouped (tracked) into fish traces. TRAKMAN produces an electronic chart recording for all valid echoes collected during a 20-min sample. Selected segments of the chart can be enlarged and echoes viewed on a Cartesian grid. Echoes that displayed a sequential progression through the beam were selected by the user and classified into fish traces (targets). TRAKMAN then produced 3 output files. The first file contained each echo that was tracked from a valid target (*.MEC file) and included the following data for each echo: estimated *X* (left-right), *Y* (up-down), and *Z* (distance from the transducer) coordinates in meters where the transducer face is the origin of the coordinate system; pulse widths measured at –6 dB, –12 dB, and –18 dB amplitude levels; combined beam pattern factor in decibels; and target strength in decibels. The second fixed-record ASCII file (*.MFS file) summarized data from all echoes associated with an individual tracked target and output the following fields by target: total number of echoes tracked; starting *X*, *Y*, and *Z* coordinates; distance traveled (m) in the *X*, *Y*, and *Z* directions; mean velocity (m/sec); and mean target strength (dB). The third file was identical to the *.RAW file described earlier except that it contained only those echoes combined into tracked targets. Direction of travel was estimated by calculating the simple linear regression of *X*-axis position (distance up- or downriver from the beam axis) on ping number, for echoes with absolute *X*-axis angle less than 5 degrees. On the right bank, a target was classified as upstream bound if the slope of the regression was negative or downstream bound if the slope was positive. On the left bank the criteria were reversed. Only upstream bound targets contributed to estimates of Chinook salmon passage. A diagram illustrating data flow can be found in Appendix C1.

Downstream moving targets (and occasionally upstream moving targets during a strong flood tide) were further classified as fish or debris primarily by looking at the angle of passage and degree of movement in the *Z*-axis (distance from transducer) as the target moved through the acoustic beam. For debris, the angle of passage through the beam is constant with little change in the range as it passes through the beam. Consequently, debris resembles a line drawn on the echogram with a straightedge. A fish typically leaves a meandering trace that reflects some level of active movement as it passes through the acoustic beam. Separate summary files were generated for tracked targets classified as debris (i.e., *.DEC and *.DFS files). Except for debris, only targets comprising echoes displaying fish-like behavior were tracked. Echoes from structures, boat wakes, and sport-fishing tackle were ignored.

Data Analysis

Tidal and Temporal Distribution

Falling tide was defined as the period of decreasing river depth readings, low tide as the period of low static readings, and rising tide as the period of both increasing readings and high static readings (i.e., high slack tide). The rising and high slack tides were combined into one category because of the very short duration of high slack tide at the sonar site. Data from both banks were combined to summarize fish passage by tide stage (falling, low, and rising) for both upstream and downstream traveling fish. Data were first filtered using target strength and range criteria.

Spatial Distribution

Knowledge of the spatial distribution of fish is desirable for developing strategies for insonifying a specific area, for determining appropriate transducer beam dimensions, and for evaluating the probability of detecting fish near the edge of the acoustic beam (Mulligan and Kieser 1996).

Fish range (*Z*-axis) distributions (distance from shore) for each bank were plotted separately for upstream and downstream moving targets. Fish range distributions were calculated using the mean distance from transducer for each target. Before 2000, range distribution comparisons were made using z_m, the distance from the face of the transducer to the target location (Miller et al. 2002). These comparisons provided information on the distribution of fish targets from the face of the transducer. However, the comparisons were poor descriptors of actual fish range distributions across the river because tripod and transducer locations change throughout the season. Beginning in 2000, estimates of distance from bank were standardized to the nearest shore transducer deployment for that bank based on distances to a fixed point (cable bipod) on the right bank (Figures 3–5):

$$z_a = z_m + |z_t - z_n| \tag{1}$$

where:

z_a = adjusted range (in meters),

z_t = distance (in meters) from right bank bipod to transducer, and

z_n = distance (in meters) from right bank bipod to nearest shore (right bank or left bank) deployment location.

z_m = distance (in meters) from face of transducer to target location.

Range distribution plots were produced with the adjusted (standardized) range estimates allowing for comparisons of actual fish target locations across the river. The end range in these distribution graphs was the maximum distance covered (generally to the thalweg) by the sonar beam on that particular bank.

For split-beam sonar data, vertical distributions were plotted by direction of travel (upstream and downstream) and tide stage. Vertical distributions were calculated from the midpoint angle off axis[9] in the vertical plane as follows:

$$\theta_v = \arcsin \frac{v_s + \left(\frac{d_v}{2} \right)}{z_m} \tag{2}$$

where:

θ_v = vertical angle-off-axis midpoint (degrees),
v_s = starting vertical coordinate (in meters), and
d_v = distance traveled in vertical direction (in meters).

Split-beam Sonar Upstream Fish Passage Estimates

The following procedures are used to estimate the number of salmon of all species that migrate upstream past the sonar site in midriver, where midriver is defined as at least 15 m from the right-bank transducer and at least 10 m from the left-bank transducer. This estimate[10] was used as the basis for all other split-beam sonar-based estimates described herein. The remaining estimates pertain only to Chinook salmon and differ in the manner in which species classification is carried out.

As mentioned above, the split-beam sonar operated 20 minutes per hour from each bank of the river, 24 hours per day. The number of salmon-sized fish (hydroacoustic variable *y*) passing midriver and upstream through the sonar beams during day *i* was estimated as follows:

$$\hat{y}_i = 24\hat{\bar{y}}_i \tag{3}$$

where

$$\hat{\bar{y}}_i = \frac{1}{n_i} \sum_{j=1}^{n_i} \hat{y}_{ij} , \tag{4}$$

and where n_i is the total number of hours (*j*) during which fish passage was estimated[11] for day *i*, and

$$\hat{y}_{ij} = \sum_{k=1}^{2} \hat{y}_{ijk} , \tag{5}$$

where $\hat{y}_{ijk}$ is the estimate of upstream midriver fish passage on bank *k* during hour *j* of day *i*.

---

9 Axis or acoustic axis refers to the center of the beam in either the vertical or horizontal plane.

10 These were known in-house as "unfiltered" estimates in the sense that TS and time-varying range thresholds had not been applied. Technically, these counts were still filtered by time-invariant minimum range criteria to exclude fish close to the transducer. Fish close to the transducer are subject to imperfect detection due to the narrowness of the sonar beams at close range. Traditionally, they have been assumed to be composed almost entirely of sockeye salmon.

11 Hours for which passage is <u>not</u> estimated include hours when equipment on both banks was not functional (<1% of time).

When the sonar was functional on bank k during hour j of day i, then hourly upstream midriver fish passage was estimated as follows:

$$\hat{y}_{ijk} = \frac{60}{m_{ijk}} c_{ijk} \tag{6}$$

where

m_{ijk} = number of minutes (usually 20) sampled from bank k during hour j of day i, and

c_{ijk} = number of upstream bound fish greater than 15 m from the right-bank transducer and greater than 10 m from the left-bank transducer, for bank k, hour j, and day i.

When the sonar system was functional on one bank but not the other, the passage on the non-functional bank k' was estimated from passage on the functional bank k as follows:

$$\hat{y}_{ijk'} = \hat{R}_{ikt} \hat{y}_{ijk} , \tag{7}$$

where the estimated bank-to-bank ratio R_{ikt}, for day i and tide stage t is calculated by pooling counts from all hours at tide stage t (set J_t) during the previous 2 days (to ensure adequate sample size):

$$\hat{R}_{ikt} = \frac{\sum_{j \in J_t} \hat{y}_{(i-2)jk'} + \sum_{j \in J_t} \hat{y}_{(i-1)jk'}}{\sum_{j \in J_t} \hat{y}_{(i-2)jk} + \sum_{j \in J_t} \hat{y}_{(i-1)jk}} . \tag{8}$$

The variance of the estimates of y, due to systematic sampling in time, was approximated (successive difference model, Wolter 1985) with adjustments for missing data as follows:

$$\hat{V}\left[\hat{y}_i\right] \cong 24^2 (1-f) \frac{\sum_{j=2}^{24} \phi_{ij} \phi_{i(j-1)} \left(\hat{y}_{ij} - \hat{y}_{i(j-1)}\right)^2}{2 \sum_{j=1}^{24} \phi_{ij} \sum_{j=2}^{24} \phi_{ij} \phi_{i(j-1)}} \tag{9}$$

where f is the sampling fraction (proportion of time sampled daily, usually 0.33), and ϕ_{ij} is 1 if $\hat{y}_{ij}$ exists for hour j of day i, or 0 if not.

The total estimate of upstream midriver fish passage during the period of sonar operation, and its variance, was the sum of all daily estimates:

$$\hat{Y} = \sum_i \hat{y}_i \tag{10}$$

and

$$\hat{V}\left[\hat{Y}\right] = \sum_i \hat{V}\left[\hat{y}_i\right]. \tag{11}$$

Split-beam Sonar Target Strength (TS)-based Chinook Salmon Passage Estimates

To produce TS-based estimates, midriver upstream bound fish counts (c_{ijk}) were filtered using 2 criteria: target strength (> –28 dB) and distance from the transducer (greater than customized range thresholds, see below). TS-based estimates were the standard metric for comparison with escapement goals. Although target strength and range thresholds do not exclude all sockeye salmon (see Introduction; Eggers 1994 and Burwen et al. 1995), we continued their use for historical comparability, while we developed other means of discriminating between fish species.

Range thresholds differed by bank and over time. Range thresholds were changed when transducer tripods were moved or when fish distribution and behavior indicated that species discrimination could be improved. The left-bank range threshold remained the same (10 m) throughout the season (16 May to 4 August). The right-bank range threshold was 15 m from 16 May to 12 July and increased to 20 m from 13 July to 4 August (Figure 4).

Target strength was calculated for individual echoes and averaged for each fish trace (Appendix A1). TS-based daily passage estimates ($\hat{y}_{TSi}$) for day i were calculated using Equations 3–10 after substituting c'_{ijk} for c_{ijk}, where

c'_{ijk} = number of upstream bound fish on bank k meeting range and target-strength criteria during t_{ijk}.

Additionally, for TS-based estimates, some sample hours were excluded when there was evidence (greater than 50% of targets in closely-spaced groups) of increased sockeye salmon abundance. Under these conditions, and at the discretion of the project leader, the entire hourly sample was dropped and the daily estimate was based on the remaining samples. Censored hourly samples are listed in Appendix D1.

Variance estimates consider only sampling error due to temporal expansion, not error due to imperfect detection or tracking of fish, nor error due to imperfect species classification. Therefore, Equation 11 represents only a minimal estimate of variance.

Downstream TS-based Chinook salmon passage for day i was estimated as follows:

$$\hat{x}_{TSi} = \hat{y}_{TSi} \frac{\sum_j \sum_k d_{ijk}}{\sum_j \sum_k c'_{ijk}}, \tag{12}$$

where d_{ijk} is the number of downstream bound fish on bank k meeting range and target-strength criteria during t_{ijk}.

Split-beam Sonar Net-Apportioned Chinook Salmon Passage Estimates

The "net-apportioned" daily estimate of Chinook salmon passage was calculated by multiplying the upstream midriver fish passage estimate by the estimated proportion of Chinook salmon ($\hat{\pi}_{NETi}$) in 5-inch and 7.5-inch drift net catches near the sonar site (Perschbacher 2012):

$$\hat{y}_{NETi} = \hat{y}_i \hat{\pi}_{NETi}. \tag{13}$$

The variance estimate followed Goodman (1960):

$$\hat{\text{var}}(\hat{y}_{NETi}) = \hat{y}_i^2\ \hat{\text{var}}(\hat{\pi}_{NETi}) + \hat{\pi}_{NETi}^2\ \hat{\text{var}}(\hat{y}_i) - \hat{\text{var}}(\hat{\pi}_{NETi})\hat{\text{var}}(\hat{y}_i) \qquad (14)$$

Split-beam Sonar Echo Length Standard Deviation (ELSD)-based Chinook Salmon Passage Estimates

Alternative estimates based on echo length standard deviation were first produced in 2002, based on work initiated in the mid-1990s that showed ELSD to be a better predictor of fish size than target strength (Burwen et al. 2003). ELSD-based estimates were generated by fitting a statistical species–age mixture model to sonar and netting data. Mixture model methodology is described below.

Mixture Models versus Thresholds

Mixture models are useful for extracting information from the observed frequency distribution of a carefully selected measurement. For example, if one were able to observe the exact length, but not the species, of every fish passing the sonar, the distribution of such measurements might look like Figure 7a. With auxiliary information about sockeye and Chinook salmon size, the shape of such a distribution can reveal much about the relative abundance of sockeye and Chinook salmon. For instance, if sockeye salmon were known not to exceed 70 cm, and small Chinook salmon were known to be rare, one could conclude that the left hand mode of the distribution is almost all sockeye salmon and that the species composition is perhaps 50:50 sockeye salmon to Chinook salmon. Mixture model analysis is merely a quantitative version of this assessment in which the shape of the overall frequency distribution is modeled and "fitted" until it best approximates the data. Uncertainty is assessed by providing a range of plausible species compositions that could have resulted in the observed frequency distribution.

As another example, imagine that many Chinook salmon are small, and that there is error in the length measurements. The effect of the measurement error is to cause the modes of the distributions to begin to overlap, reducing the ability to detect detail in the length distributions and reducing the precision of the estimates (e.g., Figure 7b). Under this scenario, it is more difficult to interpret the data, and a mixture model approach is helpful to provide objective estimates with realistic assessments of uncertainty.

Mixture models can also be fit to measurements of other quantities, like ELSD, that are related to length. Given quantitative knowledge of the relationship between length and ELSD (gleaned from tethered fish experiments, Burwen et al. 2003), it is straightforward to convert from length units to ELSD units by including the slope, intercept, and mean squared error of the relationship in the mixture model (Equation 17 below). The more closely related the surrogate measurement is to the one of interest, the more the two distributions will resemble each other and the better the resulting estimate will be. Because ELSD is a reasonably good predictor of fish length (Figure 8),[12] the observed frequency distribution of ELSD supplies valuable information about species composition, even though there is some overlap of ELSD measurements between species. An ELSD distribution with greater mass on the left-hand side indicates an abundance of sockeye salmon, whereas more mass on the right-hand side indicates more Chinook salmon (Figure 9).

---

[12] ELSD can be a good predictor of length, though not as precise as the DIDSON length estimates.

The relationship between target strength and fish length is less precise than between ELSD and fish length (Burwen et al. 2003) and it is also less predictable (the relationship changes over time). Furthermore, TS-based species discrimination is implemented in the form of a threshold (TS < –28dB = sockeye salmon, TS > –28dB = Chinook salmon), and the threshold approach has several important drawbacks. When distributions overlap between species, thresholds are unbiased only when compensating errors are equal (e.g., when the number of sockeye salmon exceeding the threshold is equal to the number of Chinook salmon beneath the threshold). But the size of the respective errors depends on the species composition itself (Figure 9): when sockeye salmon are dominant there are more misclassified sockeye salmon than misclassified Chinook salmon (and the resulting estimate of Chinook salmon proportion is too high), and when Chinook salmon are dominant there are more misclassified Chinook salmon than misclassified sockeye salmon (and the resulting estimate of Chinook salmon proportion is too low). Thus threshold-based discrimination is subject to bias that worsens for species proportions near 0 and 1. Furthermore, threshold-based estimates are sensitive to fish size distributions. For instance, in the example illustrated in Figure 9, the number of Chinook salmon misclassified as sockeye salmon (number with ELSD < 2.7) depends largely on the relative abundance of small Chinook salmon, which changes over time.[13]

The mixture model approach explicitly incorporates the expected variability in hydroacoustic measurements (known from tethered fish experiments), as well as current information about fish size distributions (from the onsite netting program). As a result, it is subject to fewer pitfalls than a threshold approach. There is less bias against extreme proportions, and the estimates are germane to the entire population of Chinook salmon, not just those Chinook salmon larger than sockeye salmon. Finally, as long as length and hydroacoustic measurements are paired in time, mixture model estimates of species proportions are less sensitive to temporal changes in fish size distribution.

Mixture Model Details[14]

Echo length standard deviation (ELSD) was calculated as follows:

$$ELSD = \sqrt{\sum_{j=1}^{n_E} \left(EL_j - \overline{EL}\right)^2 \Big/ \left(n_E - 1\right)} \qquad (15)$$

where n_E is the number of echoes and EL_j is the length of the j^{th} echo measured in 48 kHz sample units at –12 dB or higher, depending on peak echo amplitude. If peak amplitude was greater than 12 dB above the voltage threshold, then echo length was measured at 12 dB below peak amplitude. If peak amplitude was 6–12 dB above the threshold, echo length was measured at the threshold. If peak amplitude was less than 6 dB above threshold, EL_j was not defined.

Fish traces with fewer than 8 defined measurements of –12dB pulse width ($n_E < 8$) were excluded from the mixture model; they were assumed to be sockeye salmon because they generally occurred at close ranges, where the beam is very narrow. These fish generally comprised only 1–3% of all fish in the dataset.

---

[13] In fact, use of such a threshold by itself does not discriminate Chinook salmon from sockeye salmon, but rather large Chinook salmon from sockeye salmon and small Chinook salmon.

[14] Statistical notation in this section may overlap with the notation used in the remainder of the report. Specifically, the meaning of variables *x*, *y*, and *z* are unique to this section.

The probability density function (PDF) of ELSD (denoted here as *y*, for convenience) was modeled as a weighted mixture of 2 component distributions arising from sockeye salmon and Chinook salmon (Figure 10):

$$f(y) = \pi_S f_S(y) + \pi_C f_C(y) \tag{16}$$

where $f_S(y)$ and $f_C(y)$ are the PDFs of the sockeye salmon and Chinook salmon component distributions, and the weights π_S and π_C are the proportions of sockeye salmon and Chinook salmon in the population.

Individual observations of *y* for fish *i* were modeled as normal random variables whose mean is a linear function of fish length *x*:

$$y_i = \beta_0 + \beta_1 x_i + \gamma z_i + \varepsilon_i \tag{17}$$

where β_0 is the intercept; β_1 the slope; γ is the mean difference in *y* between sockeye salmon and Chinook salmon after controlling for length; z_i equals 1 if fish *i* is a sockeye salmon, or 0 if Chinook salmon; and the error ε_i is normally distributed with mean 0 and variance σ^2.

Thus, the component distributions $f_S(y)$ and $f_C(y)$ are functions of the length distributions $f_S(x)$ and $f_C(x)$ and the linear model parameters β_0, β_1, γ, and σ^2 (Figure 10). The species proportions π_S and π_C were the parameters of interest.

Length measurements were obtained from fish captured by gillnets (e.g., Eskelin 2010) immediately downstream of the sonar site. Length data were paired with hydroacoustic data from the same time periods.

Sockeye salmon and Chinook salmon return from the sea to spawn at several discrete ages. We modeled sockeye salmon and Chinook salmon length distributions as 3-component normal age mixtures:

$$f_S(x) = \theta_{S1} f_{S1}(x) + \theta_{S2} f_{S2}(x) + \theta_{S3} f_{S3}(x) \text{ and} \tag{18}$$

$$f_C(x) = \theta_{C1} f_{C1}(x) + \theta_{C2} f_{C2}(x) + \theta_{C3} f_{C3}(x) \tag{19}$$

where θ_{Ca} and θ_{Sa} are the proportions of Chinook salmon and sockeye salmon belonging to age component *a* and the distributions

$$f_{Sa}(x) \sim N(\mu_{Sa},, \tau^2_{Sa}), \text{ and} \tag{20}$$

$$f_{Ca}(x) \sim N(\mu_{Ca},, \tau^2_{Ca}) \tag{21}$$

where μ is mean length-at-age and τ is the standard deviation. The overall design was therefore a mixture of (transformed) mixtures. That is, the observed hydroacoustic data were modeled as a 2-component mixture (sockeye salmon and Chinook salmon) of echo length standard deviation (*y*), each component of which was transformed from a 3-component normal age mixture of fish length (*x*).

Bayesian statistical methods were employed because they provided realistic estimates of uncertainty and the ability to incorporate auxiliary information. We implemented the Bayesian mixture model in WinBUGS (Bayes Using Gibbs Sampler; Gilks et al. 1994). Bayesian methods require that prior probability distributions be formulated for all unknowns in the model (Gelman et al. 2004). Species proportions π_S and π_C were assigned an uninformative Dirichlet (1,1) prior.

Age proportions $\{\theta_{Sa}\}$ and $\{\theta_{Ca}\}$ were assigned informative Dirichlet priors based on a hierarchical analysis of historical data (Appendix E1). Likewise, informative normal priors based on historical data were used for the length-at-age means μ and standard deviations τ (Appendix E1). A linear statistical model of tethered fish data (Burwen et al. 2003) was integrated into the mixture model (Appendix E1) to provide information on regression parameters β_0, β_1, γ, and σ^2.

WinBUGS uses Markov chain Monte Carlo methods to sample from the joint posterior distribution of all unknown quantities in the model. A single Markov chain[15] was initiated for each daily run of the model, samples were thinned 20 to 1, and history plots were monitored to confirm convergence and mixing. The first 4,000 or more "burn-in" samples were discarded, and at least 20,000 additional samples were drawn from the posterior distribution.

The end product of a Bayesian analysis is the joint posterior probability distribution of all unknowns in the model. For point estimates, posterior means were used. Posterior standard deviations were reported as analogues to the standard error of an estimate from a classical (non-Bayesian) statistical analysis.

Sample size limitations necessitated pooling data from the first week of operation (16–22 May). Netting length data from day *d* and $d-1$ were paired with ELSD data from day *d*. WinBUGS code for the ELSD mixture model is in Appendix E2. Figure 10 is a flow chart with major components of the ELSD mixture model. See also Fleischman and Burwen (2003).

ELSD-based Chinook Salmon Passage Estimates[16]

ELSD mixture model estimates of daily Chinook salmon passage were obtained as follows. First, the proportion p_{Mi} of sonar-sampled fish that satisfied the sample size criterion ($n_E \geq 8$) and the proportion p_{Bi} that satisfied the behavior criterion (fish could not be less than 1 m of range from another fish) for day *i* were calculated. Then the ELSD frequency distribution from fish meeting both criteria was analyzed with the mixture model methods described above, yielding $\hat{\pi}_{Ci}$, the posterior mean of the Chinook salmon fraction in the reduced data set for day *i*.

The estimated number of Chinook salmon passing during day *i* was then

$$\hat{y}_{ELi} = \hat{y}_i \hat{\pi}_{Ci} p_{Mi} p_{Bi} \tag{22}$$

with estimated variance

$$\hat{\text{var}}(\hat{y}_{ELi}) = \left[\hat{y}_i^2 \,\hat{\text{var}}(\hat{\pi}_{Ci}) + \hat{\pi}_{Ci}^2 \,\hat{\text{var}}(\hat{y}_i) - \hat{\text{var}}(\hat{\pi}_{Ci})\hat{\text{var}}(\hat{y}_i)\right]\hat{p}_{Mi}^2 \hat{p}_{Bi}^2 \tag{23}$$

where $\hat{\text{var}}(\hat{\pi}_{Ci})$ is the squared posterior standard deviation from the mixture model. Uncertainty about p_{Mi} and p_{Bi} was ignored because it was negligible compared to $\hat{\text{var}}(\hat{\pi}_{Ci})$.

---

[15] During initial development of the model, multiple chains were used to assess convergence (Gelman et al. 2004). This was not necessary during production of daily estimates.

[16] These were termed "behavior-censored ELSD-based estimates" in a previous report (Miller et al. 2012).

DUAL-FREQUENCY IDENTIFICATION SONAR (DIDSON)

Acoustic Sampling

A Sound Metrics Corporation (SMC[17]) DIDSON system was operated from 17 May to 10 August, 2010. Components of the DIDSON system are listed in Table 5. Appendix F1 provides greater detail on DIDSON technology and theory.

Sonar System Configuration

DIDSON transducers were deployed on both banks of the river, mounted in a side-by-side configuration with the split-beam transducer on the same pan-and-tilt aiming device (Figure 11, panels A and B). The DIDSON was subject to the same deployment configuration and aiming protocol described above for the split-beam transducer with 1 exception, the DIDSON was aimed at a vertical angle approximately 1 degree lower than the split-beam sonar to achieve better image quality. Because silt deposition in the lens compartment can cause deterioration in both image quality and range capabilities, a custom fit fabric enclosure was used to limit silt infiltration (Figure 11, panels B and C).

Sampling Procedure

Unlike the split-beam sonar, DIDSON sampled 3 separate range strata on each bank to increase resolution (3.3–13.3 m, 13.3–23.3 m, and 23.3–33.3 m; Figure 12). The DIDSON was programmed to sample each stratum systematically for 10 min per hour according the schedule outlined in Figure 13. A sampling fraction of 10 min per hour has been used for decades in Bristol Bay for tower counts of sockeye salmon (e.g., Reynolds et al. 2007 and references cited therein).

Data Collection Parameters

The transmit power of the DIDSON sonar was fixed, and receiver gain was maximized (40 dB) during all data collection. The autofocus feature was enabled so that the sonar automatically set the lens focus to the midrange of the selected display window (e.g., for a window length of 10 m that started at 15 m, the focus range would be 20 m). The frame rate (frame per second, or fps) varied for each range stratum: 12 fps for the 3.3–13.3 m stratum, 7 fps for the 13.3–23.3 m stratum, and 5 fps for the 23.3–33.3 m stratum.

Manual DIDSON Fish Length Measurements

Software included with the DIDSON system (Control and Display software Version 5.25) was used to count and measure fish from DIDSON images. Electronic echograms similar to those generated from split-beam data provided a system to manually count, track, and size individual fish (Figure 12). Noise from stationary structures was removed from the images using Sound Metric Corporation's algorithm for dynamic background removal. Fish traces displayed on the echogram could also be displayed in video mode through a toggle function (Figure 12). In video mode, technicians used the manual measuring tools to estimate the DIDSON-based length (DL) for each fish. Date, time, frame number, range, and direction of travel were also recorded for each free-swimming fish.

Additional detail on procedures and software settings used to obtain manual fish length measurements can be found in Burwen et al. (2010) and in Appendices F1–F7.

---

[17] Product names used in this publication are included for completeness but do not constitute product endorsement.

Data Analysis

DIDSON-based Estimates of Fish Passage

DIDSON data were used to generate multiple estimates of fish passage, detailed below. All estimates apply to a midriver corridor greater than 3 m from both the left- and right-bank transducers. Note that this corridor was 19 m wider than that covered by split-beam sonar, which was greater than 15 m from the right-bank transducer and greater than 10 m from the left-bank transducer. Except where otherwise stated, all estimates apply to upstream migrating fish only.

DIDSON salmon passage estimates

The DIDSON sample design differed from split-beam sonar in that there were 3 spatial strata on each bank.[18] The number of salmon of all species exceeding 40 cm[19] that migrate upstream past the sonar site in midriver at least 3 m from the face of each sonar on day *i* was estimated following Equations 3–4, where upstream midriver fish passage on bank *k* during hour *j* of day *i* (in Equation 5) was estimated as follows:

$$\hat{y}_{ijk} = \sum_{s=1}^{3} \hat{y}_{ijks} , \tag{24}$$

where $\hat{y}_{ijks}$ is the estimate of upstream midriver fish passage for stratum *s* of bank *k* during hour *j* of day *i*.

When the sonar was functional on bank *k* during hour *j* of day *i*, hourly upstream midriver fish passage for stratum *s* was estimated as follows:

$$\hat{y}_{ijks} = \frac{60}{m_{ijks}} c_{ijks} \tag{25}$$

where

m_{ijks} = number of minutes (usually 10) sampled from bank *k* stratum *s* during hour *j* of day *i*, and

c_{ijks} = number of upstream bound fish greater than 40 cm in stratum *s* of bank *k* during hour *j* of day *i*.

When the DIDSON was functional on one bank but not the other, the passage on the non-functional bank was estimated from passage on the functional bank following Equations 7 and 8. The variance followed Equation 9, and seasonal totals followed Equations 10 and 11 as before.

DIDSON Chinook salmon passage estimates

The number of Chinook salmon passing upstream on day *i* was estimated by multiplying the DIDSON midriver upstream salmon passage estimate *y* by the estimated proportion of Chinook salmon ($\hat{\pi}_{Ci}$) derived by fitting the DIDSON length mixture model described below:

$$\hat{z}_i = \hat{y}_i \hat{\pi}_{Ci} . \tag{26}$$

---

[18] Different focus settings are required for short, medium, and long ranges in order to produce high-resolution images.

[19] As measured from the DIDSON image. This quantity is intended to separate salmon from non-salmon species. It also corresponds approximately to the smallest fish gilled in the inriver netting project (Perschbacher 2012).

Variance estimates follow Goodman (1960):

$$\hat{\text{var}}(\hat{z}_i) = \hat{y}_i^2\, \hat{\text{var}}(\hat{\pi}_{Ci}) + \hat{\pi}_{Ci}^2\, \hat{\text{var}}(\hat{y}_i) - \hat{\text{var}}(\hat{\pi}_{Ci})\hat{\text{var}}(\hat{y}_i). \quad (27)$$

Cumulative estimates were obtained by summing daily estimates and variances.

DIDSON-length mixture model estimates of species composition

DIDSON-based estimates of the proportion of passing fish that were Chinook salmon were obtained by fitting a mixture model to DIDSON length data. The mixture model was identical to the ELSD mixture model (see Equations 15–21) except that DIDSON length was substituted for ELSD and there was no γ parameter in the model. Thus the following was substituted for Equation 17:

$$y_i = \beta_0 + \beta_1 x_i + \varepsilon_i. \quad (28)$$

A subset[20] of tethered fish data from 2007 DIDSON experiments (Burwen et al. 2010) was used to inform the β_0 and β_1 parameters. Species proportions π_S and π_C were assigned a Dirichlet (0.1,0.9) prior.[21] Prior distributions for age proportions $\{\theta_{Sa}\}$ and $\{\theta_{Ca}\}$ were constructed with nested beta (0.5,0.5) prior distributions. Netting probability of capture was assumed to be equal for all 3 age classes. Netting length data from days $d-3$ through $d+3$ were paired with DIDSON length data from day d.[22] A single Markov chain[23] was initiated for each daily run of the model, samples were thinned 10 to 1, and history plots were monitored to confirm convergence and mixing. The first 5,000 or more "burn-in" samples were discarded, and at least 10,000 additional samples were drawn from the posterior distribution.

WinBUGS code for the DIDSON length mixture model is in Appendix E3.

As with the ELSD mixture model results, posterior means are reported as point estimates, and posterior standard deviations as standard errors.

DIDSON-length threshold large fish passage estimates

Upstream large fish passage in midriver during day *i* was calculated following Equations 1–9 after redefining c_{ijk} in Equation 6 to be the number of upstream bound fish greater than 3 m from the right- and left-bank transducers exceeding 75 cm in length as measured by the DIDSON during t_{ijk}.

Downstream large fish passage in midriver during day *i* was calculated following Equations 1–9 after redefining c_{ijk} in Equation 6 to be the number of downstream bound fish greater than 3 m from the right- and left-bank transducers exceeding 75 cm in length as measured by the DIDSON during t_{ijk}.

---

[20] Mixture model results were more robust to length measurement error if only a minimal number of tethered fish data points was used.

[21] This is a very mildly informative prior distribution, equivalent to a single additional observation, and centered on 10% Chinook salmon rather than 50% for the non-informative beta (0.5,0.5).

[22] Netting sample-size limitations were addressed differently between the ELSD and DIDSON-length mixture models. The ELSD model employed informative priors on age composition, developed from a hierarchical analysis of historical netting data. The DIDSON length model assigned non-informative priors to age composition parameters, but pooled 7 days of netting data centered on the current day to pair with a single day of DIDSON length data.

[23] During initial development of the model, multiple chains were used to assess convergence (Gelman et al. 2004). This was not necessary during production of daily estimates.

Daily DIDSON-equivalent estimates of Chinook salmon passage

DIDSON-length mixture model (DLMM) estimates of inriver abundance could be produced for only 48 of 87 days in 2010, due to various hardware, software, and logistical problems. However, DLMM estimates were correlated with catches of Chinook salmon in the inriver netting project (available all 87 days) and with DIDSON-length threshold estimates (available 54 days including 6 days when DLMM estimates were missing). By fitting a daily abundance model (Appendices N1–N4) to sonar and netting data, these relationships were leveraged to produce "DIDSON-equivalent" estimates for the 39 days when direct estimates were not available.

Three indices I of daily Chinook salmon abundance were used: (1) the catch rate of Chinook salmon in nets deployed at RM 8.5 (Perschbacher 2012); (2) the split-beam net-apportioned estimate of Chinook salmon passage (Equation 13); and (3) the DIDSON-length threshold estimate of Chinook salmon passage (see previous section: DIDSON-length threshold large fish passage estimates). Each was an independent measure of the relative midriver abundance of Chinook salmon on day d:

$$I_{id} = q_i w_d \tag{30}$$

where q_i is the mean ratio of index I_{id} to midriver abundance w_d. To allow for non-stationary relationships between each index and true abundance, an autoregressive lag-1 (AR[1]) error term was specified (Pankratz 1991):

$$\ln(I_{id}) = \ln(q_i w_d) + \phi_i \nu_{i,d-1} + \varepsilon_{id} \tag{31}$$

where ϕ_i is the AR(1) coefficient, the $\{\nu_{i,d-1}\}$ are model residuals, and

$$\nu_{i,d-1} = \ln(I_{id}) - \ln(q_i w_d) \tag{32}$$

for the previous day, and the $\{\varepsilon_{id}\}$ are independently and normally distributed process errors with "white noise" variance σ^2_i. Parameters q_i, ϕ_i, and σ_i were estimated from the data. OpenBUGS code for the daily abundance model is in Appendix N1.

Predicted values of abundance specific to each index, with and without the AR(1) term, were produced for illustrative purposes (Appendices N3–N4) as follows:

$$N_{PWid} = \exp\left(\ln(I_{id}) + \phi_i \nu_{i,d-1}\right)/q_i \ , \tag{33}$$

$$N_{PWOid} = I_{id}/q_i \ . \tag{34}$$

Model fitting was implemented in the Bayesian software program OpenBUGS (Lunn et al. 2009). Block updaters were disabled before compilation, but no other problems with mixing or convergence were encountered. After confirming that mixing and convergence were adequate, a single chain of 69,000 samples was used to approximate the posterior distribution of the model parameters. As with the results of other Bayesian analyses in this report, posterior means are reported as point estimates, and posterior standard deviations as standard errors. See McKinley and Fleischman (2013) for a description of similar methods applied to a reconstruction of annual Kenai River Chinook salmon abundances.

RESULTS

SPLIT-BEAM SONAR

Spatial and Temporal Distribution of Split-beam Sonar Targets

In 2010, 79,323 split-beam targets were manually tracked, 8,700 during the early run and 70,623 during the late run. Of these, approximately 20% met the TS-based criteria for classification as Chinook salmon (TS greater than –28 dB, range greater than 10 m from left bank transducer and greater than 15–20 m from the right bank transducer [see Split-beam Sonar Target Strength (TS)-based Chinook Salmon Passage Estimates in Methods section]; sample period not dropped based on fish behavior, Appendix D1). Spatial and temporal distribution of these "filtered" targets is described below.

The percentage of filtered targets that exhibited upstream movement was 98% for the early run and 99% for the late run (Appendices G1–G2). Daily upstream percentages varied from 75% to 100% during the early run and from 90% to 100% during the late run.

Upstream moving filtered targets were observed mostly during the falling tide for both the early (63.7%) and late (55.1%) run (Table 6, Figure 14). Likewise, downstream passage occurred primarily during the falling tide for both the early (57.8%) and late (53.9%) run.

During the early run, more upstream moving filtered targets (57%) were observed on the left bank than on the right bank (Table 7). During the late run, a little more than half of upstream moving filtered targets (54%) were observed on the right bank (Table 7).

Early-run upstream and downstream moving filtered targets were distributed throughout the insonified range on both banks, with a relatively even distribution of upstream moving targets on the left bank (Figure 15). The right bank exhibited a pronounced peak in upstream passage near the offshore end of the insonified range (Figure 15).

During the late run, upstream moving filtered targets on the left bank were also relatively evenly distributed throughout the insonified range (Figure 16). Upstream moving filtered targets on the right bank and downstream moving targets on both banks exhibited offshore peaks in passage (Figure 16).

The effect of tide stage on the range distribution (distance from transducer) of filtered targets was more pronounced on the right bank than on the left bank during both runs (Figures 17 and 18). Upstream moving targets on the left bank were relatively evenly distributed during all three tide stages. Upstream moving targets on the right bank exhibited a higher offshore distribution during the falling and low tides, and a more uniform distribution during the rising tide (Figures 17 and 18).

Although filtered targets were generally bottom oriented during the early and late runs, vertical distribution did vary by direction of travel, tide stage, and run (Appendices H1–H2). During the early run, 77% of the upstream moving filtered targets on the left bank and 76% on the right bank were on or below the acoustic axis (Figure 19). Sixty-four percent of downstream moving filtered targets on the left bank and 72% on the right bank were on or below the acoustic axis (Figure 19). Mean vertical position of downstream moving targets (0.11°, SD = 0.45, n = 28) on the left bank was significantly higher (t = 3.04, P < 0.01) than that of upstream moving targets (−0.15°, SD = 0.31, n = 2,815). On the right bank, mean vertical position of downstream moving targets (−0.21°, SD = 0.53, n = 65) was not significantly higher (t = 0.14, P = 0.46) than that of upstream moving targets (−0.22°, SD = 0.38, n = 2,214). Upstream traveling targets were, on average, distributed higher in the water column during rising tides, particularly on the left bank (Figure 20).

During the late run, 62% of upstream moving filtered targets on the left bank and 55% on the right bank were on or below the acoustic axis (Figure 21). Fifty-five percent of downstream moving filtered targets on the left bank and 43% on the right bank were on or below the acoustic axis (Figure 21). There was no significant difference (t = 0.08, P = 0.47) between the mean vertical position of upstream moving targets (−0.04°, SD = 0.28, n = 11,733) and downstream moving targets (−0.03°, SD = 0.31, n = 130) on the left bank. On the right bank, the mean vertical position of downstream moving targets (0.04°, SD = 0.29, n = 227) was significantly higher (t = 2.97, P < 0.01) than the vertical position of upstream moving targets (−0.01°, SD = 0.25, n = 18,741). Vertical distribution of upstream moving targets was higher during the rising tide on both banks (Figure 22).

Split-beam Sonar Estimates of Upstream Fish Passage

Daily split-beam estimates of upstream fish passage were generated for 16 May through 4 August.[24] A total of 542 hours of split-beam acoustic data were processed from the right bank and 564 hours from the left bank during the 81-day season. This represented 28% and 29% of the total available sample time (1,944 hours) for the right and left banks, respectively.

Note that all split-beam fish passage estimates apply to a corridor in midriver that is greater than 15 m from the right-bank transducer and greater than 10 m from the left-bank transducer. This differs from the wider DIDSON corridor, which is greater than 3 m from both transducers.

Split-beam sonar upstream fish passage estimates were 20,577 (SE 375) early-run fish and 158,073 (SE 2,869) late-run fish. Peak early-run daily passage occurred on 30 June and peak late-run passage on 31 July (Tables 8–9).

Split-beam Sonar TS-based Estimates of Chinook Salmon Passage

Daily upstream midriver TS-based estimates of Chinook salmon passage were generated for 16 May through 4 August, totaling 13,248 (SE 235) early-run fish and 48,343 (SE 726) late-run fish (Tables 8–9). Peak daily passage based on these estimates occurred on 15 June for the early run and 21 July for the late run. All historical daily TS-based estimates for the years 1987–2010 are compiled in Appendices I1 and I2.[25]

Split-beam Sonar Net-apportioned Estimates of Chinook Salmon Passage

Net-apportioned estimates of upstream Chinook salmon passage were 2,644 (SE 196) fish during the early run and 12,269 (SE 768) fish during the late run (Tables 8–9). Peak daily passage based on net-apportioned estimates occurred on 11 June for the early run and 30 July for the late run.

Split-beam Sonar ELSD-based Estimates of Chinook Salmon Passage

ELSD-based estimates of upstream Chinook salmon passage were 8,497 (SE 428) fish during the early run and 32,941 (SE 2,401) fish during the late run (Tables 8–9). Peak daily passage based

[24] Split-beam sonar data were not processed after 4 August due to numerous fish holding in the sonar beam, making it difficult to accurately track fish targets. DIDSON video images suggest that these fish were probably pink salmon.

[25] TS-based estimates will no longer be generated after 2010.

on ELSD mixture-model estimates occurred on 30 June during the early run and 23 July during the late run.

DUAL-FREQUENCY IDENTIFICATION SONAR (DIDSON)

Long-range high-resolution DIDSON was deployed from both banks and sampled the midsection of the river for 86 days (17 May–10 August) in 2010. Fish measurement data were missing or unreliable during 32% of early-run and 7% of late-run samples, primarily due to chronic focus-related problems that caused degraded image resolution.[26] In total, 66,727 fish 40 cm or longer were measured from DIDSON images, including 59,528 on the 48 days for which DIDSON estimates of Chinook salmon passage were produced (see DIDSON Estimates of Chinook Salmon Passage section below). Such fish are often referred to generically as "salmon" in this report.[27]

Size Distribution and Species Composition

Small fish (presumably sockeye salmon) predominated in both early and late runs, as evidenced by large left-hand modes in the DIDSON length (DL) frequency distributions (Figure 23, top panels). The modes of the DL distributions line up well[28] with mid eye to tail fork length distributions from salmon measured by the inriver netting project (Figure 23, bottom panels). The DL distributions are broader than the corresponding mid eye to tail fork distributions because there is greater error associated with measuring length from DIDSON images. The shapes of the frequency distributions suggest that fish measuring greater than approximately 75–80 cm are probably Chinook salmon. Of fish measuring 40 cm or longer, 3.9% were 75 cm or longer and 3.3% were 80 cm or longer. In this report, "large Chinook salmon" are defined as fish greater than 75 cm DIDSON length.[29]

Spatial and Temporal Distribution

During the early run, salmon of all sizes favored the left bank of the insonified zone (Figure 24). During the late run, large Chinook salmon continued to favor the left bank, but small salmon migrating during 2 of 3 tide stages (falling and rising) favored the right bank (Figure 24). During both the early and late runs, most (60–68%) upstream bound large (DL $\geq$ 75 cm) Chinook salmon were observed from the left bank transducer (Table 10).

Large Chinook salmon migrated closer to shore in the early run than in the late run. For instance, distribution by range stratum (3–13 m, 13–23 m, 23–33 m) differed between runs (early [33%, 39%, 27%] versus late [25%, 36%, 39%] derived from summed values for left and right banks in Table 10). The temporal distribution of large Chinook salmon among tide stages also differed by run, from 20%, 61%, and 20% on the rising, falling, and low tides during the early run to 44%, 39%, and 16% during the late run (Table 10, last column). Note that late-run distribution by tide

---

[26] Image resolution was reduced in the far-range (23–33 m) strata, however there was little evidence that this seriously impacted the ability to distinguish large from small fish. This was corroborated by the results of supplementary tethered fish experiments conducted in 2010 (not shown).

[27] A minimum threshold of 40 cm includes virtually all Chinook salmon and effectively excludes nonsalmon species. For example, among Chinook salmon caught in gillnets at RM 8.5 in 2010, only 1% were less than 40 cm mid eye to tail fork. The proportion of fish over 40 cm that were not salmon was not estimated because nonsalmon species were not measured; however the fraction was very small.

[28] Lengths from the netting data are not representative across species because non-Chinook salmon were sampled (measured) at only one-half the rate of Chinook salmon. Chinook salmon are therefore disproportionately represented in the netting length data.

[29] Although the species of individual fish cannot be determined with certainty from DIDSON images, probably very few fish longer than DL = 75 cm are not Chinook salmon.

differed greatly from that of split-beam filtered targets (18% rising, 55% falling, 27% low; Table 6 and Figure 14). The natural distribution of tide stages was 27% rising, 49% falling, and 24% low; comparing this to the tidal distribution of salmon (quoted above from Table 10) indicates that large Chinook salmon displayed a slight "preference" for the falling tide in the early run and a stronger preference for the rising tide in the late run.

The proportion of all upstream-bound salmon that were classified as large Chinook salmon varied by run, bank, range stratum, and tide stage (Table 11). A greater proportion of salmon were large Chinook salmon in the early run (7.4%) than in the late run (3.7%). During the early run, relatively more salmon were large Chinook salmon on the right bank (9.5%) than on the left bank (6.7%), with the highest fraction (11.5%) occurring in the stratum nearest the right bank shore (Table 11). During the late run, when small salmon often favored the right bank (Figure 24, as mentioned above), relatively more salmon were large Chinook salmon on the left bank (5.0%) than on the right bank (2.6%), and the right-bank nearshore stratum had the lowest fraction (1.2%) of large Chinook salmon.

During the early run, upstream moving salmon that passed during low tide had the highest fraction of large Chinook salmon (10.1%), followed by the rising tide (9.0%), and the falling tide (6.5%). Although smaller percentages of large Chinook salmon were present, a similar pattern held during the late run, when fish migrating during low tide were composed of 5.0% large Chinook salmon, followed by 4.4% during rising tide, and 2.8% during falling tide (Table 11).

Spatial and temporal patterns of migration of small, medium, and large salmon are displayed relative to tide stage in Appendices K1–K5. In general, large Chinook salmon (in this case, defined as >90 cm) were interspersed throughout the sampled range, and were only mildly clustered in space and time. Smaller salmon exhibited more clustering than large Chinook salmon, and their migration timing was strongly influenced by tide cycle (Appendices K1–K5).

Direction of Travel

Among fish that were greater than or equal to 75 cm DIDSON length (DL), 97.4% were upstream bound in the early run, and 98.4% were upstream bound in the late run (Appendices J1–J2). Daily percentages of fish greater than 75 cm DL that were upstream bound ranged from 67% (19 May; 2 of 3 fish) to 100% (many days; Appendices J1–J2).

Matched-sample Comparison of DIDSON and Split-beam Data

Some DIDSON samples could be matched with split-beam data from the same time and range strata (e.g., Figure 25). During the early run, summing over all valid matching samples,[30] there were 1,205 upstream bound fish detected by the DIDSON and 937 detected by the split-beam sonar (Appendices L1–L2). Of the DIDSON-detected fish, only 87 exceeded the 75-cm threshold as measured by the DIDSON. With the split-beam sonar, 680 (7.8 times as many) exceeded the TS threshold of −28 dB. During the late run, also summing over matching left-bank mid-range samples, there were 8,826 upstream bound fish detected by the DIDSON and 5,505 detected by the split-beam sonar. Of the DIDSON fish, only 470 exceeded the 75-cm threshold as measured by the DIDSON. With the split-beam sonar, 3,060 (6.5 times as many) exceeded the TS threshold of −28 dB.

[30] Only left bank mid-range strata were included because no other spatial strata overlapped completely between the DIDSON and the split beam sonar.

During the early run, summing over all matching samples, there were 142 fish that exceeded the ELSD threshold of 3.1 units, 1.6 times as many as the 87 that exceeded the 75-cm DIDSON threshold. During the late run, there were 775 fish that exceeded the ELSD threshold of 3.1 units, which was also 1.6 times the DIDSON threshold.

DIDSON Estimates of Upstream Salmon Passage

Daily DIDSON estimates of upstream salmon passage for 48 days between 11 June and 4 August (Tables 12–13) were generally more than double the corresponding split-beam sonar estimates of upstream fish passage (Figure 26). This difference can be attributed partially to the greater ability of the DIDSON to distinguish individual fish migrating in dense schools, which was responsible for a 43% increase in daily estimates (Figure 26). In addition, the DIDSON was able to count and measure fish as close as 3 m from the DIDSON transducer, compared to 10 m (left bank) or 15 m (right bank) from the split-beam transducer, yielding an additional 19 m of insonified range and an approximate 50% increase in total salmon passage estimates (Figure 26).

DIDSON Estimates of Chinook Salmon Passage

Daily proportions of upstream bound salmon that were Chinook salmon were estimated using a DIDSON-length (DL) mixture model (see DIDSON length mixture model estimates of species composition in Methods section) for 48 days between 11 June and 4 August, totaling 15 days in the early run and 33 days in the late run (Tables 12–13). These proportions, which ranged from 1.2% on 28 July to 20.5% on 4 July, were multiplied by DIDSON estimates of upstream salmon passage to produce DIDSON estimates of upstream Chinook salmon passage (Tables 12–13). The DL mixture model also produced daily estimates of Chinook salmon age composition (Tables 14–15). These estimates incorporated length information from DIDSON as well from inriver gillnet catches.

DIDSON-length Threshold Large Fish Passage Estimates

"Threshold" estimates of fish equal or exceeding DIDSON lengths of 75 cm, 80 cm, and 90 cm were produced for 15 days in the early run and 33 days in the late run (Appendices M1–M2). A DIDSON length of 90 cm corresponds approximately[31] to the boundary between age-5 and age-6 Chinook salmon.[32]

DIDSON-equivalent Estimates of Chinook Salmon Passage

By fitting a daily abundance model (see Daily DIDSON-equivalent estimates of Chinook salmon passage in Methods section) to DIDSON-length mixture model estimates (DLMM), DIDSON-length threshold estimates (DLT), net-apportioned split-beam estimates (NASB), and catch rate in the RM-8.5 netting project (NCPUE), "DIDSON-equivalent" (DSEQ) estimates were generated for the 39 days (31 of 46 early-run days and 8 of 41 late-run days) when DLMM estimates were not available. Relationships of the three abundance indices DLT, NASB, and NCPUE to DLMM were non-stationary, and inclusion of an AR(1) term in the model provided much improved predictive ability (Appendices N3–N4). Daily DSEQ estimates summed to 3,124 (CV = 0.18) Chinook salmon for the early run and 2,241 (CV = 0.15) Chinook salmon for the late run. Relative uncertainty of individual daily DSEQ estimates ranged from

31 But recall the potential pitfalls of using thresholds when fish size overlaps between (age) categories (see Mixture Models versus Thresholds in Methods section).

32 Ages are total age from spawning event to spawning migration.

CV = 0.15 (5 August) to 0.71 (18 May). The greatest absolute uncertainty (SE = 138) associated with a daily DSEQ estimate occurred on 5 June (Tables 12–13).

Estimates of Midriver Chinook Salmon Passage

DIDSON-based estimates of total upstream Chinook salmon passage, produced by summing daily DIDSON-based (DSMM or DSEQ) estimates, were 5,874 (SE 645) Chinook salmon during the early run (16 May – 30 June) and 18,401 (SE 698) during the late run (1 July–10 August; Tables 12 and 13). Reconstructed (DSEQ) estimates comprised 53% and 12% of the total upstream Chinook salmon passage, and 79% and 20% of the variance for the early and late runs, respectively. These DIDSON-based estimates are germane to a midriver water column located between, and at least 3 m from, the transducers at RM 8.5. They supplant the preliminary numbers reported by Fleischman and McKinley (2013: Table 4) and McKinley and Fleischman (2013: Table 5).

DISCUSSION AND RECOMMENDATIONS

Deployment of DIDSON on both banks of the Kenai River in 2010 provided the most extensive opportunity to date to obtain accurate assessments of Chinook salmon passage in the Kenai River and to evaluate the validity of comparable split-beam estimates. Key conclusions from the 2010 season were as follows:

1) *Chinook salmon comprised only a small proportion of fish in the Kenai River, even in midriver.* Using a DIDSON length of 75 cm as a cutoff between large Chinook salmon and all other salmon, only 7.4% and 3.6% of fish measured during the early and late runs, respectively, were classified as large Chinook salmon (derived from values in Appendices M1–M2 and Tables 12–13). Chinook salmon of all sizes, as estimated by the DIDSON-length mixture model (DLMM), comprised 12.1% (early run) and 4.8% (late run) of upstream bound salmon (derived from values in Tables 12–13). The largest daily proportion of Chinook salmon from the DLMM was 21% (on 4 July; Table 13). Thus, fish swimming midriver between the RM-8.5 sonar transducers in 2010 were composed overwhelmingly of sockeye salmon and other small salmon.

2) *Large Chinook salmon were well-mixed with smaller salmon in space and time.* According to DIDSON length measurement data, large Chinook salmon were interspersed throughout the sampled range, and were only mildly clustered in space or time (Appendices K1–K5). Small (presumably mostly sockeye) salmon did not consistently exhibit schooling behavior and their migration past the sonar site was not restricted to discrete time periods. No combination of bank, range stratum, and tide stage harbored more than 16% large Chinook salmon in 2010 (Table 11). When samples were classified according to whether or not they were censored from the TS-based estimates, both censored and non-censored samples contained over 90% small fish (not shown). Thus it is not feasible to isolate Chinook salmon from other salmon by censoring data based on range or time criteria.

3) *The target strength threshold of −28 dB was ineffective at distinguishing between large and small salmon.* In matched split-beam sonar and DIDSON samples, 6 to 8 times as many fish exceeded the TS threshold of −28 dB as exceeded the DIDSON

length of 75 cm, indicating that many small fish are misclassified as large Chinook salmon using TS methodology (Appendices L1–L2). This explains why the TS-based split-beam estimates of Chinook salmon abundance were too high compared to DIDSON estimates. For the 48 days when DIDSON and TS-based estimates were both available, the TS-based estimates were 2.7 times higher (derived from values in Tables 8–9 and 12–13).[33]

4) *The ELSD-based split-beam estimates of Chinook salmon abundance were higher than DIDSON estimates in 2010*. For the 48 days when DIDSON and ELSD-based estimates were both available, the ELSD-based estimates of Chinook salmon abundance were 1.9 times higher, despite being germane to a smaller spatial subset of the river cross-section (see DIDSON Estimates of Upstream Salmon Passage in Results section; Figure 26). These results contrast with those of 2009, when ELSD- and DIDSON-based estimates were nearly equal for comparable dates and spatial strata (Miller et al. 2012). The reason for the difference between estimates for 2009 and 2010 is unknown. Potential factors include 1) large numbers of small fish in midriver (the split-beam estimate of 187,553 upstream bound fish in midriver was the largest of the 9 years that this estimate has been recorded), 2) very small fractions of large Chinook salmon during some portions of the run (small Chinook salmon fractions: Tables 12–13; small age-6+ fractions: Tables 14–15; also Appendices M1–M2), and 3) greater than expected variability in the relationship between ELSD and fish length (not shown).

5) *Substantial numbers of large Chinook salmon migrated in the stratum nearest the right-bank transducer.* With split-beam sonar, it is not possible to count or estimate the size of close-range fish, thus the DIDSON permits monitoring a larger proportion of the river without moving the transducers. In 2010, 33% (early run) and 25% (late run) large Chinook salmon (DL $\geq$ 75 cm) migrated in the stratum nearest shore (calculated from Table 10), and during the early run, large Chinook salmon comprised similar or greater proportions of total salmon in nearshore strata than in offshore strata (Table 11). This finding suggests that some Chinook salmon may migrate near shore undetected by the split-beam sonar and unsampled by the nets, even though earlier studies using the DIDSON had failed to detect them (unpublished data).[34]

6) *Using DIDSON estimates as a standard for comparison, other Chinook salmon abundance measures were of varying similarity in 2010.* TS-based estimates of Chinook salmon were consistently higher than DIDSON estimates, as were ELSD-based estimates for most of 2010 (Figure 27), which is not surprising given the comparison between matched split-beam sonar and DIDSON data (see Matched-sample Comparison of DIDSON and Split-beam Data in Results section). Although sockeye salmon were most abundant during mid-July (RM-19 sockeye sonar; Figure 28), the DIDSON detected significant numbers of small salmon migrating midriver at

[33] This ratio would have been even higher had not some samples with evidence of abundant sockeye salmon been excluded.

[34] This finding is also consistent with 2010 Funny River weir counts, which were seemingly too high to be explained by 2010 DIDSON estimates of Chinook salmon passage.

RM 8.5 during most of the season (Appendices K1–K5). Daily catch rates in the nets and net-apportioned split-beam sonar estimates tracked DLMM estimates well enough (Figures 27, 28, 29) to enable reconstruction of DIDSON-equivalent estimates for days without DIDSON data (Appendices N1–N3). However the relationships of these indices to DLMM were not constant and there were periods of time when agreement was poor (Figures 28–29). These potential shortcomings will be important to consider when interpreting historical data.

RECOMMENDATIONS

Produce DIDSON-based estimates on a regular basis and supply to fishery managers. Mixture model estimates based on DIDSON-measured fish lengths appear to be a viable long-term solution for assessing Kenai River Chinook salmon in the presence of more numerous sockeye salmon. Many of the logistical requirements for such an assessment have now been successfully worked out. New escapement goals based on these more reliable estimates of abundance will be required.

Discontinue producing TS-based estimates. Comparisons of TS-based estimates with DIDSON estimates and other indices of Chinook salmon abundance show that the assumptions underpinning TS-based estimates of Chinook salmon abundance are not valid. The inability of TS and range to exclude sockeye salmon can result in overestimating Chinook salmon abundance by large and unpredictable amounts. Daily TS-based estimates often diverged greatly from other indices for extended periods of time (Figure 27), and the late-run 2010 TS-based estimate was the second highest since 2002 for a run that, according to other measures, was one of the smallest (Fleischman and McKinley 2013).

Continue to operate the inriver netting project in the same standardized protocol as has been practiced since 2002. Consistent data produced by this project may prove to be highly valuable for reconstructing historical abundance.

Investigate the possibility of Chinook salmon migrating upstream in blind spots behind the usual transducer placements. DIDSON detected substantial numbers of Chinook salmon in the range strata nearest the transducers, which cannot be sampled by split-beam sonar.[35] Thus the conventional assumption that nearly all Chinook salmon swim in midriver may no longer be credible. The 2010 data suggest that Chinook salmon are more likely to migrate close to the left bank shore than to the right (Figure 24). Additional investigation is contingent upon availability of a third DIDSON for placement closer to shore.

Closely scrutinize ELSD estimates in 2011. Although ELSD-based estimates remain a large improvement over TS-based estimates (Miller et al. 2012), they failed to track DIDSON estimates in 2010 as well as they had in 2009, indicating that they may not provide reliable information under all conditions.

---

[35] Except for 10–13 m from the left bank transducer.

ACKNOWLEDGEMENTS

We would like to thank Mark Jensen for his assistance in overseeing the day-to-day operation of the project, for providing computer programming and networking support, and for his assistance in processing and analyzing the data. We would also like to thank Mike Hopp, Kara Bethune, Brandon Key, and Gabe Cazares for meticulously collecting the sonar data and for their high level of motivation throughout the long field season. Trevor Davis and Don Eide spent many hours processing DIDSON data and collecting fish image measurements. We would like to express our gratitude to Melissa Brown with Hi-Lo Charters for allowing us to use her dock for project deployment and breakdown. Finally, thanks to Division of Sport Fish staff in Soldotna who provided logistical support throughout the season.

REFERENCES CITED

Alexandersdottir, M., and L. Marsh. 1990. Abundance estimates of the escapement of Chinook salmon into the Kenai River, Alaska, by analysis of tagging data, 1989. Alaska Department of Fish and Game, Fishery Data Series No. 90-55, Anchorage. http://www.adfg.alaska.gov/FedAidPDFs/fds90-55.pdf

Benke, A. C., and C. E. Cushing. 2005. Rivers of North America. Elsevier Academic Press, Burlington, Massachusetts.

Bernard, D. R., and P. A. Hansen. 1992. Mark-recapture experiments to estimate the abundance of fish: a short course given by the Division of Sport Fish, Alaska Department of Fish and Game in 1991. Alaska Department of Fish and Game, Special Publication No. 92-4, Anchorage. http://www.adfg.alaska.gov/FedAidPDFs/sp92-04.pdf

Bosch, D., and D. Burwen. 1999. Estimates of Chinook salmon abundance in the Kenai River using split-beam sonar, 1997. Alaska Department of Fish and Game, Fishery Data Series No. 99-3, Anchorage. http://www.adfg.alaska.gov/FedAidPDFs/fds99-03.pdf

Bosch, D., and D. Burwen. 2000. Estimates of Chinook salmon abundance in the Kenai River using split-beam sonar, 1998. Alaska Department of Fish and Game, Fishery Data Series No. 00-12, Anchorage. http://www.adfg.alaska.gov/FedAidPDFs/fds00-12.pdf

Burger, C. V., R. L. Wilmot, and D. B. Wangaard. 1985. Comparison of spawning areas and times for two runs of Chinook salmon (*Oncorhynchus tshawytscha*) in the Kenai River, Alaska. Canadian Journal of Fisheries and Aquatic Sciences 42(4):693-700.

Burwen, D., and D. Bosch. 1998. Estimates of Chinook salmon abundance in the Kenai River using split-beam sonar, 1996. Alaska Department of Fish and Game, Fishery Data Series No. 98-2, Anchorage. http://www.adfg.alaska.gov/FedAidPDFs/fds98-02.pdf

Burwen, D., J. Hasbrouck, and D. Bosch. 2000. Investigations of alternate sites for Chinook salmon sonar on the Kenai River. Alaska Department of Fish and Game, Fishery Data Series No. 00-43, Anchorage. http://www.adfg.alaska.gov/FedAidPDFs/fds00-43.pdf

Burwen, D. L., and D. E. Bosch. 1995a. Estimates of Chinook salmon abundance in the Kenai River using dual-beam sonar, 1993. Alaska Department of Fish and Game, Fishery Data Series No. 95-31, Anchorage. http://www.adfg.alaska.gov/FedAidPDFs/fds95-31.pdf

Burwen, D. L., and D. E. Bosch. 1995b. Estimates of Chinook salmon abundance in the Kenai River using dual-beam sonar, 1994. Alaska Department of Fish and Game, Fishery Data Series No. 95-38, Anchorage. http://www.adfg.alaska.gov/FedAidPDFs/fds95-38.pdf

Burwen, D. L., and D. E. Bosch. 1996. Estimates of Chinook salmon abundance in the Kenai River using split-beam sonar, 1995. Alaska Department of Fish and Game, Fishery Data Series No. 96-9, Anchorage. http://www.adfg.alaska.gov/FedAidPDFs/fds96-09.pdf

Burwen, D. L., D. E. Bosch, and S. J. Fleischman. 1995. Evaluation of hydroacoustic assessment techniques for Chinook salmon on the Kenai River using split- beam sonar. Alaska Department of Fish and Game, Fishery Data Series No. 95-45, Anchorage. http://www.adfg.alaska.gov/FedAidPDFs/fds95-45.pdf

Burwen, D. L., D. E. Bosch, and S. J. Fleischman. 1998. Evaluation of hydroacoustic assessment techniques for Chinook salmon on the Kenai River, 1995. Alaska Department of Fish and Game, Fishery Data Series No. 98-3, Anchorage. http://www.adfg.alaska.gov/FedAidPDFs/fds98-03.pdf

Burwen, D. L., and S. J. Fleischman. 1998. Evaluation of side-aspect target strength and pulse width as hydroacoustic discriminators of fish species in rivers. Canadian Journal of Fisheries and Aquatic Sciences 55(11):2492-2502.

Burwen, D. L., S. J. Fleischman, and J. D. Miller. 2007. Evaluation of a dual-frequency imaging sonar for estimating fish size in the Kenai River. Alaska Department of Fish and Game, Fishery Data Series No. 07 44, Anchorage. http://www.adfg.alaska.gov/FedAidPDFs/fds07-44.pdf

REFERENCES CITED (Continued)

Burwen, D. L., S. J. Fleischman, and J. D. Miller. 2010. Accuracy and precision of manual fish length measurements from DIDSON sonar images. Transactions of the American Fisheries Society, 139:1306-1314.

Burwen, D. L., S. J. Fleischman, J. D. Miller, and M. E. Jensen. 2003. Time-based signal characteristics as predictors of fish size and species for a side-looking hydroacoustic application in a river. ICES Journal of Marine Science 60:662-668.

Carlon, J. A., and M. Alexandersdottir. 1989. Abundance estimates of the escapement of Chinook salmon into the Kenai River, Alaska, by analysis of tagging data, 1988. Alaska Department of Fish and Game, Fishery Data Series No. 107, Juneau. http://www.adfg.alaska.gov/FedAidPDFs/fds-107.pdf

Cochran, W. G. 1977. Sampling techniques. 3rd edition. John Wiley and Sons, New York.

Conrad, R. H. 1988. Abundance estimates of the escapement of Chinook salmon into the Kenai River, Alaska, by analysis of tagging data, 1987. Alaska Department of Fish and Game, Fishery Data Series No. 67, Juneau. http://www.adfg.alaska.gov/FedAidPDFs/fds-067.pdf

Conrad, R. H., and L. L. Larson. 1987. Abundance estimates for Chinook salmon (*Oncorhynchus tshawytscha*) in the escapement into the Kenai River, Alaska, by analysis of tagging data, 1986. Alaska Department of Fish and Game, Fishery Data Series No. 34, Juneau. http://www.adfg.alaska.gov/FedAidPDFs/fds-034.pdf

Eggers, D. M. 1994. On the discrimination of sockeye and Chinook salmon in the Kenai River based on target strength determination with 420 kHz dual-beam sonar. Alaska Fishery Research Bulletin 1(2):125-139. http://www.adfg.alaska.gov/FedAidpdfs/AFRB.01.2.125-139.pdf

Eggers, D. M., P. A. Skvorc II, and D. L. Burwen. 1995. Abundance estimates of Chinook salmon in the Kenai River using dual-beam sonar. Alaska Fishery Research Bulletin 2(1):1-22. http://www.adfg.alaska.gov/FedAidpdfs/AFRB.02.1.001-022.pdf

Ehrenberg, J. E. 1983. A review of *in situ* target strength estimation techniques. FAO (Food and Agriculture Organization of the United Nations) Fisheries Report 300:85-90.

Eskelin, A. 2007. Chinook salmon creel survey and inriver gillnetting study, lower Kenai River, Alaska, 2005. Alaska Department of Fish and Game, Fishery Data Series No. 07-87, Anchorage. http://www.adfg.alaska.gov/FedAidPDFs/fds07-87.pdf

Eskelin, A. 2010. Chinook salmon creel survey and inriver gillnetting study, lower Kenai River, Alaska, 2007. Alaska Department of Fish and Game, Fishery Data Series No. 10-63, Anchorage. http://www.adfg.alaska.gov/FedAidpdfs/FDS10-63.pdf

Fleischman, S. J., and D. L. Burwen. 2003. Mixture models for the species apportionment of hydroacoustic data, with echo-envelope length as the discriminatory variable. ICES Journal of Marine Science 60:592-598.

Fleischman, S. J., and T. R. McKinley. 2013. Run reconstruction, spawner–recruit analysis, and escapement goal recommendation for late-run Chinook salmon in the Kenai River. Alaska Department of Fish and Game, Fishery Manuscript Series No. 13-02, Anchorage. http://www/adfg/alaska.gov/FedAidpdfs/FMS13-02

Foote, K. G., and D. N. MacLennan. 1984. Comparison of copper and tungsten carbide calibration spheres. Journal of the Acoustical Society of America 75:612-616.

Gamblin, M., L. E. Marsh, P. Berkhahn, and S. Sonnichsen. 2004. Area management report for the recreational fisheries of the Northern Kenai Peninsula, 2000 and 2001. Alaska Department of Fish and Game, Fishery Management Report No. 04-04, Anchorage. http://www.adfg.alaska.gov/FedAidPDFs/fmr04-04.pdf

Gelman, A., J. B. Carlin, H. S. Stern, and D. B. Rubin. 2004. Bayesian data analysis. 3rd edition. Chapman and Hall, Boca Raton, Florida.

Gilks, W. R., A. Thomas, and D. J. Spiegelhalter. 1994. A language and program for complex Bayesian modeling. The Statistician 43:169-178. http://www.mrc-bsu.cam.ac.uk/bugs Accessed 01/2010.

Goodman, L. A. 1960. On the exact variance of products. Journal of the American Statistical Association 55:708-713.

REFERENCES CITED (Continued)

Hammarstrom, S. L., and J. J. Hasbrouck. 1998. Estimation of the abundance of late-run Chinook salmon in the Kenai River based on exploitation rate and harvest, 1996. Alaska Department of Fish and Game, Fishery Data Series No. 98-6, Anchorage. http://www.adfg.alaska.gov/FedAidPDFs/fds98-06.pdf

Hammarstrom, S. L., and J. J. Hasbrouck. 1999. Estimation of the abundance of late-run Chinook salmon in the Kenai River based on exploitation rate and harvest, 1997. Alaska Department of Fish and Game, Fishery Data Series No. 99-8, Anchorage. http://www.adfg.alaska.gov/FedAidPDFs/fds99-08.pdf

Hammarstrom, S. L., L. Larson, M. Wenger, and J. Carlon. 1985. Kenai Peninsula Chinook and coho salmon studies. Alaska Department of Fish and Game. Federal Aid in Fish Restoration. Annual Performance Report, 1984-1985, Project F-9-17(26)G-II-L, Juneau. http://www.adfg.alaska.gov/FedAidPDFs/FREDf-9-17(26)G-II-L.pdf

Hammarstrom, S. L., and L. L. Larson. 1986. Cook Inlet Chinook and coho salmon studies. Alaska Department of Fish and Game. Federal Aid in Fish Restoration, Annual Performance Report, 1985-1986, Project F-9-18, 27 (G-32-1,2,4,5), Juneau.

Howe, A. L., G. Fidler, A. E. Bingham, and M. J. Mills. 1996. Harvest, catch, and participation in Alaska sport fisheries during 1995. Alaska Department of Fish and Game, Fishery Data Series No. 96-32, Anchorage. http://www.adfg.alaska.gov/FedAidPDFs/fds96-32.pdf

Howe, A. L., G. Fidler, and M. J. Mills. 1995. Harvest, catch, and participation in Alaska sport fisheries during 1994. Alaska Department of Fish and Game, Fishery Data Series No. 95-24, Anchorage. http://www.adfg.alaska.gov/FedAidPDFs/fds95-24.pdf

Howe, A. L., R. J. Walker, C. Olnes, K. Sundet, and A. E. Bingham. 2001a. Revised Edition. Harvest, catch, and participation in Alaska sport fisheries during 1996. Alaska Department of Fish and Game, Fishery Data Series No. 97-29 (revised), Anchorage. http://www.adfg.alaska.gov/FedAidPDFs/fds97-29(revised).pdf

Howe, A. L., R. J. Walker, C. Olnes, K. Sundet, and A. E. Bingham. 2001b. Revised Edition. Harvest, catch, and participation in Alaska sport fisheries during 1997. Alaska Department of Fish and Game, Fishery Data Series No. 98-25 (revised), Anchorage. http://www.adfg.alaska.gov/FedAidPDFs/fds98-25(revised).pdf

Howe, A. L., R. J. Walker, C. Olnes, K. Sundet, and A. E. Bingham. 2001c. Revised Edition. Participation, catch, and harvest in Alaska sport fisheries during 1998. Alaska Department of Fish and Game, Fishery Data Series No. 99-41 (revised), Anchorage. http://www.adfg.alaska.gov/FedAidPDFs/fds99-41(revised).pdf

Howe, A. L., R. J. Walker, C. Olnes, K. Sundet, and A. E. Bingham. 2001d. Participation, catch, and harvest in Alaska sport fisheries during 1999. Alaska Department of Fish and Game, Fishery Data Series No. 01-08, Anchorage. http://www.adfg.alaska.gov/FedAidPDFs/fds01-08.pdf

HTI (Hydroacoustic Technology Inc.). 1996. Model 340 digital echo processor (split-beam) operator's manual, version 1.6 Hydroacoustic Technology Inc., Seattle.

HTI (Hydroacoustic Technology Inc.). 1997. Model 241/243/244 split-beam digital echo sounder system operator's manual, version 1.6. Hydroacoustic Technology Inc., Seattle.

HTI (Hydroacoustic Technology Inc.). 2009. Transducer calibration for HTI Model 244 split-beam system, March 30, 2009. Report of Hydroacoustic Technology, Inc. to Alaska Department of Fish and Game, Sport Fish Division, Anchorage.

Jennings, G. B., K. Sundet, and A. E. Bingham. 2007. Participation, catch, and harvest in Alaska sport fisheries during 2004. Alaska Department of Fish and Game, Fishery Data Series No. 07-40, Anchorage. http://www.adfg.alaska.gov/FedAidPDFs/fds07-40.pdf

Jennings, G. B., K. Sundet, and A. E. Bingham. 2009a. Estimates of participation, catch, and harvest in Alaska sport fisheries during 2005. Alaska Department of Fish and Game, Fishery Data Series No. 09-47, Anchorage. http://www.adfg.alaska.gov/FedAidPDFs/FDS09-47.pdf

Jennings, G. B., K. Sundet, and A. E. Bingham. 2009b. Estimates of participation, catch, and harvest in Alaska sport fisheries during 2006. Alaska Department of Fish and Game, Fishery Data Series No. 09-54, Anchorage. http://www.adfg.alaska.gov/FedAidPDFs/FDS09-54.pdf

Jennings, G. B., K. Sundet, and A. E. Bingham. 2010a. Estimates of participation, catch, and harvest in Alaska sport fisheries during 2007. Alaska Department of Fish and Game, Fishery Data Series No. 10-02, Anchorage. http://www.adfg.alaska.gov/FedAidpdfs/Fds10-02.pdf

Jennings, G. B., K. Sundet, and A. E. Bingham. 2010b. Estimates of participation, catch, and harvest in Alaska sport fisheries during 2008. Alaska Department of Fish and Game, Fishery Data Series No. 10-22, Anchorage. http://www.adfg.alaska.gov/FedAidpdfs/FDS10-22.pdf

Jennings, G. B., K. Sundet, and A. E. Bingham. 2011. Estimates of participation, catch, and harvest in Alaska sport fisheries during 2009. Alaska Department of Fish and Game, Fishery Data Series No. 11-45, Anchorage. http://www.adfg.alaska.gov/FedAidpdfs/FDS11-45

Jennings, G. B., K. Sundet, A. E. Bingham, and D. Sigurdsson. 2004. Participation, catch, and harvest in Alaska sport fisheries during 2001. Alaska Department of Fish and Game, Fishery Data Series No. 04-11, Anchorage. http://www.adfg.alaska.gov/FedAidPDFs/fds04-11.pdf

Jennings, G. B., K. Sundet, A. E. Bingham, and D. Sigurdsson. 2006a. Participation, catch, and harvest in Alaska sport fisheries during 2002. Alaska Department of Fish and Game, Fishery Data Series No. 06-34, Anchorage. http://www.adfg.alaska.gov/FedAidpdfs/fds06-34.pdf

Jennings, G. B., K. Sundet, A. E. Bingham, and D. Sigurdsson. 2006b. Participation, catch, and harvest in Alaska sport fisheries during 2003. Alaska Department of Fish and Game, Fishery Data Series No. 06-44, Anchorage. http://www.adfg.alaska.gov/FedAidpdfs/fds06-44.pdf

Lunn, D., D. Spiegelhalter, A. Thomas, and N. Best. 2009. The BUGS project: Evolution, critique and future directions. Statistics in Medicine 28(25):3049-3067.

MacLennan, D. N., and E. J. Simmonds. 1992. Fisheries acoustics. Chapman & Hall, London.

Marsh, L. E. 2000. Angler effort and harvest of Chinook salmon by the recreational fisheries in the lower Kenai River, 1998. Alaska Department of Fish and Game, Fishery Data Series No. 00-21, Anchorage. http://www.adfg.alaska.gov/FedAidPDFs/fds00-21.pdf

McBride, D. N., M. Alexandersdottir, S. Hammarstrom, and D. Vincent-Lang. 1989. Development and implementation of an escapement goal policy for the return of Chinook salmon to the Kenai River. Alaska Department of Fish and Game, Fishery Manuscript No. 8, Juneau. http://www.adfg.alaska.gov/FedAidPDFs/fms-008.pdf

McKinley, T. R., and S. J. Fleischman. 2013. Run reconstruction, spawner–recruit analysis, and escapement goal recommendation for early-run Chinook salmon in the Kenai River. Alaska Department of Fish and Game, Fishery Manuscript Series No. 13-03, Anchorage. http://www.adfg.alaska.gov/FedAidPDFs/FMS13-03.pdf

Miller, J. D., D. Bosch, and D. Burwen. 2002. Estimates of Chinook salmon abundance in the Kenai River using split-beam sonar, 1999. Alaska Department of Fish and Game, Fishery Data Series No. 02-24, Anchorage. http://www.adfg.alaska.gov/FedAidPDFs/fds02-24.pdf

Miller, J. D., and D. Burwen. 2002. Estimates of Chinook salmon abundance in the Kenai River using split-beam sonar, 2000. Alaska Department of Fish and Game, Fishery Data Series No. 02-09, Anchorage. http://www.adfg.alaska.gov/FedAidPDFs/fds02-09.pdf

Miller, J. D., D. L. Burwen, and S. J. Fleischman. 2003. Estimates of Chinook salmon abundance in the Kenai River using split-beam sonar, 2001. Alaska Department of Fish and Game, Fishery Data Series No. 03-03, Anchorage. http://www.adfg.alaska.gov/FedAidPDFs/fds03-03.pdf

Miller, J. D., D. L. Burwen, and S. J. Fleischman. 2004. Estimates of Chinook salmon abundance in the Kenai River using split-beam sonar, 2002. Alaska Department of Fish and Game, Fishery Data Series No. 04-29, Anchorage. http://www.adfg.alaska.gov/FedAidPDFs/fds04-29.pdf

Miller, J. D., D. L. Burwen, and S. J. Fleischman. 2005. Estimates of Chinook salmon abundance in the Kenai River using split-beam sonar, 2003. Alaska Department of Fish and Game, Fishery Data Series No. 05-59, Anchorage. http://www.adfg.alaska.gov/FedAidPDFs/fds05-59.pdf

Miller, J. D., D. L. Burwen, and S. J. Fleischman. 2007a. Estimates of Chinook salmon abundance in the Kenai River using split-beam sonar, 2004. Alaska Department of Fish and Game, Fishery Data Series No. 07-57, Anchorage. http://www.adfg.alaska.gov/FedAidPDFs/fds07-57.pdf

Miller, J. D., D. L. Burwen, and S. J. Fleischman. 2007b. Estimates of Chinook salmon abundance in the Kenai River using split-beam sonar, 2005. Alaska Department of Fish and Game, Fishery Data Series No. 07-92, Anchorage. http://www.adfg.alaska.gov/FedAidpdfs/Fds07-92.pdf

Miller, J. D., D. L. Burwen, and S. J. Fleischman. 2010. Estimates of Chinook salmon passage in the Kenai River using split-beam sonar, 2006. Alaska Department of Fish and Game, Fishery Data Series No. 10-40, Anchorage. http://www.adfg.alaska.gov/FedAidpdfs/FDS10-40.pdf

Miller, J. D., D. L. Burwen, and S. J. Fleischman. 2011. Estimates of Chinook salmon passage in the Kenai River using split-beam sonar, 2007. Alaska Department of Fish and Game, Fishery Data Series No. 11-52, Anchorage. http://www.adfg.alaska.gov/FedAidpdfs/FDS11-52

Miller, J. D., D. L. Burwen, and S. J. Fleischman. 2012. Estimates of Chinook salmon passage in the Kenai River using split-beam sonar, 2008-2009. Alaska Department of Fish and Game, Fishery Data Series No. 12-73, Anchorage. http://www.adfg.alaska.gov/FedAidPDFs/FDS12-73.pdf

Mills, M. J. 1979. Alaska statewide sport fish harvest studies. Alaska Department of Fish and Game, Federal Aid in Fish Restoration, Annual Performance Report 1978-1979, Project F-9-11(20)SW-I-A, Juneau. http://www.adfg.alaska.gov/FedAidPDFs/FREDf-9-11(20)SW-I-A.pdf

Mills, M. J. 1980. Alaska statewide sport fish harvest studies. Alaska Department of Fish and Game. Federal Aid in Fish Restoration, Annual Performance Report, 1979-1980, Project F-9-12(21) SW-I-A, Juneau. http://www.adfg.alaska.gov/FedAidPDFs/FREDf-9-12(21)SW-I-A.pdf

Mills, M. J. 1981a. Alaska statewide sport fish harvest studies. 1979 data. Alaska Department of Fish and Game, Federal Aid in Fish Restoration, Annual Performance Report 1980-1981, Project F-9-13(22a)SW-I-A, Juneau. http://www.adfg.alaska.gov/FedAidPDFs/FREDf-9-13(22a)SW-I-A.pdf

Mills, M. J. 1981b. Alaska statewide sport fish harvest studies. 1980 data. Alaska Department of Fish and Game, Federal Aid in Fish Restoration, Annual Performance Report 1980-1981, Project F-9-13(22b)SW-I-A, Juneau. http://www.adfg.alaska.gov/FedAidPDFs/FREDf-9-13(22b)SW-I-A.pdf

Mills, M. J. 1982. Alaska statewide sport fish harvest studies. Alaska Department of Fish and Game, Federal Aid in Fish Restoration, Annual Performance Report 1981-1982, Project F-9-14(23)SW-I-A, Juneau. http://www.adfg.alaska.gov/FedAidPDFs/FREDf-9-14(23)SW-I-A.pdf

Mills, M. J. 1983. Alaska statewide sport fish harvest studies. Alaska Department of Fish and Game, Federal Aid in Fish Restoration, Annual Performance Report 1982-1983, Project F-9-15(24)SW-I-A, Juneau. http://www.adfg.alaska.gov/FedAidPDFs/FREDf-9-15(24)SW-I-A.pdf

Mills, M. J. 1984. Alaska statewide sport fish harvest studies. Alaska Department of Fish and Game, Federal Aid in Fish Restoration, Annual Performance Report 1983-1984, Project F-9-16(25)SW-I-A, Juneau. http://www.adfg.alaska.gov/FedAidPDFs/FREDf-9-16(25)SW-I-A.pdf

Mills, M. J. 1985. Alaska statewide sport fish harvest studies. Alaska Department of Fish and Game, Federal Aid in Fish Restoration, Annual Performance Report 1984-1985, Project F-9-17(26)SW-I-A, Juneau. http://www.adfg.alaska.gov/FedAidPDFs/FREDf-9-17(26)SW-I-A.pdf

Mills, M. J. 1986. Alaska statewide sport fish harvest studies. Alaska Department of Fish and Game, Federal Aid in Fish Restoration, Annual Performance Report 1985-1986, Project F-10-1(27)RT-2, Juneau. http://www.adfg.alaska.gov/FedAidPDFs/FREDf-10-1(27)RT-2.pdf

REFERENCES CITED (Continued)

Mills, M. J. 1987. Alaska statewide sport fisheries harvest report, 1986. Alaska Department of Fish and Game, Fishery Data Series No. 2, Juneau. http://www.adfg.alaska.gov/FedAidPDFs/fds-002.pdf

Mills, M. J. 1988. Alaska statewide sport fisheries harvest report, 1987. Alaska Department of Fish and Game, Fishery Data Series No. 52, Juneau. http://www.adfg.alaska.gov/FedAidPDFs/fds-052.pdf

Mills, M. J. 1989. Alaska statewide sport fisheries harvest report, 1988. Alaska Department of Fish and Game, Fishery Data Series No. 122, Juneau. http://www.adfg.alaska.gov/FedAidPDFs/fds-122.pdf

Mills, M. J. 1990. Harvest and participation in Alaska sport fisheries during 1989. Alaska Department of Fish and Game, Fishery Data Series No. 90-44, Anchorage. http://www.adfg.alaska.gov/FedAidPDFs/fds90-44.pdf

Mills, M. J. 1991. Harvest, catch, and participation in Alaska sport fisheries during 1990. Alaska Department of Fish and Game, Fishery Data Series No. 91-58, Anchorage. http://www.adfg.alaska.gov/FedAidPDFs/fds91-58.pdf

Mills, M. J. 1992. Harvest, catch, and participation in Alaska sport fisheries during 1991. Alaska Department of Fish and Game, Fishery Data Series No. 92-40, Anchorage. http://www.adfg.alaska.gov/FedAidPDFs/fds92-40.pdf

Mills, M. J. 1993. Harvest, catch, and participation in Alaska sport fisheries during 1992. Alaska Department of Fish and Game, Fishery Data Series No. 93-42, Anchorage. http://www.adfg.alaska.gov/FedAidPDFs/fds93-42.pdf

Mills, M. J. 1994. Harvest, catch, and participation in Alaska sport fisheries during 1993. Alaska Department of Fish and Game, Fishery Data Series No. 94-28, Anchorage. http://www.adfg.alaska.gov/FedAidPDFs/fds94-28.pdf

Mulligan, T. J., and R. Kieser. 1996. A split-beam echo-counting model for riverine use. International Council for the Exploration of the Sea Journal of Marine Science 53:403-406.

Pankratz, A. 1991. Forecasting with dynamic regression models. John Wiley and Sons, New York.

Perschbacher, J. 2012. Chinook salmon creel survey and inriver gillnetting study, lower Kenai River, Alaska, 2010. Alaska Department of Fish and Game, Fishery Data Series No. 12-75, Anchorage. http://www.adfg.alaska.gov/FedAidPDFs/FDS12-75.pdf

Reimer, A. 2004. Chinook salmon creel survey and inriver gillnetting study, lower Kenai River, Alaska, 2002. Alaska Department of Fish and Game, Fishery Data Series No. 04-28, Anchorage. http://www.adfg.alaska.gov/FedAidPDFs/fds04-28.pdf

Reimer, A. M., W. W. Jones, and L. E. Marsh. 2002. Chinook salmon creel survey and inriver gillnetting study, lower Kenai River, Alaska, 1999 and 2000. Alaska Department of Fish and Game, Fishery Data Series No. 02-25, Anchorage. http://www.adfg.alaska.gov/FedAidPDFs/fds02-25.pdf

Reynolds, J. H., C. A. Woody, N. E. Gove, and L. F. Fair. 2007. Efficiently estimating salmon escapement uncertainty using systematically sampled data. Pages 121-129 [*In*] C. A. Woody, editor. Sockeye salmon evolution, ecology, and management. American Fisheries Society, Symposium No. 54, Anchorage.

Simmonds, J., and D. MacLennan. 2005. Fisheries acoustics: theory and practice. 2nd edition. Blackwell Science, Ames, Iowa.

USDA (United States Department of Agriculture). 1992. Kenai River landowner's guide. Prepared by the U. S. Department of Agriculture, Soil conservation Service (SCS) for the Kenai Soil and Water Conservation District, Kenai, Alaska.

Walker, R. J., C. Olnes, K. Sundet, A. L. Howe, and A. E. Bingham. 2003. Participation, catch, and harvest in Alaska sport fisheries during 2000. Alaska Department of Fish and Game, Fishery Data Series No. 03-05, Anchorage. http://www.adfg.alaska.gov/FedAidPDFs/fds03-05.pdf

REFERENCES CITED (Continued)

Westerman, D. L., and T. M. Willette. 2011. Upper Cook Inlet salmon escapement studies, 2010. Alaska Department of Fish and Game, Fishery Data Series No. 11-66, Anchorage. http://www.adfg.alaska.gov/FedAidpdfs/FDS11-66

Wolter, K. M. 1985. Introduction to variance estimation. Springer-Verlag, New York.

WRCC (Western Region Climate Center). 2008. Kenai FAA Airport, Alaska. Website Western U.S. Climate Historical Summaries, Climatological Data Summaries, Alaska, accessed February 4, 2008. http://www.wrcc.dri.edu/cgi-bin/cliMAIN.pl?4546

TABLES

Table 1.–Main components of the split-beam sonar system used in 2010.

System component	Description
Sounder	Hydroacoustics Technology Inc. (HTI) Model 244 Split-Beam Echo sounder operating at 200 kHz
Data processing computer	Dell Dimension 2350 personal computer
Transducers	(2) HTI Split-Beam transducers: Left Bank: nominal beam widths: 2.9°×10.2° Right Bank: nominal beam widths: 2.8°×10.0°
Chart recorder	HTI model 403 digital dual-channel chart recorder
Oscilloscope	Nicolet model 310 digital storage oscilloscope
Video display	Hydroacoustic Assessments HARP-HC
Remote pan and tilt aiming controller	Remote Ocean Systems Model PTC-1 Pan and Tilt Controller
Remote pan and tilt aiming unit	Remote Ocean Systems Model PT-25 Remote Pan and Tilt Unit
Heading and angular measurement device	JASCO Research Ltd. AIM-2000 Underwater Measurement Device

Table 2.–Results of 2010 HTI and *in situ* calibration verifications using a 38.1-mm tungsten carbide standard sphere.

Transducer	Location	Date	Mean target strength (dB)	SD	*N*	Range (m)	Noise (mV)	Threshold (mV)
Right bank								
	HTI[a]	2 Dec 09	-38.6	0.2	542	6	N/A[b]	N/A[b]
	Kenai River	18 May 10	-38.7	1.96	526	12.9	150	175
	Kenai River	2 Aug 10	-38.7	1.89	774	13.6	150	175
Left bank								
	HTI[a]	3 Dec 09	-38.8	0.34	513	6	N/A[b]	N/A[b]
	Kenai River	18 May 10	-38.8	1.83	227	13.8	75	100
	Kenai River	2 Aug 10	-39.2	1.81	1,128	12.8	75	100

[a] Measurements taken at Hydroacoustic Technology Inc. facility during system calibration.

[b] Not available or not applicable.

Table 3.–Hydroacoustics Technology Inc. model 244 digital echo sounder settings used in 2010.

Echo sounder parameter	Value
Transmit power	25 dB
System gain (G_r)	−18 dB
TVG	$40\log_{10}R$
Transmitted pulse width	0.20 msec
Ping rate right bank	11 pings/sec
Ping rate left bank	16 pings/sec

Table 4.–Echo acceptance criteria for digital echo processing, 2010.

Bank	Pulse width[a] (ms) at −6 dB	Vertical angle off axis (°)	Horizontal angle off axis (°)	Threshold mV (dB)	Minimum range (m)
Right	0.04 to 10.0	–2.5 to 2.0	–5.0 to 5.0	706 (–35 dB)	2
Left	0.04 to 10.0	–2.5 to 2.0	–5.0 to 5.0	431 (–35 dB)	2

Note: criteria are for 16 May–4 Aug 2010.

[a] Pulse width filters have not been used since 1996 (Burwen and Bosch 1998) in order to retain information potentially useful for species classification (Burwen et al. 2003; Fleischman and Burwen 2003).

Table 5.–Components of the DIDSON sonar system used in 2010.

System component	Description
Sounder	DIDSON-LR operating at 1.2 MHz
Orientation sensor	Honeywell Truepoint Compass (internal)
Lens	Large Lens Assembly with ~3°×15° beam pattern
Data collection computer	Dell Latitude E6500 laptop computer
Remote pan-and-tilt aiming controller	Remote Ocean Systems Model PTC-1 Pan and Tilt Controller
Remote pan-and-tilt aiming unit	Remote Ocean Systems Model P-25 Remote Pan and Tilt Unit

Table 6.–Percentage of filtered split-beam targets by tide stage and direction of travel for the 2010 early run (16 May–30 June) and late run (1 July–4 August) at RM 8.5, Kenai River.

Run	Direction of travel		Tide stage: Rising	Falling	Low	Total
Early						
	Upstream					
		Row %	17.3%	63.7%	19.0%	100.0%
		Column %	97.6%	98.3%	98.0%	98.1%
	Downstream					
		Row %	21.7%	57.8%	20.5%	100.0%
		Column %	2.4%	1.7%	2.0%	1.9%
Late						
	Upstream					
		Row %	17.8%	55.1%	27.2%	100.0%
		Column %	99.2%	98.8%	98.5%	98.8%
	Downstream					
		Row %	11.4%	53.9%	34.8%	100.0%
		Column %	0.8%	1.2%	1.5%	1.2%

Note: results for test of independence for early run was $\chi^2 = 4.44$, df = 2, $P = 0.11$, and for late run was $\chi^2 = 25.50$, df = 2, $P < 0.01$.

Note: Data have been filtered by range (distance from transducer) and target strength criteria.

Table 7.–Percentage of filtered split-beam targets by riverbank and direction of travel for the 2010 early (16 May–30 June) and late run (1 July–4 August) at RM 8.5, Kenai River.

Run	Bank		Direction of travel: Upstream	Downstream	Upstream and downstream
Early					
	Right bank		43%	71%	44%
	Left bank		57%	29%	56%
		Total	100%	100%	100%
Late					
	Right bank		54%	62%	54%
	Left bank		46%	38%	46%
		Total	100%	100%	100%

Table 8.–Estimated upstream fish passage based on split-beam sonar (all species; internally termed "unfiltered" estimates), TS-based split-beam sonar (Chinook only), ELSD-based (these were termed "behavior-censored ELSD-based estimates" in a previous report [Miller et al. 2012]), split-beam sonar (Chinook only), and net-apportioned split-beam sonar (Chinook only), Kenai River RM 8.5, early run, 2010.

	Upstream Fish		TS-based		ELSD-based		Net Apportioned	
Date	Passage	SE	Passage	SE	Passage	SE	Passage	SE
16 May	45	14	32	9	22	7	26	18
17 May	63	25	39	19	31	15	0	0
18 May	64	21	41	19	32	14	0	0
19 May	111	24	75	17	55	20	111	24
20 May	58	15	40	12	29	11	41	14
21 May	42	8	27	7	21	7	0	0
22 May	105	12	51	10	52	17	25	19
23 May	45	14	36	13	15	9	9	6
24 May	69	12	48	8	21	10	0	0
25 May	75	10	57	8	32	11	11	13
26 May	69	11	69	11	27	11	24	13
27 May	66	15	60	12	27	13	16	12
28 May	37	12	28	10	13	7	15	6
29 May	42	11	36	10	13	6	28	15
30 May	39	9	36	8	15	7	9	7
31 May	36	10	24	9	7	6	7	5
1 Jun	42	8	25	7	13	7	0	0
2 Jun	30	9	15	7	3	3	0	0
3 Jun	35	10	32	9	12	6	12	6
4 Jun	215	21	165	21	43	15	22	12
5 Jun	332	26	266	20	91	25	116	37
6 Jun	301	28	259	24	73	20	58	36
7 Jun	266	27	215	22	82	20	30	13
8 Jun	953	78	572	53	282	49	81	51
9 Jun	703	54	592	48	281	46	115	33
10 Jun	845	76	635	61	234	53	95	40
11 Jun	805	85	533	57	297	55	159	33
12 Jun	727	112	437	51	161	55	145	70
13 Jun	819	89	480	67	277	54	45	14
14 Jun	1,011	109	474	46	320	75	147	21
15 Jun	983	79	687	57	356	68	138	23
16 Jun	643	50	502	44	489	82	51	28
17 Jun	577	56	417	36	144	37	61	19
18 Jun	560	64	381	35	167	39	89	23
19 Jun	542	39	405	34	236	47	83	31
20 Jun	480	35	344	29	133	32	60	51

-continued-

Table 8.–Part 2 of 2.

	Upstream Fish		TS-based		ELSD-based		Net Apportioned	
Date	Passage	SE	Passage	SE	Passage	SE	Passage	SE
21 Jun	490	53	306	42	106	30	53	32
22 Jun	820	54	537	40	333	146	118	9
23 Jun	1,194	115	581	57	273	84	36	33
24 Jun	882	74	509	48	363	79	32	16
25 Jun	819	59	495	39	304	106	106	44
26 Jun	645	47	421	36	313	129	50	35
27 Jun	1,028	65	657	47	619	176	52	14
28 Jun	698	47	464	34	577	73	84	67
29 Jun	816	76	517	45	486	99	150	56
30 Jun	1,350	138	626	52	1015	174	136	44
Total	20,577	375	13,248	235	8,497	428	2,644	196

Table 9.–Estimated upstream fish passage based on split-beam sonar (all species; internally termed “unfiltered” estimates), TS-based split-beam sonar (Chinook only), ELSD-based (these were termed “behavior-censored ELSD-based estimates” in a previous report ([Miller et al. 2012]), split-beam sonar (Chinook only), and net-apportioned split-beam sonar (Chinook only), Kenai River late run, 2010.

	Upstream Fish		TS-based		ELSD-based		Net Apportioned	
Date	Passage	SE	Passage	SE	Passage	SE	Passage	SE
1 Jul	1,492	102	843	54	546	206	192	92
2 Jul	1,563	210	639	42	913	237	364	151
3 Jul	2,051	255	740	64	568	204	78	34
4 Jul	2,248	246	943	78	1560	230	175	72
5 Jul	1,819	164	940	80	1182	378	253	123
6 Jul	2,291	238	942	84	1084	463	426	55
7 Jul	3,644	536	1,495	114	1665	1,000	262	170
8 Jul	3,533	555	1,600	84	1929	663	212	41
9 Jul	846	90	505	62	261	84	76	19
10 Jul	1,679	165	781	69	215	78	65	31
11 Jul	3,340	284	1,002	103	237	99	207	59
12 Jul	3,077	359	1,311	101	360	141	262	150
13 Jul	4,017	528	1,090	118	301	111	145	78
14 Jul	3,167	342	1,009	72	263	96	219	156
15 Jul	3,064	320	1,062	100	429	159	184	102
16 Jul	5,093	700	1,525	125	634	272	693	179
17 Jul	6,785	812	1,661	186	1,177	403	387	87
18 Jul	6,163	637	1,672	137	1,019	318	388	273
19 Jul	2,209	240	1,131	129	364	113	179	86
20 Jul	6,165	553	1,937	126	1,671	836	808	159
21 Jul	7,279	588	2,654	148	564	308	495	279
22 Jul	6,246	485	1,627	149	2,386	746	156	70
23 Jul	4,644	368	2,216	170	2,879	819	385	129
24 Jul	6,213	454	2,562	128	2,050	698	199	52
25 Jul	6,355	535	1,388	86	1,010	383	140	102
26 Jul	3,840	273	1,396	101	710	220	369	99
27 Jul	5,577	554	1,542	131	402	150	379	72
28 Jul	8,576	785	1,761	183	712	314	420	126
29 Jul	6,469	489	1,470	230	1,164	372	369	132
30 Jul	7,460	623	1,686	186	627	251	1,201	342
31 Jul	12,333	1,148	1,659	177	1,344	436	358	33
1 Aug	6,999	627	1,716	156	812	248	994	89
2 Aug	3,895	319	1,249	65	647	131	327	27
3 Aug	3,619	213	1,312	86	590	142	492	29
4 Aug[a]	4,322	136	1,277	81	666	140	411	13
Total	158,073	2,869	48,343	726	32,941	2,401	12,269	768

[a] Counting operations were terminated after 4 August due to numerous fish holding and milling in the beam, which hampered the ability to accurately track targets.

Table 10.–Percentage of upstream bound large Chinook salmon (DIDSON length ≥ 75 cm) by riverbank, range stratum (distance from transducer), and tide stage sampled by DIDSON for 15 days of the 2010 early run (11–30 June) and for 33 days of the 2010 late run (1 July–4 August).

		Left Bank				Right Bank				
		Range Stratum				Range Stratum				
Run	Tide Stage	3–13 m	13–23 m	23–33 m	All Strata	3–13 m	13–23 m	23–33 m	All Strata	Both Banks
Early										
	Rising	6	6	2	14	2	2	3	6	20
	Falling	12	16	10	38	5	10	8	23	61
	Low	8	5	4	16	1	1	1	3	20
	All Stages	25	26	16	68	8	13	11	33	100
Late										
	Rising	7	9	7	23	5	6	11	22	44
	Falling	6	9	10	25	2	5	7	14	39
	Low	4	5	3	13	0	1	2	4	16
	All Stages	17	24	19	60	8	12	20	40	100

Note: columns may not sum due to rounding.

Table 11.–Percentage of upstream bound salmon that were classified as large Chinook salmon (DIDSON length ≥ 75cm) by riverbank, range stratum (distance from transducer), and tide stage; for 15 days of the 2010 early run (11–30 June) and 33 days of the 2010 late run (1 July–4 August).

		Left Bank				Right Bank				
		Range Stratum				Range Stratum				
Run	Tide Stage	3–13 m	13–23 m	23–33 m	All Strata	3–13 m	13–23 m	23–33 m	All Strata	Both Banks
Early										
	Rising	7.0	11.9	10.0	9.0	13.5	7.2	8.3	8.9	9.0
	Falling	5.5	6.1	4.8	5.5	10.6	9.9	8.2	9.4	6.5
	Low	10.9	9.2	8.8	9.8	15.4	14.3	8.1	11.5	10.1
	All Stages	6.8	7.3	5.8	6.7	11.5	9.7	8.2	9.5	7.4
Late										
	Rising	4.9	6.5	6.6	5.9	1.7	3.3	7.8	3.5	4.4
	Falling	3.1	4.1	4.8	4.0	0.8	1.7	3.4	1.9	2.8
	Low	5.8	8.1	4.8	6.2	0.7	2.4	5.9	2.9	5.0
	All Stages	4.2	5.5	5.3	5.0	1.2	2.4	5.2	2.6	3.7

Table 12.–DIDSON-based estimates of upstream salmon passage, DL mixture model (DLMM) proportion of Chinook salmon, and DLMM and DSEQ (DIDSON equivalent) Chinook salmon passage, RM 8.5 Kenai River, early run, 2010.

	DIDSON upstream salmon		DLMM Chinook salmon		DLMM Chinook salmon			DSEQ Chinook salmon		
Date	Passage	SE	Proportion	SE	Passage	SE	CV	Passage	SE	CV
16 May								40	18	0.45
17 May								7	4	0.63
18 May								7	4	0.64
19 May								134	63	0.47
20 May								73	34	0.46
21 May								7	4	0.61
22 May								40	19	0.46
23 May								24	12	0.49
24 May								3	2	0.47
25 May								27	12	0.46
26 May								59	29	0.48
27 May								30	15	0.50
28 May								60	31	0.51
29 May								65	33	0.51
30 May								25	13	0.50
31 May								27	14	0.52
1 Jun								3	2	0.52
2 Jun								3	2	0.52
3 Jun								44	23	0.52
4 Jun								93	48	0.51
5 Jun								285	147	0.52
6 Jun								124	61	0.50
7 Jun								77	39	0.50
8 Jun								241	116	0.48
9 Jun								286	132	0.46
10 Jun								247	112	0.45
11 Jun	1,417	145	0.158	0.032	224	50	0.22			
12 Jun	1,290	190	0.184	0.044	238	66	0.28			
13 Jun	1,375	163	0.149	0.047	205	68	0.33			
14 Jun	2,090	223	0.119	0.029	248	66	0.27			
15 Jun	1,431	106	0.094	0.027	134	40	0.30			
16 Jun	1,115	81	0.152	0.047	169	54	0.32			
17 Jun								174	74	0.42
18 Jun								191	86	0.45
19 Jun								235	108	0.46
20 Jun								182	76	0.42
21 Jun	1,139	150	0.163	0.036	186	47	0.25			
22 Jun	1,694	165	0.124	0.031	210	56	0.27			
23 Jun	1,881	130	0.053	0.017	99	33	0.34			
24 Jun	1,586	122	0.083	0.025	132	41	0.31			
25 Jun	1,396	113	0.178	0.044	248	65	0.26			
26 Jun	953	85	0.106	0.04	101	39	0.39			
27 Jun	1,610	130	0.108	0.038	174	62	0.36			
28 Jun	1,102	80	0.169	0.057	186	64	0.34			
29 Jun								310	126	0.40
30 Jun	2,586	269	0.076	0.028	195	74	0.38			
Early run total for DLMM and DSEQ								5,874	645	0.11

Note: All estimates are of upstream bound fish in midriver between and at least 3 m from the transducers.

Table 13.–DIDSON-based estimates of upstream salmon passage, DL mixture model (DLMM) proportion of Chinook salmon, and DLMM and DSEQ (DIDSON equivalent) Chinook salmon passage, RM 8.5 Kenai River, late run, 2010.

	DIDSON upstream salmon		DLMM Chinook salmon		DLMM Chinook salmon			DSEQ Chinook salmon		
Date	Passage	SE	Proportion	SE	Passage	SE	CV	Passage	SE	CV
1 Jul	2,870	204	0.085	0.026	244	76	0.31			
2 Jul	2,478	340	0.099	0.031	246	83	0.34			
3 Jul								104	42	0.41
4 Jul	3,340	308	0.205	0.065	685	226	0.33			
5 Jul	3,582	250	0.141	0.035	504	131	0.26			
6 Jul	3,825	415	0.080	0.022	306	88	0.29			
7 Jul	6,391	970	0.052	0.013	334	95	0.29			
8 Jul	6,747	1268	0.040	0.010	270	83	0.31			
9 Jul	1,440	125	0.182	0.046	261	70	0.27			
10 Jul	2,774	266	0.128	0.030	354	91	0.26			
11 Jul	5,519	431	0.041	0.011	227	61	0.27			
12 Jul	5,888	507	0.117	0.018	689	119	0.17			
13 Jul								331	139	0.42
14 Jul	6,245	692	0.060	0.012	372	83	0.22			
15 Jul	6,685	974	0.046	0.009	305	74	0.24			
16 Jul	12,019	1454	0.061	0.009	729	138	0.19			
17 Jul	19,867	4040	0.039	0.006	772	191	0.25			
18 Jul	16,921	1902	0.050	0.008	854	160	0.19			
19 Jul	5,076	424	0.136	0.018	691	109	0.16			
20 Jul	15,410	1391	0.100	0.012	1,544	228	0.15			
21 Jul	16,192	1449	0.040	0.007	645	124	0.19			
22 Jul	14,316	1461	0.055	0.007	788	124	0.16			
23 Jul	9,210	915	0.043	0.008	392	80	0.20			
24 Jul	22,579	1917	0.027	0.004	607	99	0.16			
25 Jul	13,849	1368	0.024	0.004	336	61	0.18			
26 Jul	7,174	550	0.046	0.007	332	54	0.16			
27 Jul	10,170	960	0.023	0.005	231	53	0.23			
28 Jul	16,628	1823	0.012	0.002	193	45	0.23			
29 Jul	13,415	1190	0.031	0.004	409	69	0.17			
30 Jul	15,189	1509	0.018	0.003	267	53	0.20			
31 Jul	25,335	2827	0.014	0.002	347	73	0.21			
1 Aug	14,490	1600	0.042	0.006	612	114	0.19			
2 Aug	10,531	1074	0.048	0.006	507	79	0.16			
3 Aug	9,523	732	0.057	0.006	546	72	0.13			
4 Aug	12,918	610	0.042	0.005	545	68	0.13			
5 Aug								623	96	0.15
6 Aug								324	60	0.19
7 Aug								283	58	0.21
8 Aug								242	54	0.22
9 Aug								149	36	0.24
10 Aug								202	53	0.26
Late run total for DLMM and DSEQ								18,401	698	0.04

Note: All estimates are of upstream bound fish in midriver between and at least 3 m from the transducers.

Table 14.–Daily estimates of Chinook salmon age composition derived from fitting a mixture model to length measurements from DIDSON and inriver gillnet catches, RM 8.5 Kenai River, early run, 2010.

	Ages 3 and 4		Age 5		Ages 6 and 7	
Date	Proportion	SE	Proportion	SE	Proportion	SE
11 Jun	0.30	0.08	0.66	0.09	0.04	0.03
12 Jun	0.32	0.08	0.66	0.09	0.03	0.03
13 Jun	0.39	0.10	0.57	0.10	0.04	0.04
14 Jun	0.36	0.09	0.55	0.09	0.09	0.05
15 Jun	0.35	0.09	0.59	0.09	0.06	0.05
16 Jun	0.42	0.09	0.52	0.09	0.07	0.04
17 Jun						
18 Jun						
19 Jun						
20 Jun						
21 Jun	0.18	0.08	0.78	0.09	0.04	0.05
22 Jun	0.33	0.10	0.61	0.10	0.06	0.05
23 Jun	0.28	0.09	0.69	0.10	0.03	0.04
24 Jun	0.31	0.09	0.60	0.11	0.09	0.07
25 Jun	0.38	0.10	0.49	0.10	0.13	0.06
26 Jun	0.55	0.09	0.33	0.10	0.12	0.07
27 Jun	0.58	0.09	0.31	0.09	0.11	0.06
28 Jun	0.56	0.09	0.29	0.08	0.16	0.06
29 Jun						
30 Jun	0.64	0.08	0.20	0.07	0.16	0.06
Weighted mean	0.39		0.53		0.08	

Note: No estimates were produced for 16 May through 10 June. Estimates apply to upstream bound fish in midriver between and at least 3 m from the transducers. In the mixture model, ages 3 and 4 are pooled, as are ages 6 and 7. Means are weighted by daily DLMM estimates.

Table 15.–Daily estimates of Chinook salmon age composition derived from fitting a mixture model to length measurements from DIDSON and inriver gillnet catches, RM 8.5 Kenai River, late run, 2010.

	Ages 3 and 4		Age 5		Ages 6 and 7	
Date	Proportion	SE	Proportion	SE	Proportion	SE
1 Jul	0.67	0.07	0.13	0.06	0.2	0.06
2 Jul	0.68	0.07	0.17	0.07	0.15	0.06
3 Jul						
4 Jul	0.70	0.07	0.15	0.06	0.15	0.05
5 Jul	0.66	0.07	0.11	0.06	0.23	0.06
6 Jul	0.59	0.08	0.21	0.07	0.2	0.06
7 Jul	0.54	0.08	0.25	0.08	0.21	0.07
8 Jul	0.47	0.08	0.24	0.08	0.29	0.08
9 Jul	0.47	0.08	0.20	0.08	0.34	0.08
10 Jul	0.38	0.09	0.37	0.09	0.24	0.07
11 Jul	0.32	0.08	0.18	0.09	0.49	0.09
12 Jul	0.35	0.08	0.38	0.08	0.27	0.07
13 Jul						
14 Jul	0.33	0.08	0.34	0.08	0.33	0.07
15 Jul	0.34	0.07	0.23	0.09	0.43	0.08
16 Jul	0.27	0.08	0.32	0.10	0.41	0.10
17 Jul	0.29	0.08	0.37	0.08	0.34	0.07
18 Jul	0.35	0.08	0.28	0.08	0.37	0.08
19 Jul	0.34	0.08	0.14	0.08	0.52	0.07
20 Jul	0.26	0.09	0.29	0.07	0.44	0.07
21 Jul	0.26	0.08	0.30	0.10	0.44	0.09
22 Jul	0.20	0.06	0.36	0.12	0.44	0.12
23 Jul	0.21	0.07	0.17	0.09	0.62	0.09
24 Jul	0.14	0.07	0.37	0.09	0.49	0.09
25 Jul	0.07	0.04	0.25	0.13	0.68	0.13
26 Jul	0.09	0.05	0.35	0.10	0.57	0.10
27 Jul	0.11	0.05	0.23	0.11	0.67	0.12
28 Jul	0.10	0.05	0.37	0.14	0.53	0.14
29 Jul	0.09	0.05	0.46	0.10	0.45	0.10
30 Jul	0.09	0.05	0.32	0.11	0.59	0.11
31 Jul	0.09	0.05	0.38	0.12	0.53	0.12
1 Aug	0.08	0.05	0.44	0.07	0.48	0.08
2 Aug	0.05	0.04	0.23	0.09	0.71	0.09
3 Aug	0.02	0.03	0.19	0.07	0.79	0.07
4 Aug	0.03	0.03	0.26	0.09	0.71	0.09
5 Aug						
6 Aug						
7 Aug						
8 Aug						
9 Aug						
10 Aug						
Weighted mean	0.28		0.28		0.43	

Note: Estimates apply to upstream bound fish in midriver between and at least 3 m from the transducers. In the mixture model, ages 3 and 4 are pooled, as are ages 6 and 7. Means are weighted by daily DLMM estimates.

FIGURES

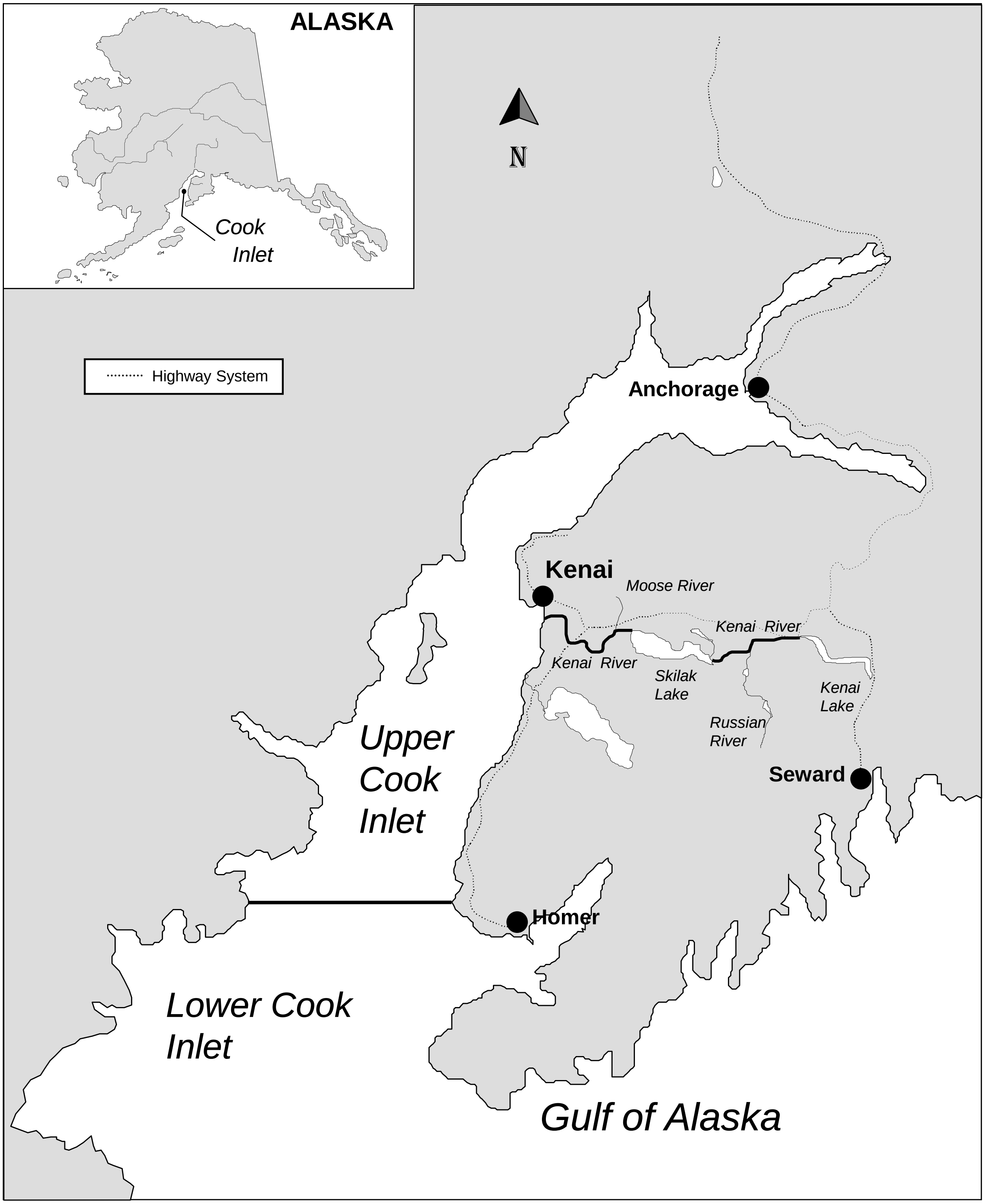

Figure 1.–Cook Inlet showing location of Kenai River.

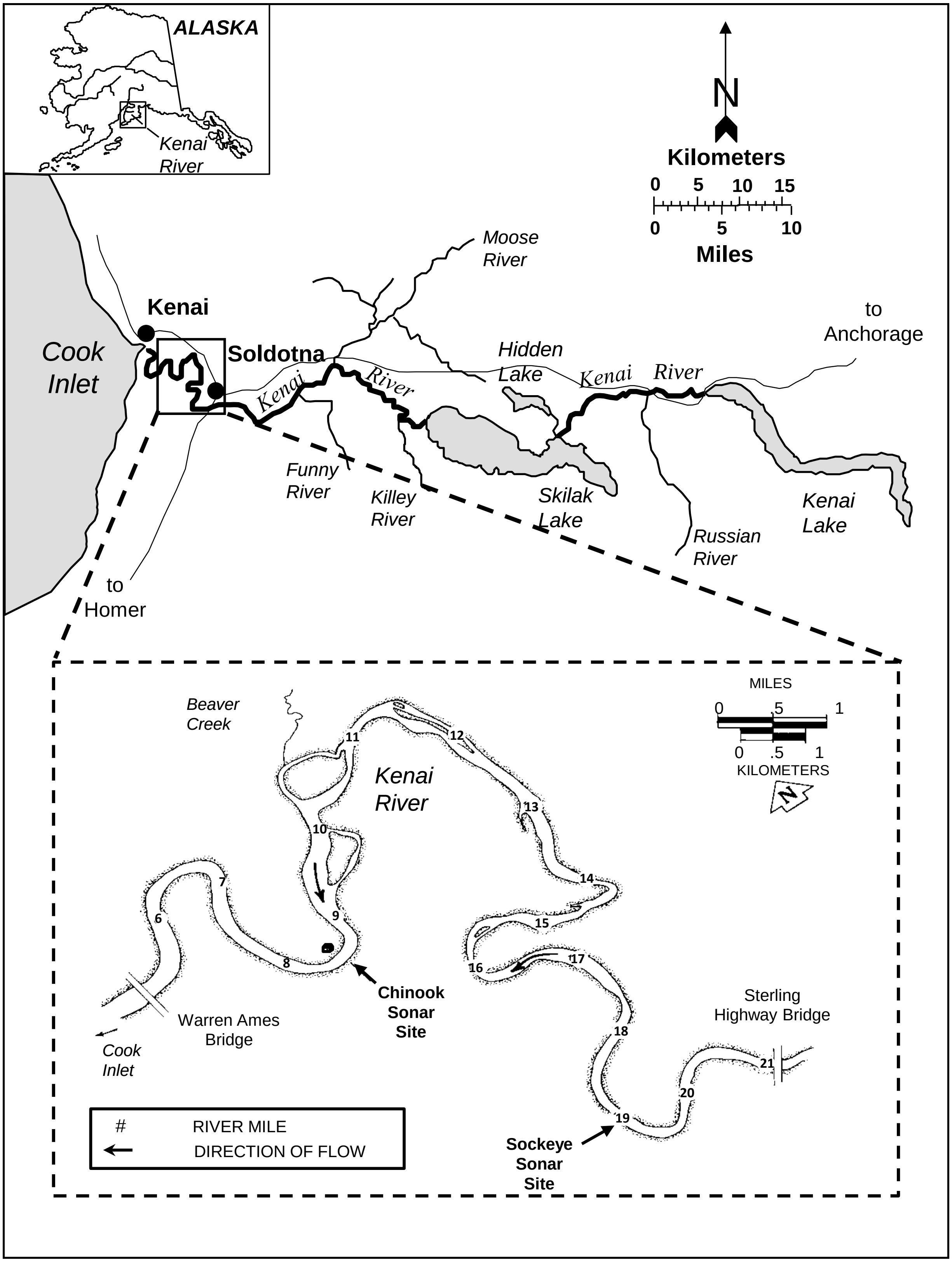

Figure 2.–Kenai River sonar site locations, 2010.

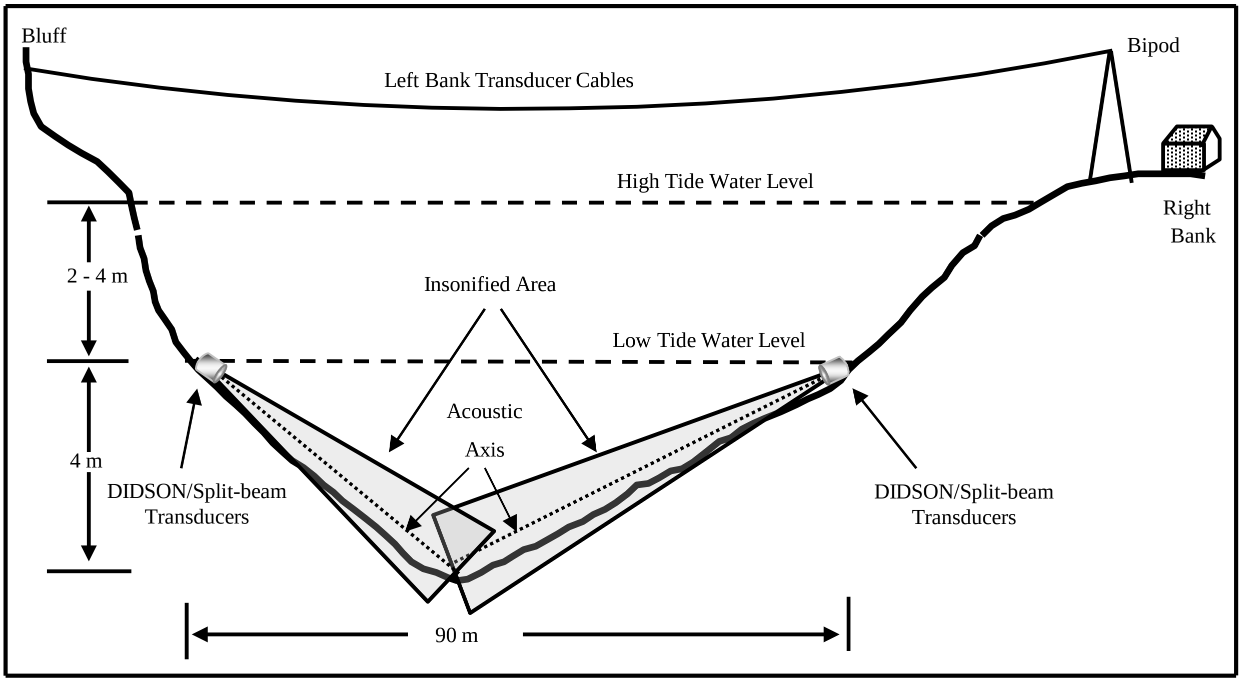

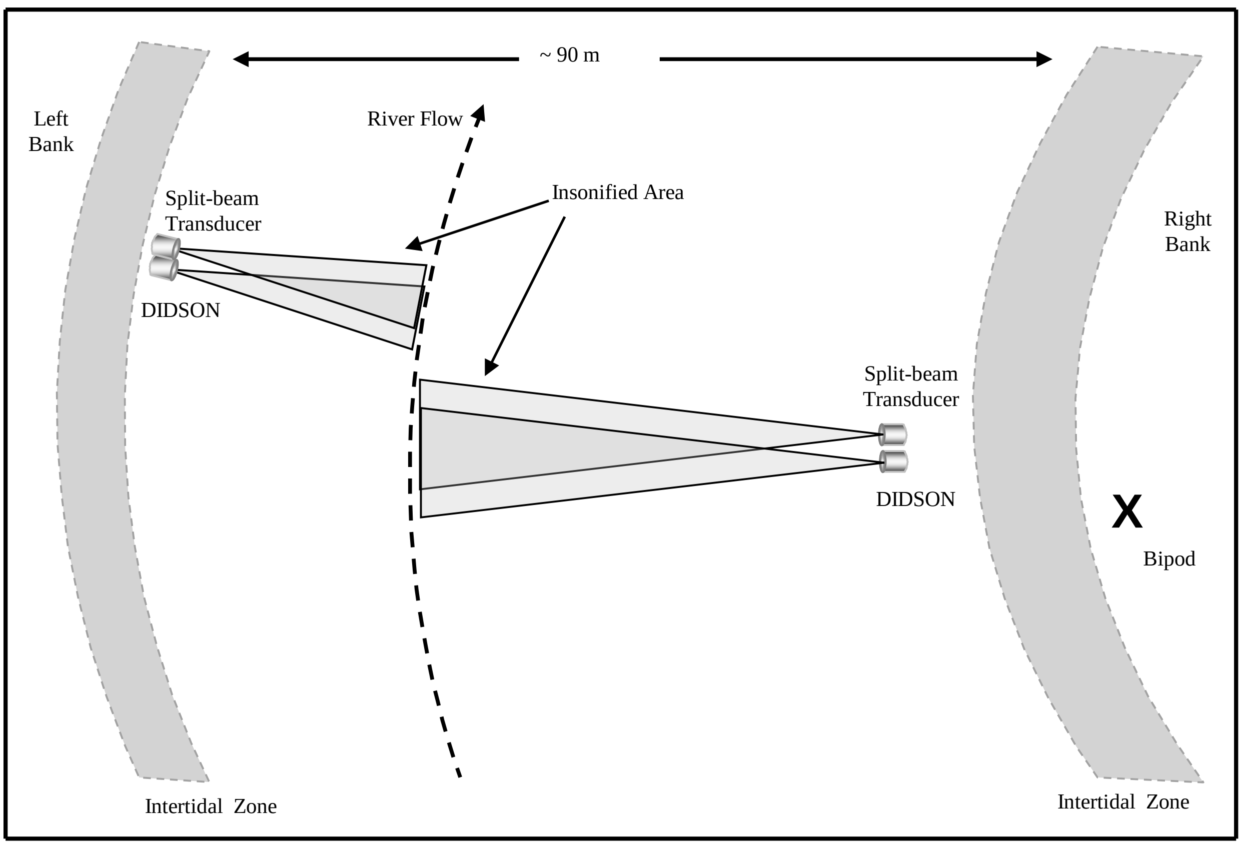

Note: Distance from bipod to thalweg (shown as dashed line depicting lowest course of the river) is approximately 88 m.

Figure 3.–Cross-sectional (top) and aerial (bottom) diagrams of sonar site illustrating insonified portions of RM 8.5 of the Kenai River, 2010.

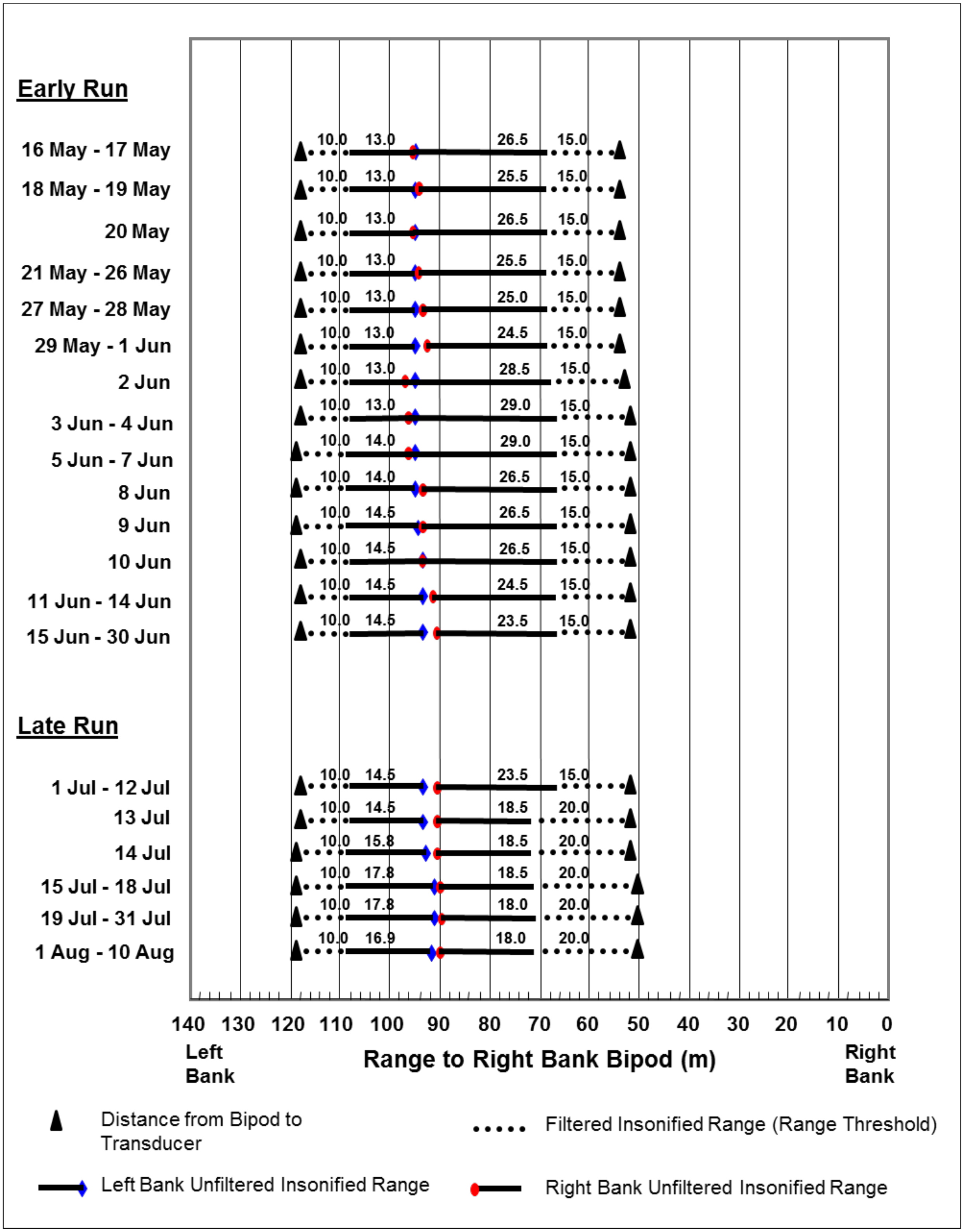

Figure 4.–Daily right- and left-bank transducer placement and insonified ranges relative to bipod tower located on the right bank, Kenai River RM 8.5, 2010.

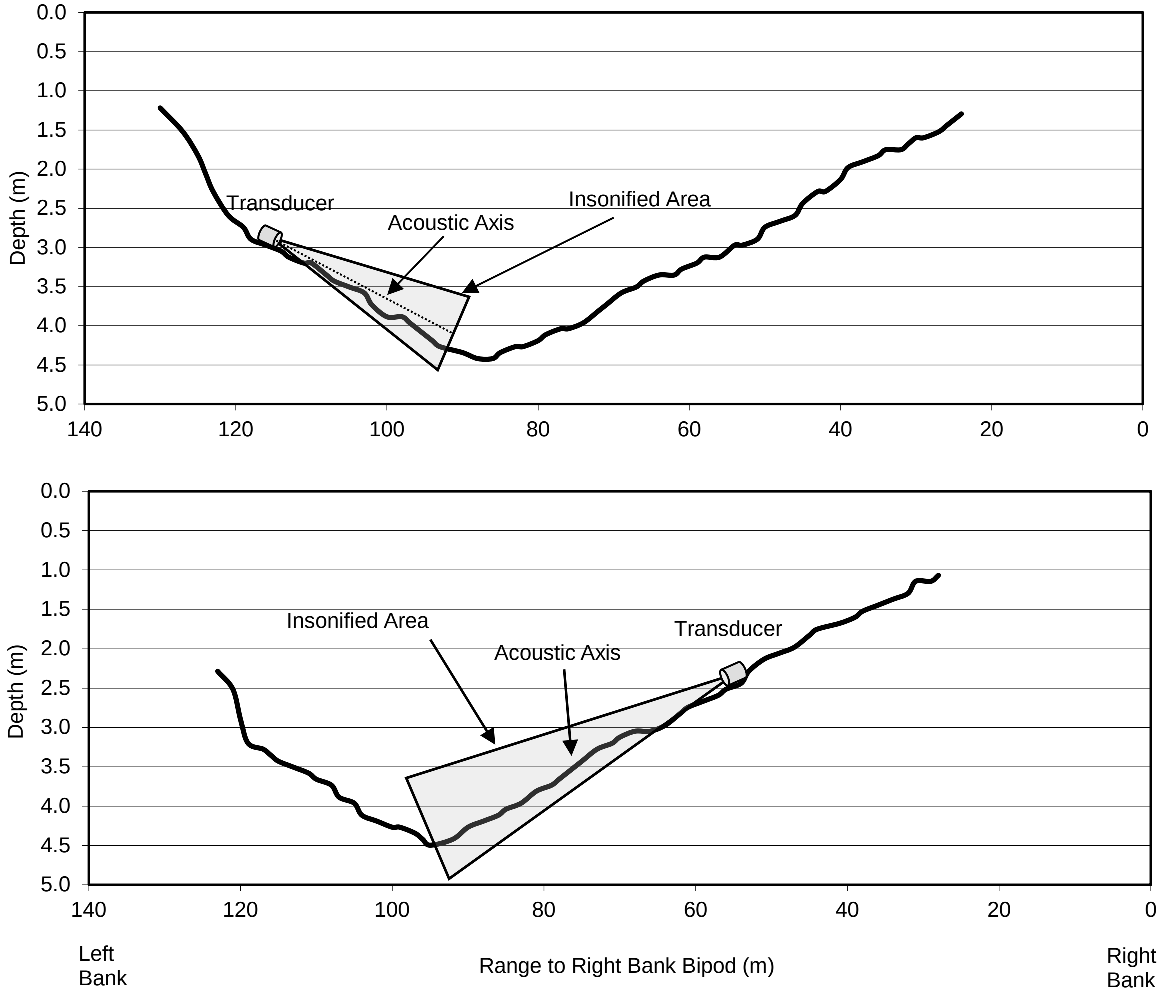

Figure 5.–Bottom profiles for the left bank transducer (top) and right bank transducer (bottom) at the Kenai River Chinook salmon sonar site with approximate transducer placement and sonar beam coverage for 16 May 2010.

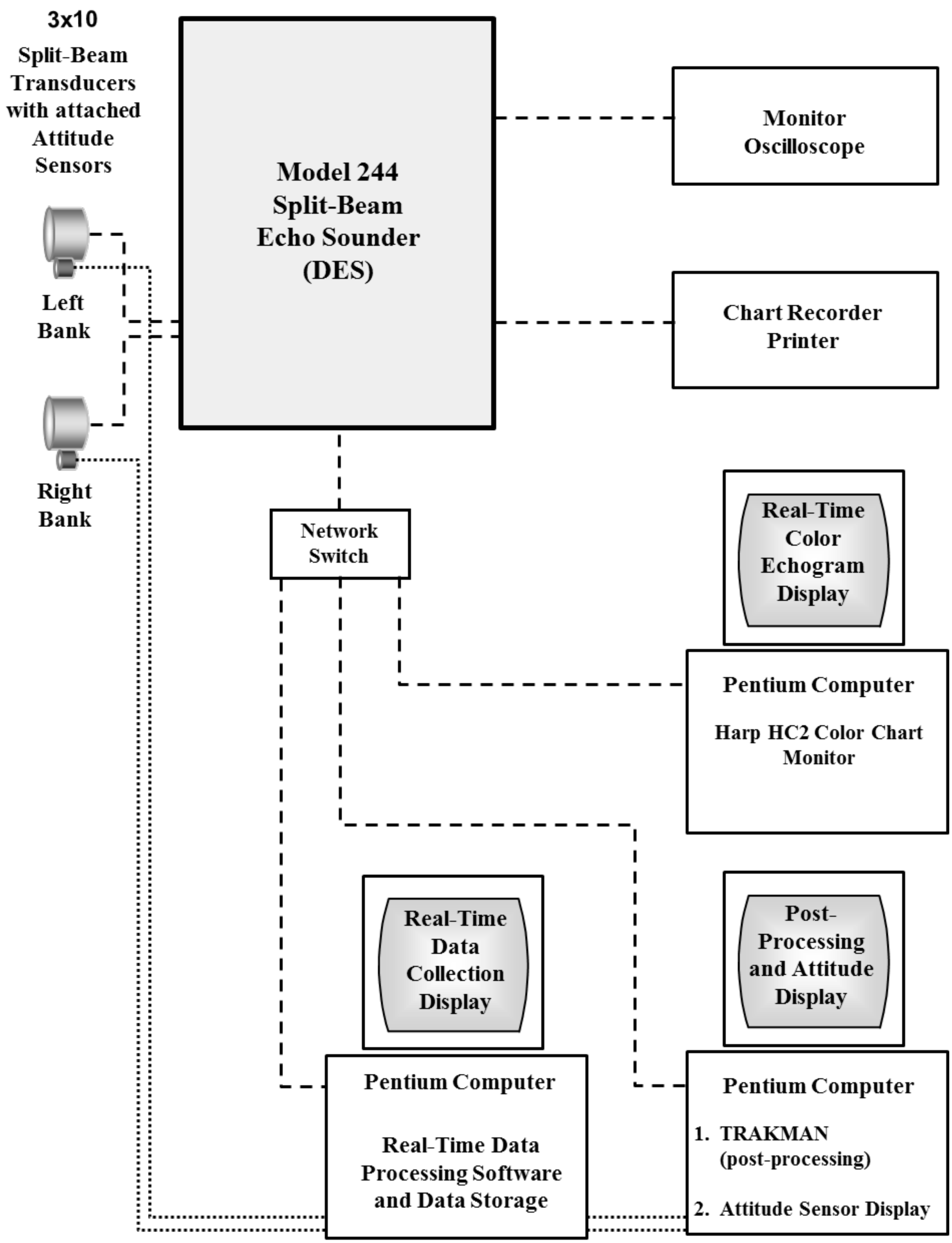

Figure 6.–Diagram of 2010 split-beam sonar system configuration and data flow.

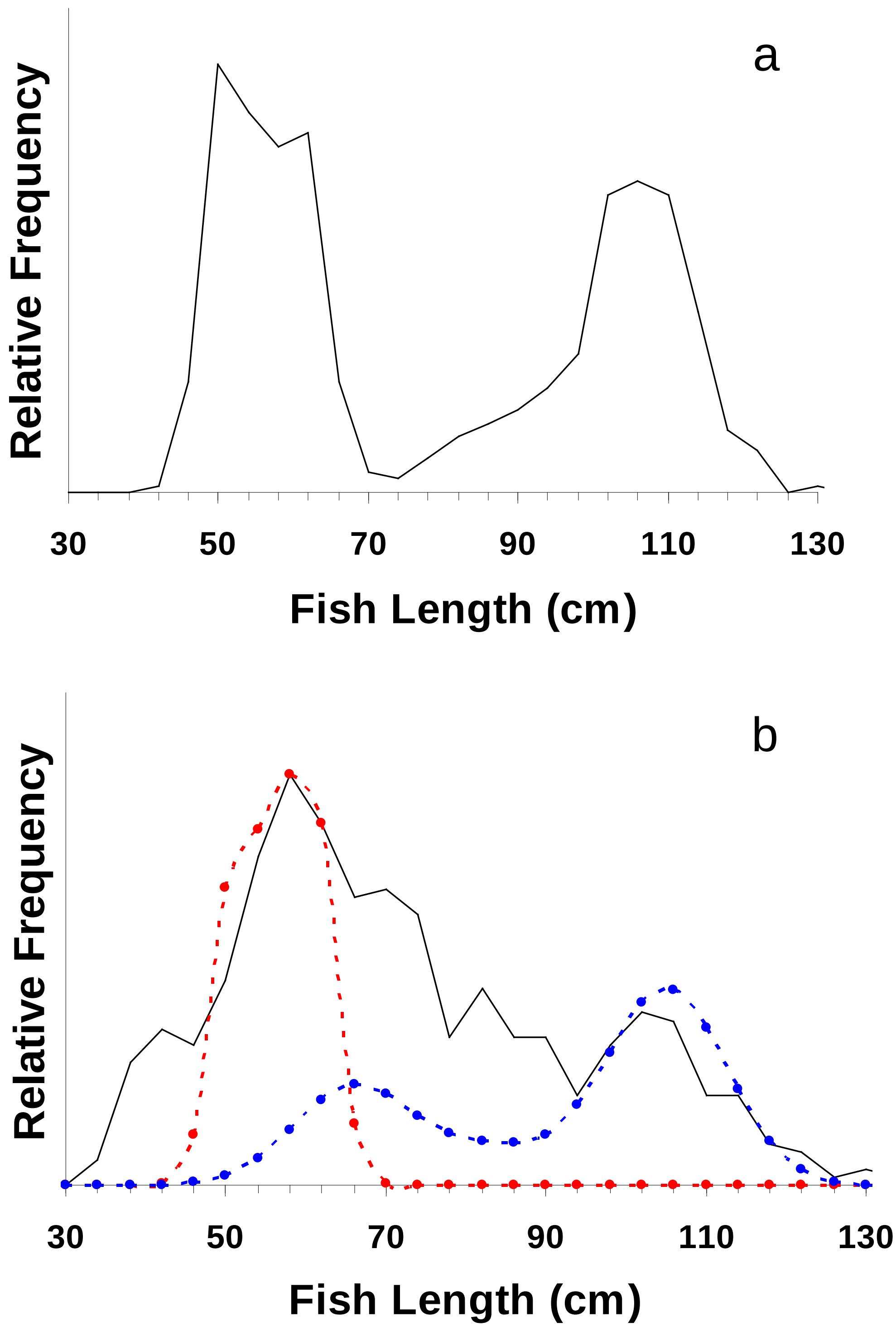

Note: true length distributions of sockeye salmon (red dashed line) and Chinook salmon (blue dashed line) are shown.

Figure 7.–Hypothetical frequency distributions of fish length measurements (black solid lines) at the Kenai River sonar site for true species composition 50% sockeye salmon, 50% Chinook salmon. Top graph (a) depicts hypothetical distribution when there are few small Chinook salmon and no measurement error. Bottom graph (b) depicts hypothetical distribution when 40% of Chinook salmon are small and measurement error standard deviation is 10 cm.

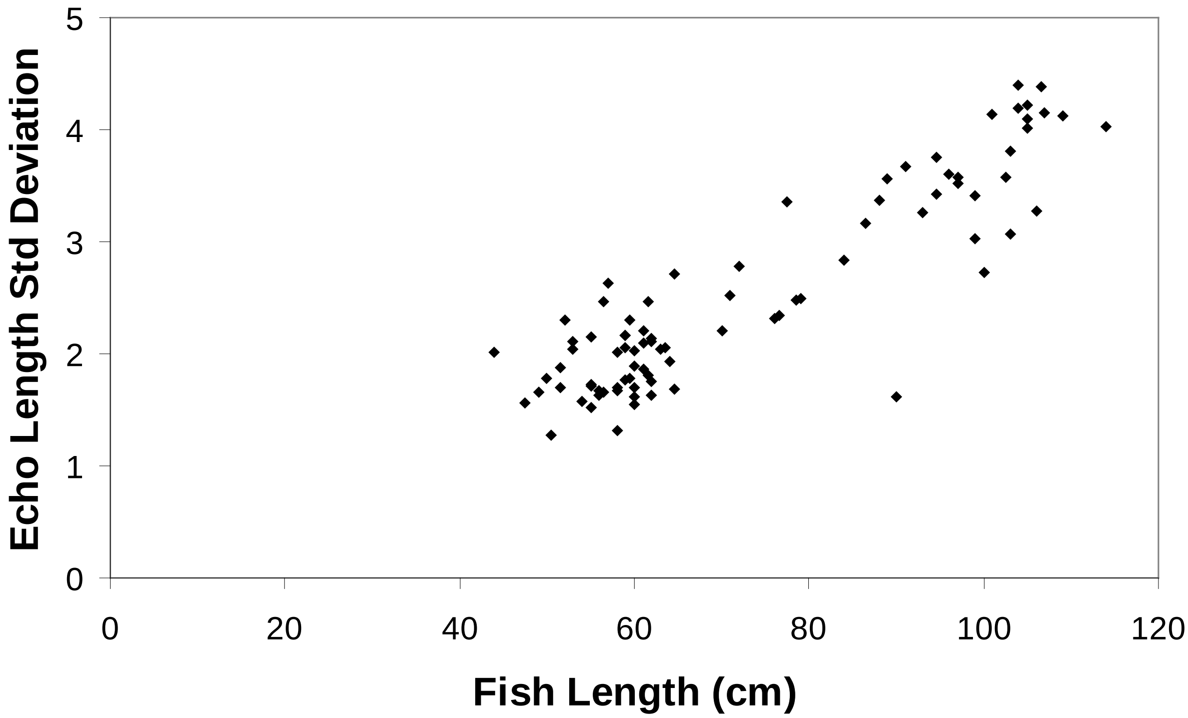

Source: data from Burwen and Fleischman (1998).

Figure 8.–Echo length standard deviation versus fish length for tethered Pacific salmon in the Kenai River, 1995.

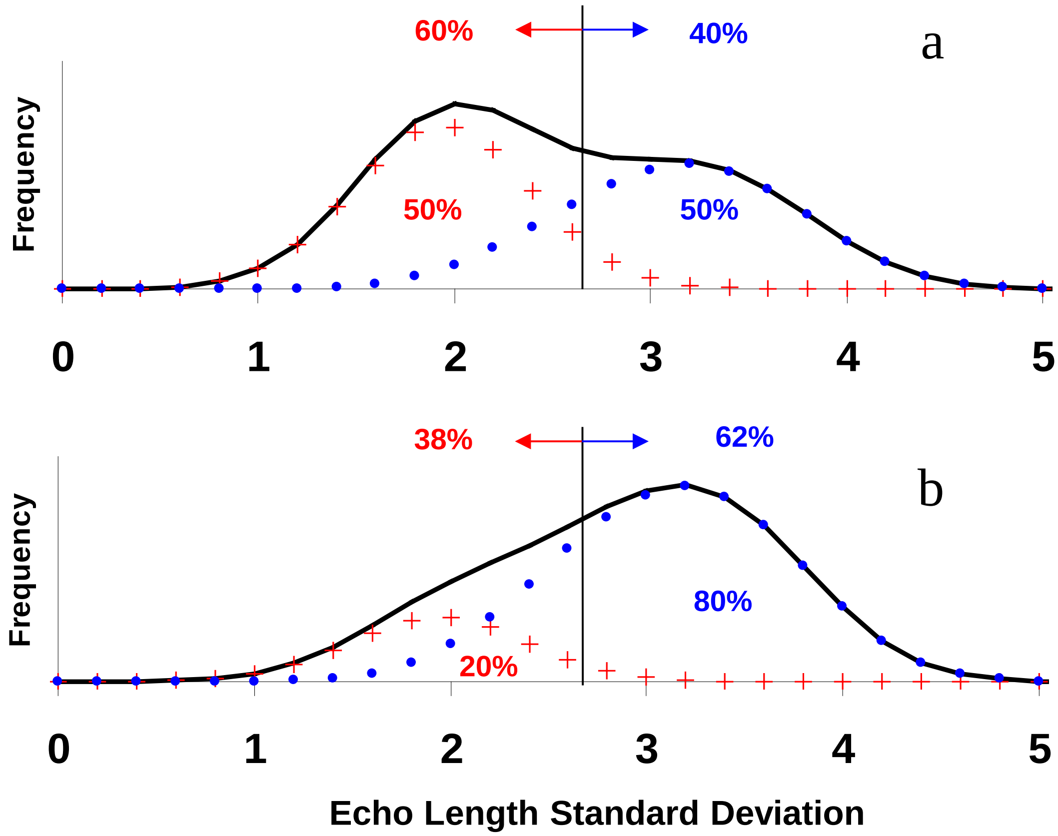

Note: Threshold-based discrimination is subject to bias when discriminating variables are imprecise. Solid lines are simulated frequency distributions of echo length standard deviation arising from component distributions due to sockeye salmon (plus symbols) and Chinook salmon (solid symbols).

Figure 9.–An example of threshold-based discrimination of Chinook and sockeye salmon. Top graph (a) depicts a simulated frequency distribution if the true species composition is 50% sockeye, 50% Chinook salmon, and a threshold criterion of 2.7 is used; estimated species composition will be 60:40. Bottom graph (b) depicts a simulated frequency distribution if the true species composition is 20:80, and the same threshold criterion of 2.7 is used; estimated species composition will be 38:62.

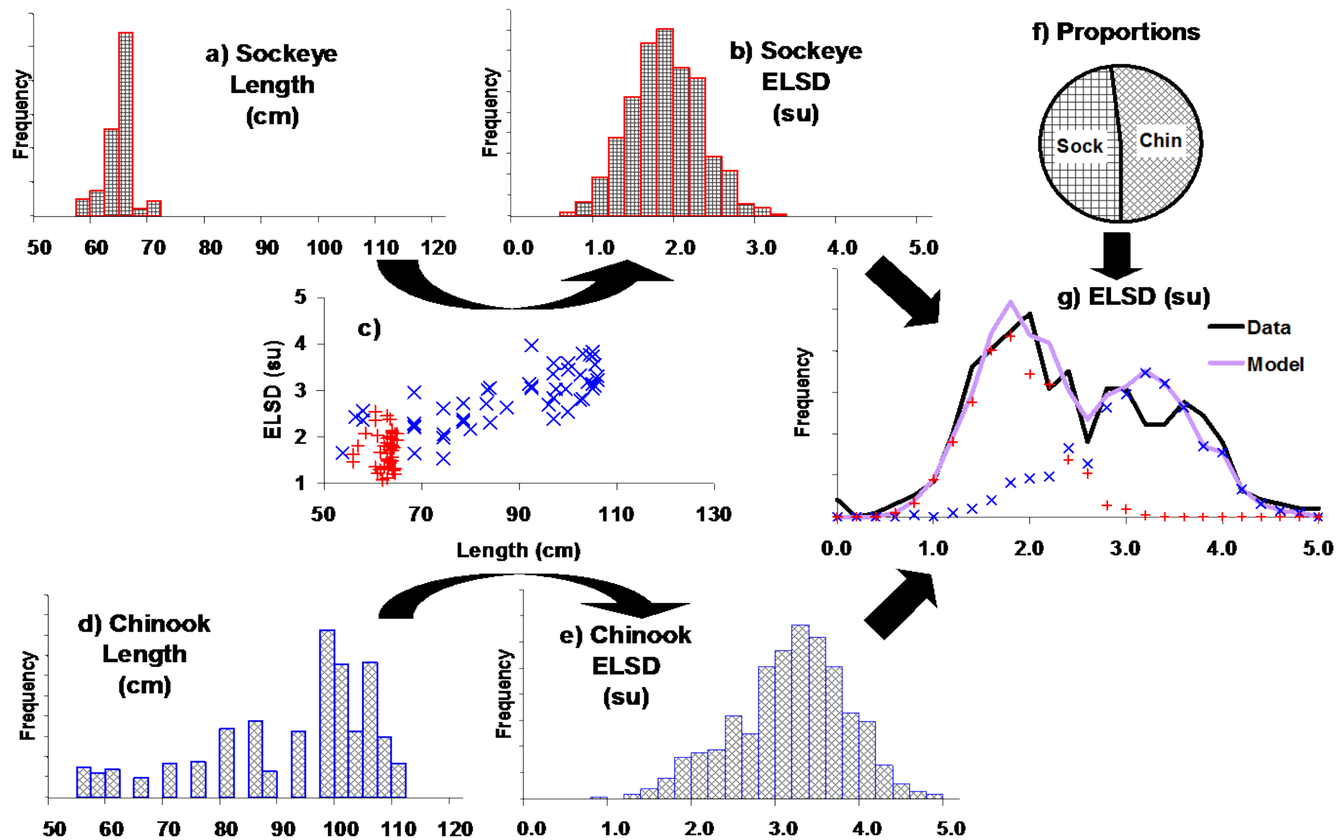

Note: Plus symbol = sockeye salmon, x = Chinook salmon. Checkered pattern = sockeye salmon, cross-hatched = Chinook salmon. Units for ELSD are 48 kHz digital sampling units.

Figure 10.–Flow chart of a mixture model. The frequency distribution of echo length standard deviation (ELSD, panel g) is modeled as a weighted mixture of species-specific ELSD distributions (panels b and e), which in turn are the products of species-specific size distributions (panels a and d) and the relationship between ELSD and fish length (panel c). The weights (species proportions, panel f) are the parameters of interest.

Figure 11.–DIDSON-LR with a high-resolution lens (on left in photos A and B) mounted next to a split-beam transducer (on right in photos A and B). A custom fit fabric enclosure shown in photo B protects against silt buildup in front of the lens as shown in photo C.

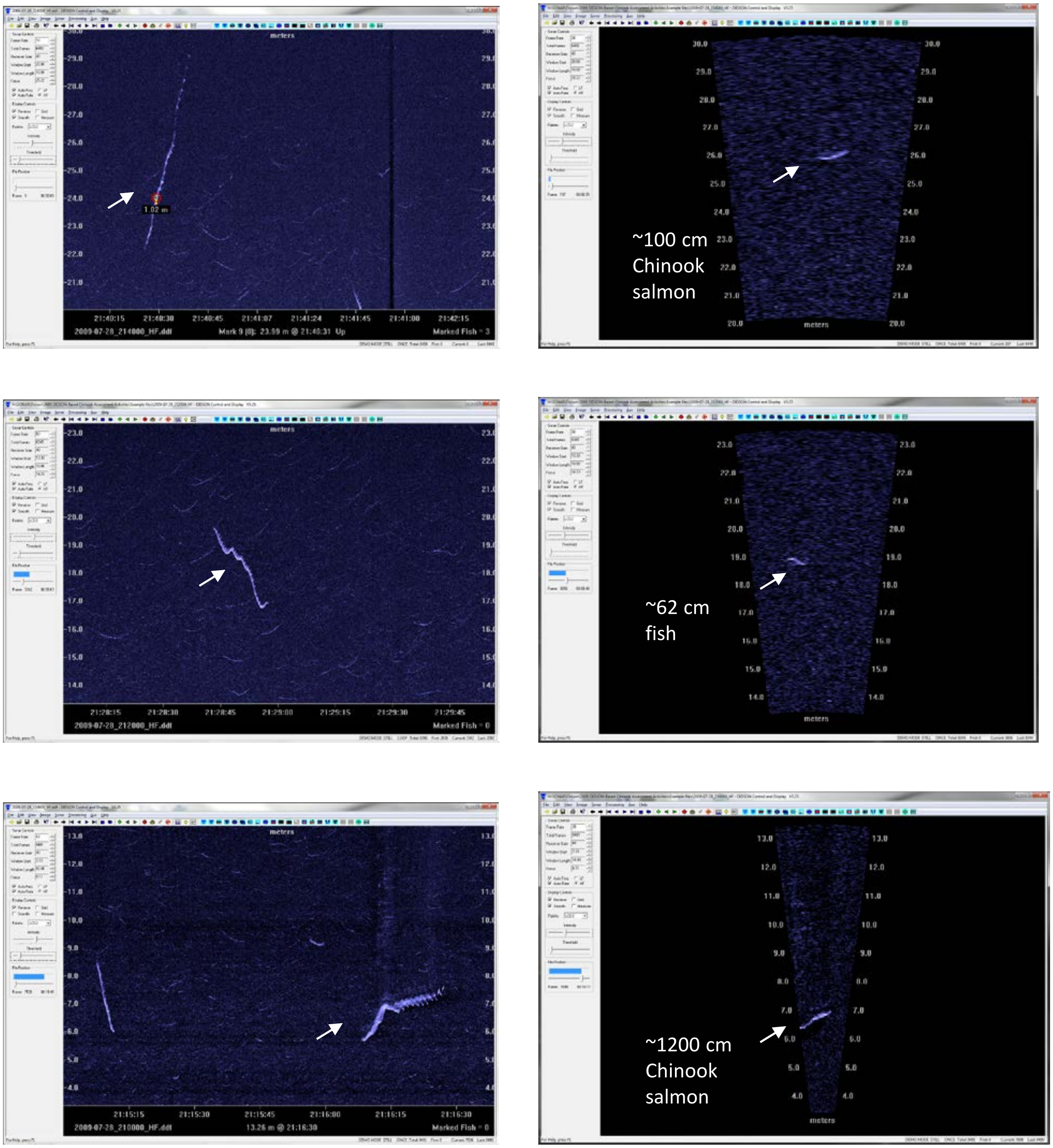

Note: the echograms display approximately 800 frames, whereas the video displays the single frame on which the measurement was taken.

Figure 12.–Example fish traces with their measured sizes are shown on DIDSON echogram (at left) and video (at right) displays for each of the 3 range strata: 3.3–13.3 m (bottom), 13.3–23.3 m (middle), and 23.3–33.3 (top).

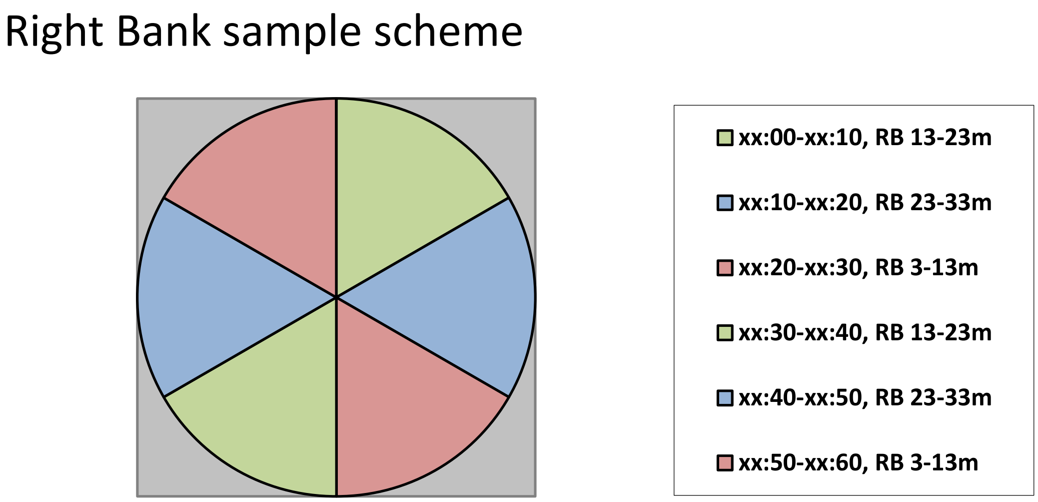

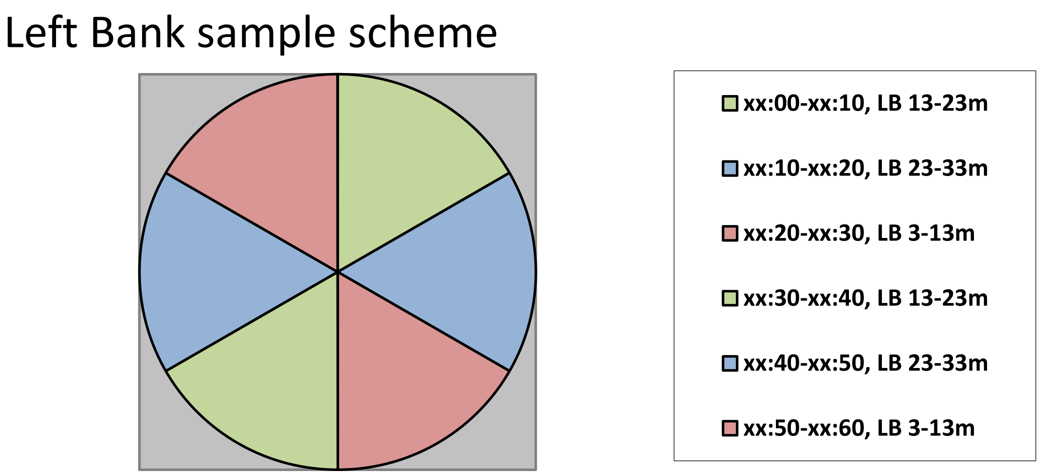

Note: Time presented in hours and minutes (hh:mm) format.

Figure 13.–Right (top) and left (bottom) bank range strata sampling schedules for 2010.[36]

[36] The DIDSON caused “cross talk” (interference) for the split-beam sonar. Because the cross talk was most prevalent when sampling the 23–33 m stratum, sampling of this stratum was scheduled during the time period xx:40–xx:60 (last 20 minutes of the hour) when the split-beam sonar was least likely to be used.

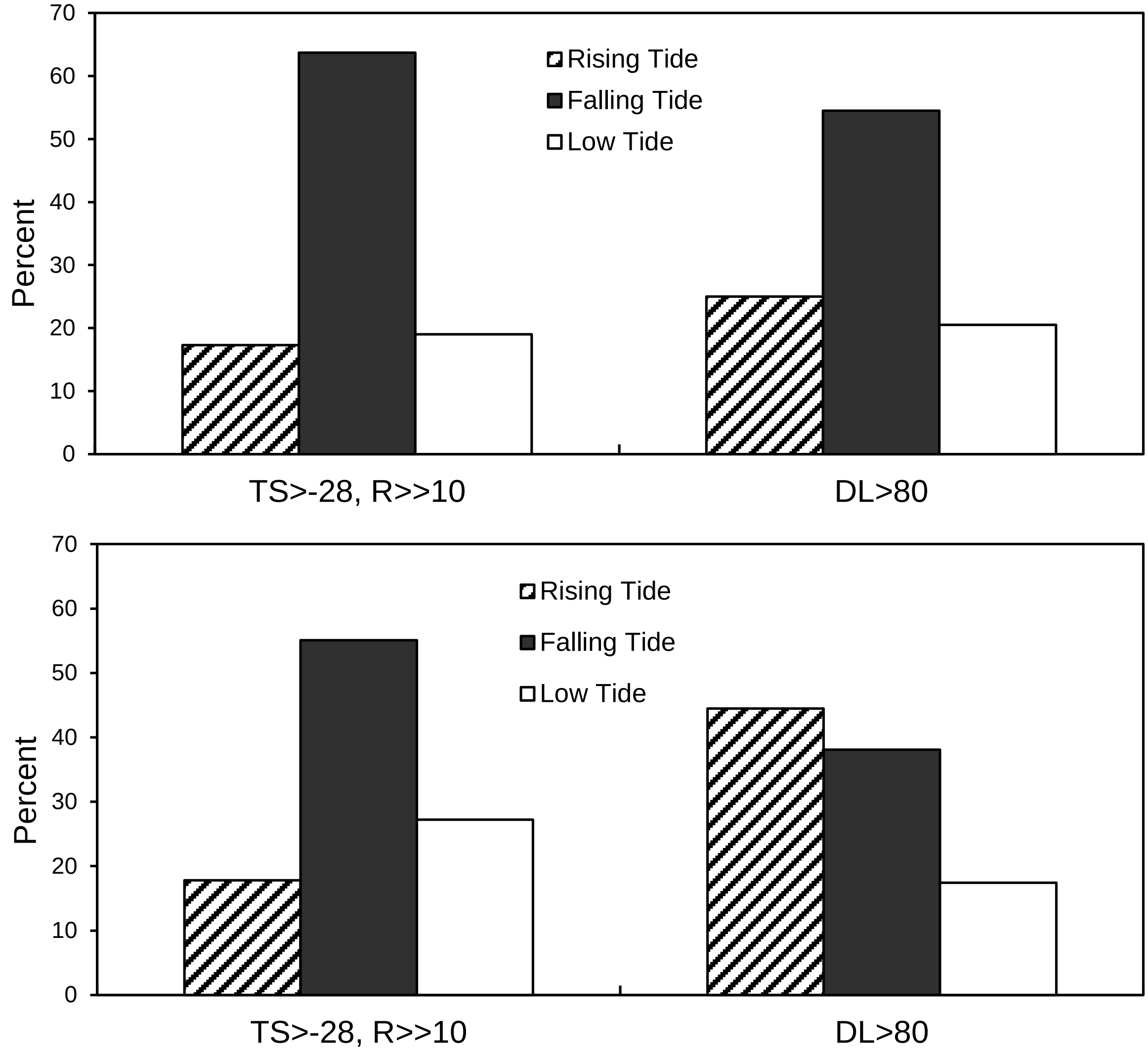

Note: Data have been filtered by range (distance from transducer) and target strength criteria. TS = target strength; R = range; and DL = DIDSON length.

Figure 14.–Percentage of filtered split-beam and DIDSON upstream bound fish by tide stage for the early (top) and late (bottom) runs, Kenai River RM 8.5, 2010.

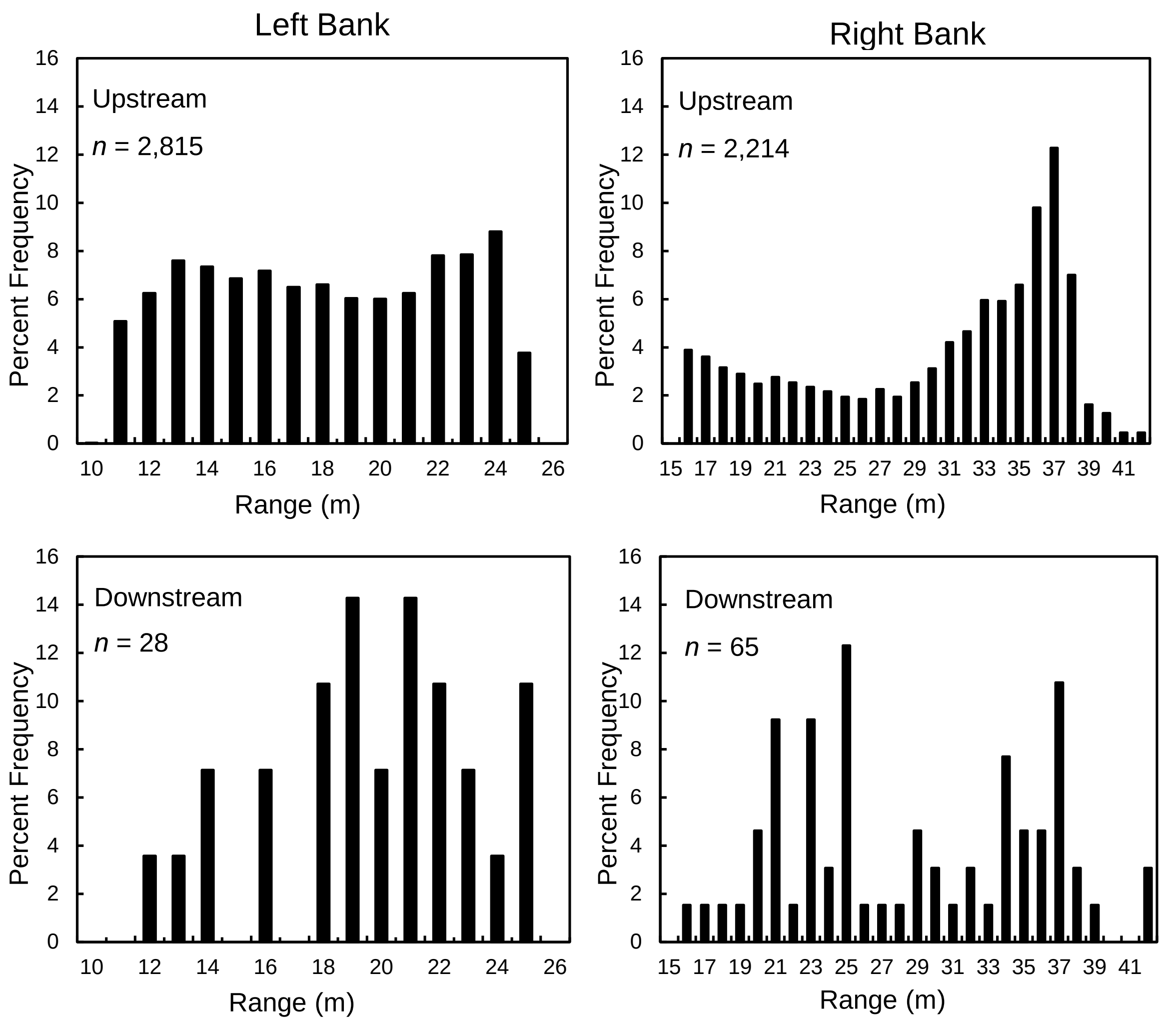

Note: Data have been filtered by range (distance from transducer) and target strength criteria.

Figure 15.–Standardized distance from transducer of early-run upstream and downstream moving filtered split-beam targets by bank, Kenai River RM 8.5, 2010.

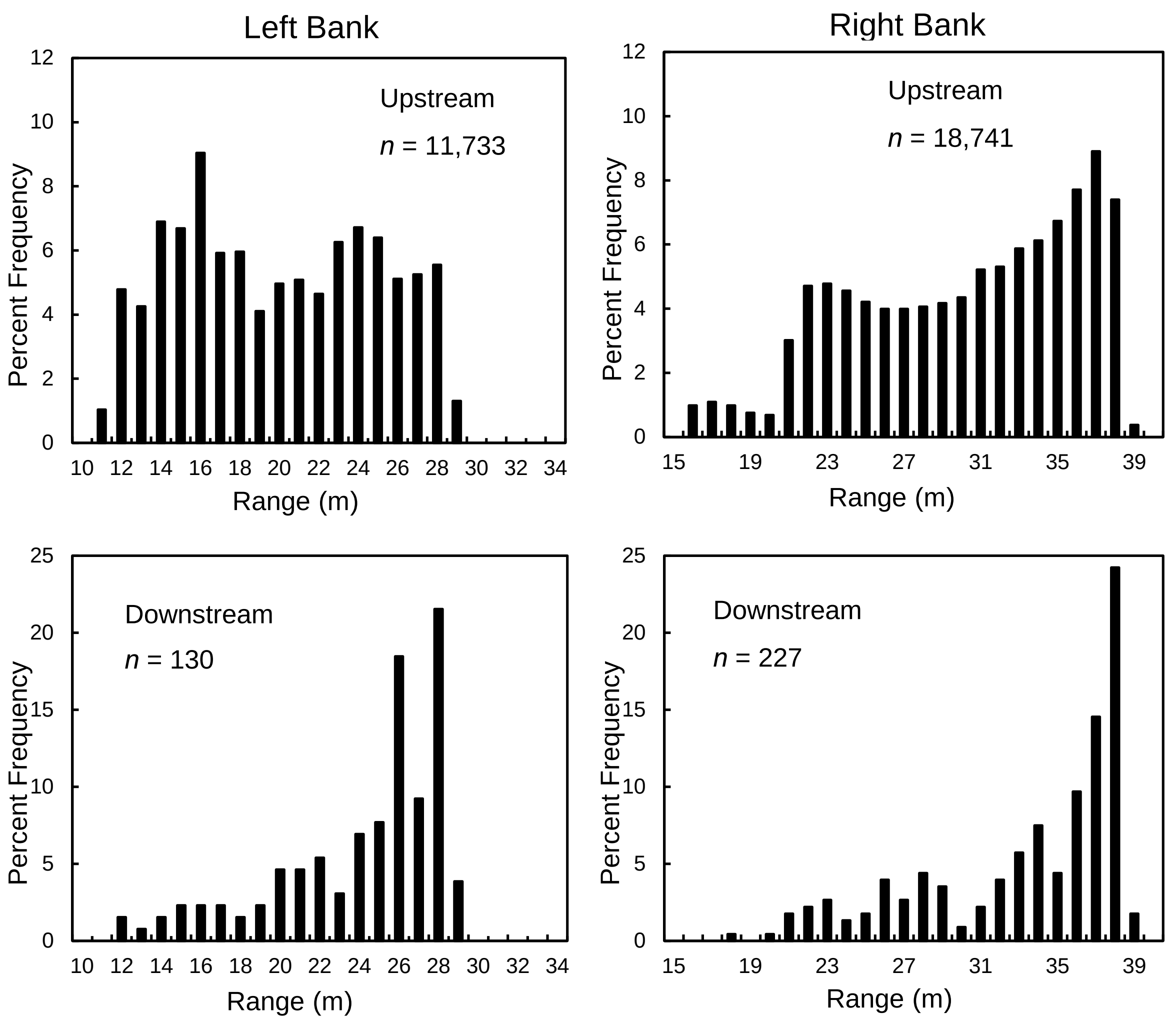

Note: Data have been filtered by range (distance from transducer) and target strength criteria.

Figure 16.–Standardized distance from transducer of late-run upstream and downstream moving filtered split-beam targets by bank, Kenai River RM 8.5, 2010.

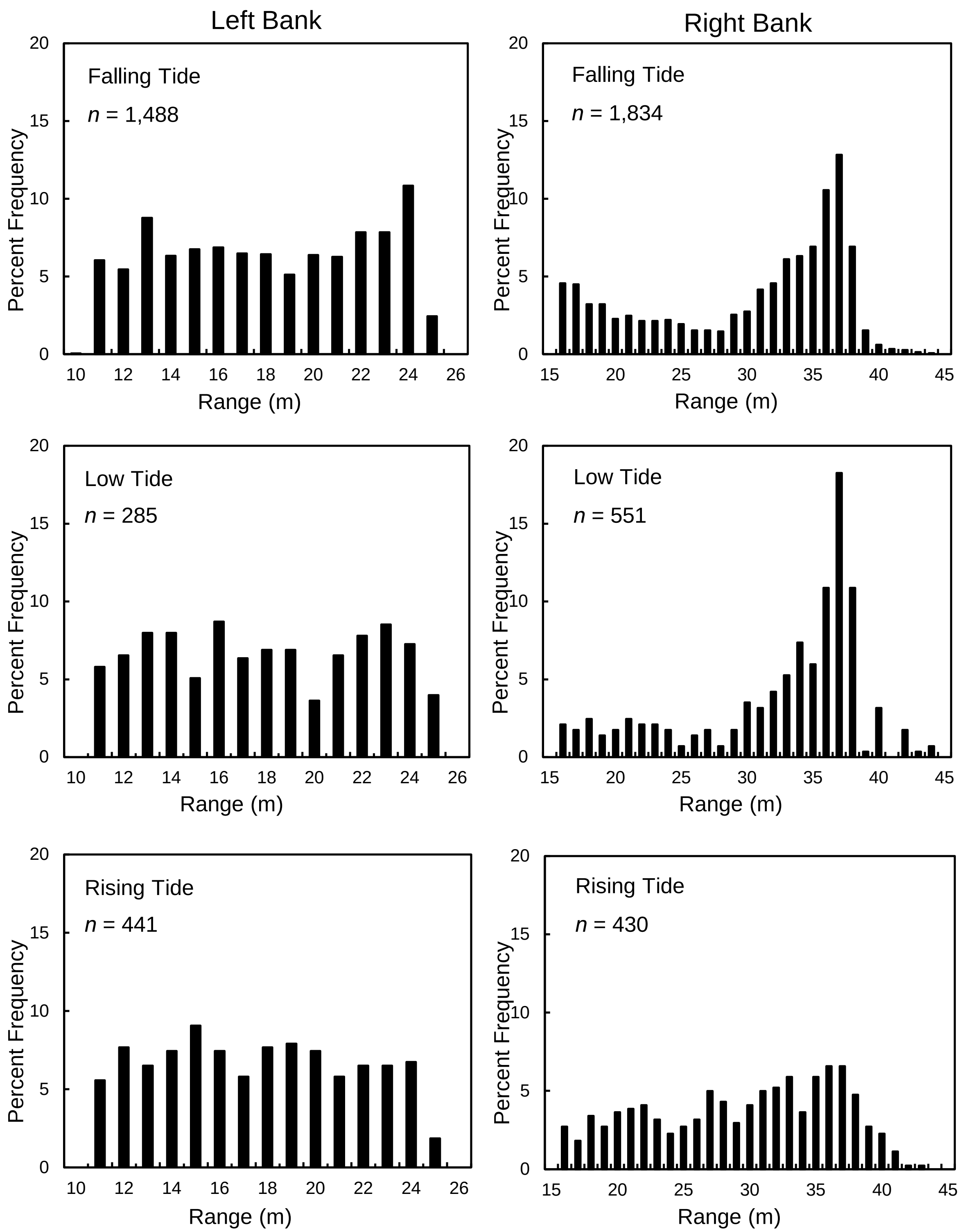

Note: Data have been filtered by range (distance from transducer) and target strength criteria.

Figure 17.–Standardized distance from transducer of early-run upstream moving filtered split-beam targets by tide stage and bank, Kenai River RM 8.5, 2010.

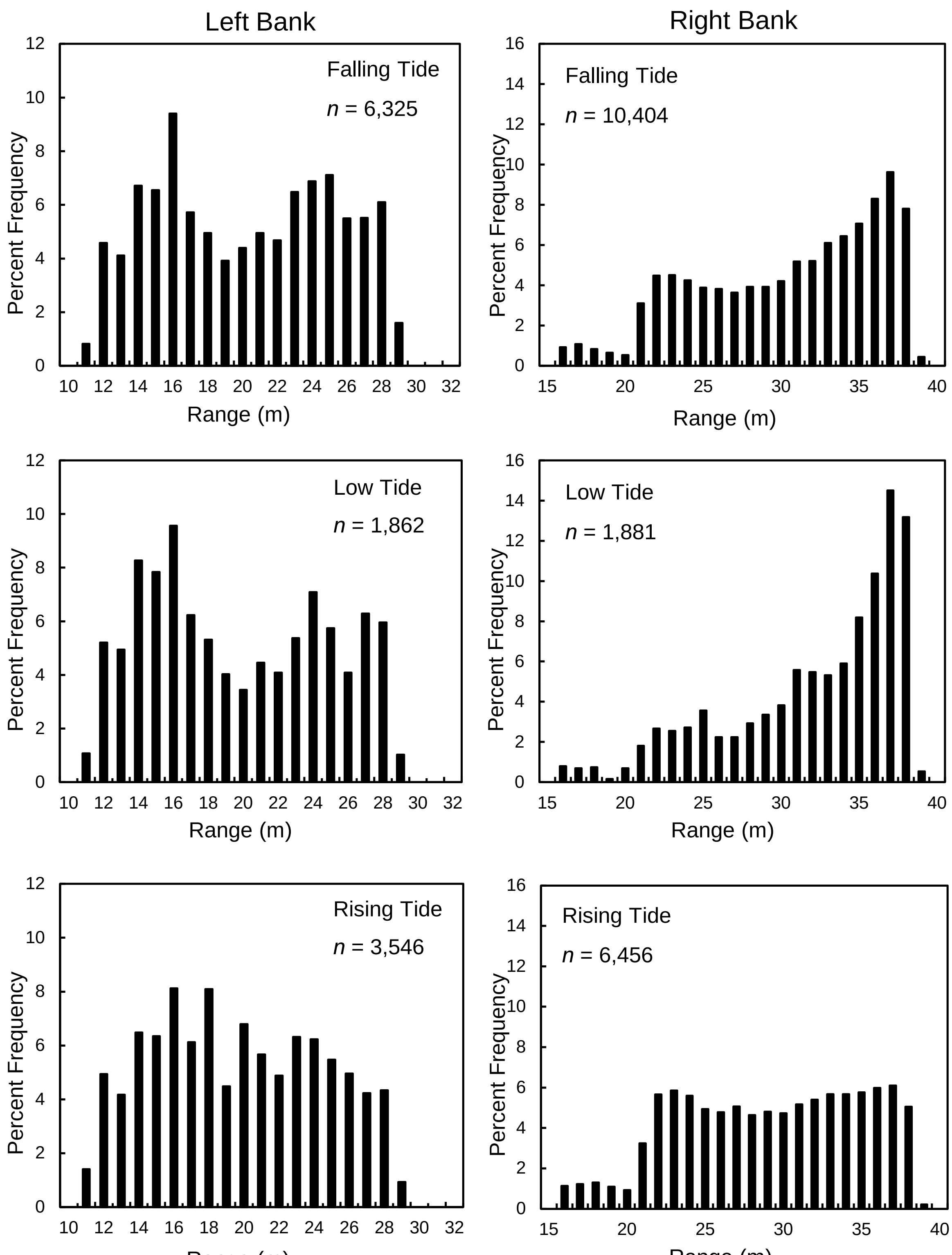

Note: Data have been filtered by range (distance from transducer) and target strength criteria.

Figure 18.–Standardized distance from transducer of late-run upstream moving filtered split-beam targets by tide stage and bank, Kenai River RM 8.5, 2010.

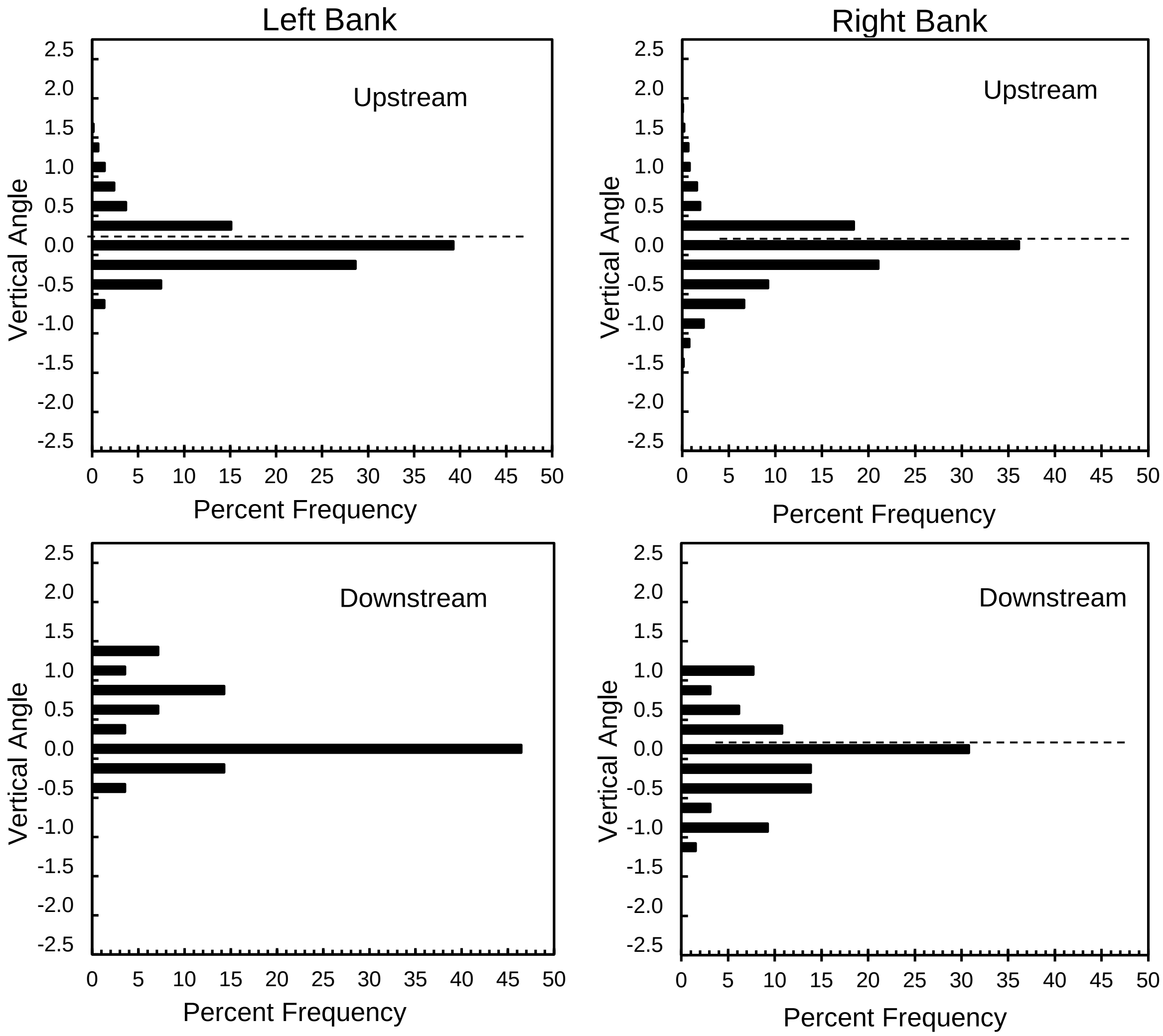

Note: Data have been filtered by range (distance from transducer) and target strength criteria. Acoustic axis = 0.0.

Figure 19.–Vertical distributions above and below the acoustic axis of early-run upstream and downstream moving filtered split-beam targets by bank, Kenai River RM 8.5, 2010.

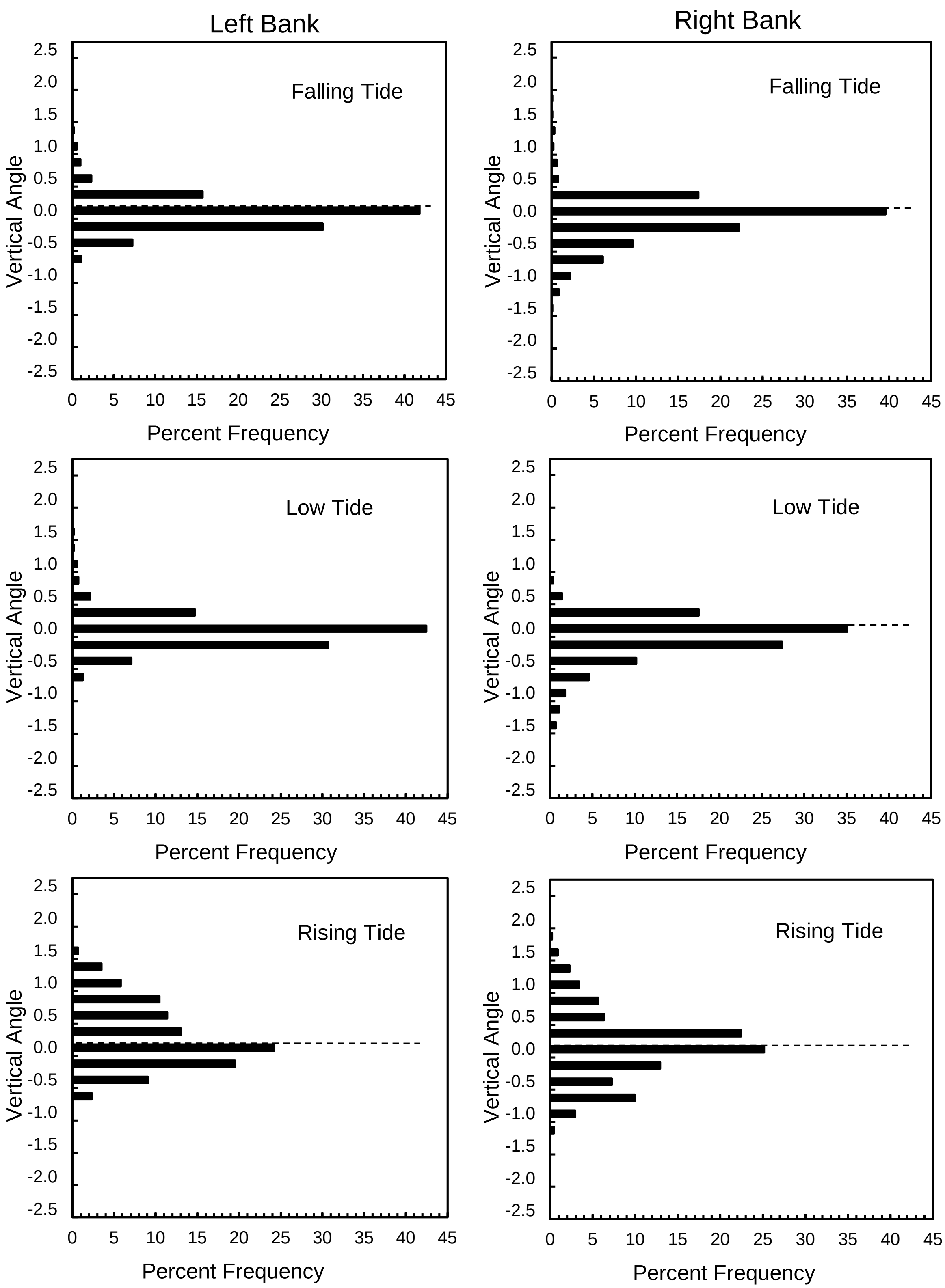

Note: Data have been filtered by range (distance from transducer) and target strength criteria. Acoustic axis = 0.0.

Figure 20.–Vertical distributions above and below the acoustic axis of early-run upstream moving filtered split-beam targets by tide stage and bank, Kenai River RM 8.5, 2010.

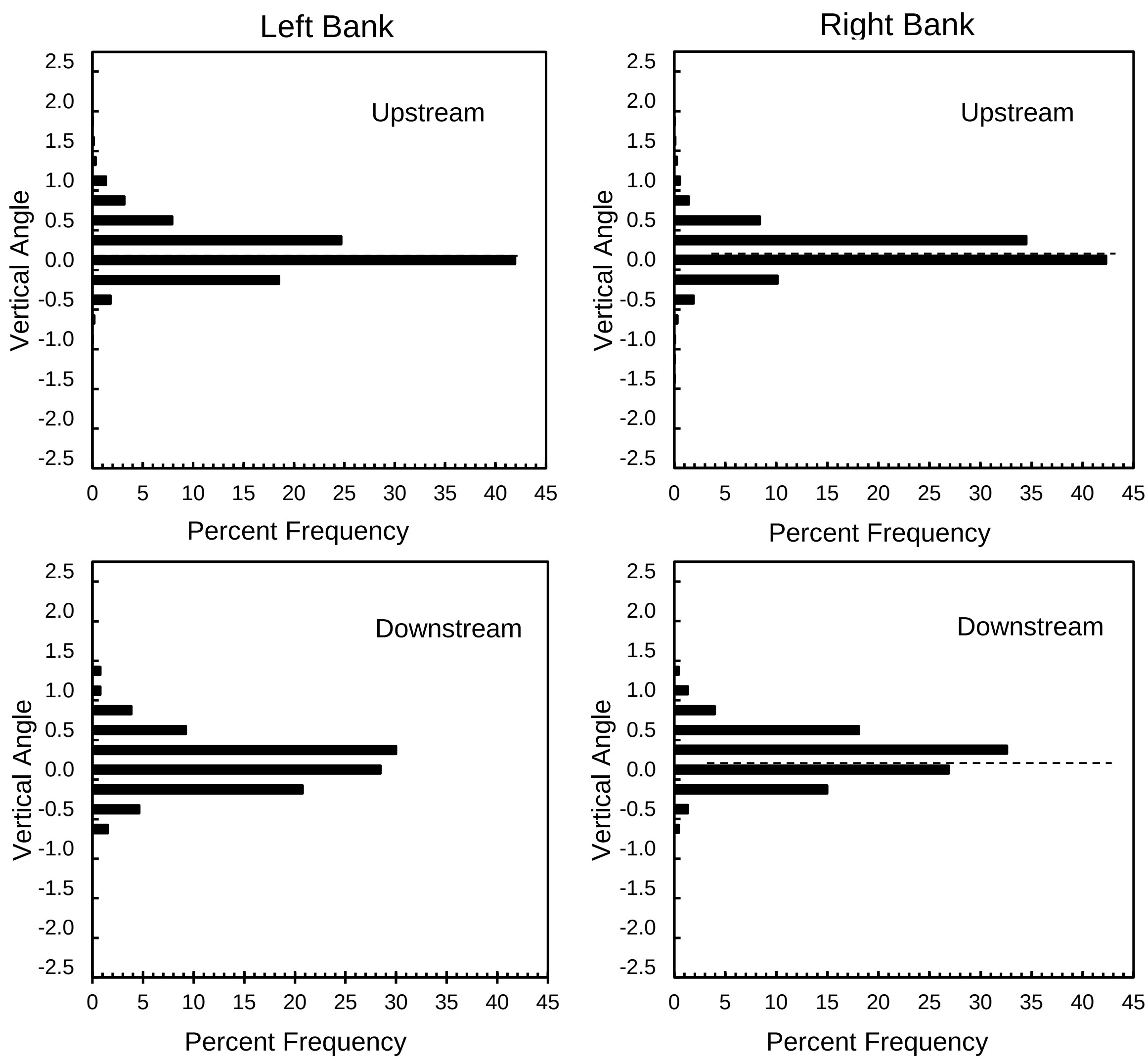

Note: Data have been filtered by range (distance from transducer) and target strength criteria. Acoustic axis = 0.0.

Figure 21.–Vertical distributions above and below the acoustic axis of late-run upstream and downstream moving filtered split-beam targets by bank, Kenai River RM 8.5, 2010.

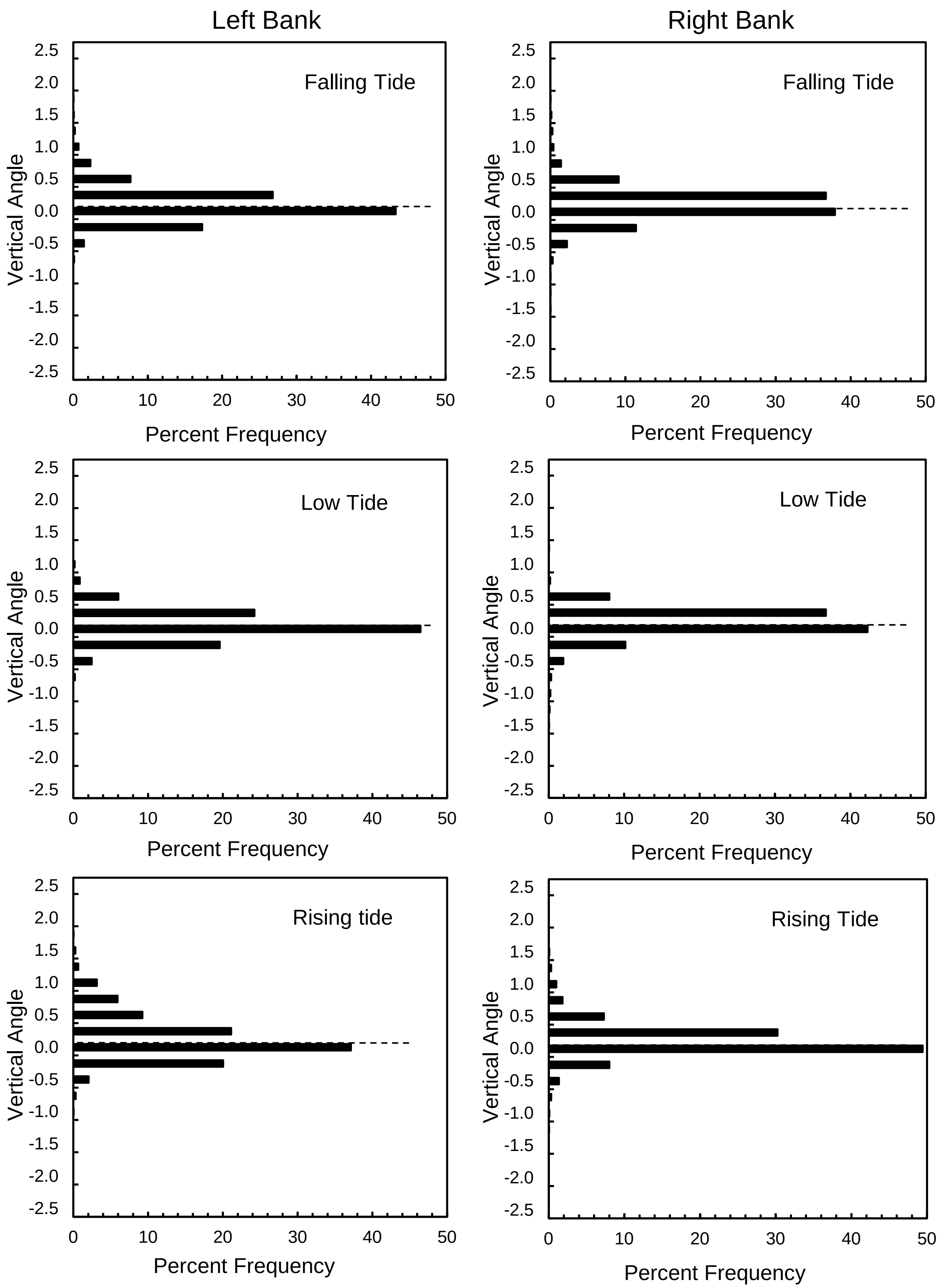

Note: Data have been filtered by range (distance from transducer) and target strength criteria. Acoustic axis = 0.0.

Figure 22.–Vertical distributions above and below the acoustic axis of late-run upstream moving filtered split-beam targets by tide stage and bank, Kenai River RM 8.5, 2010.

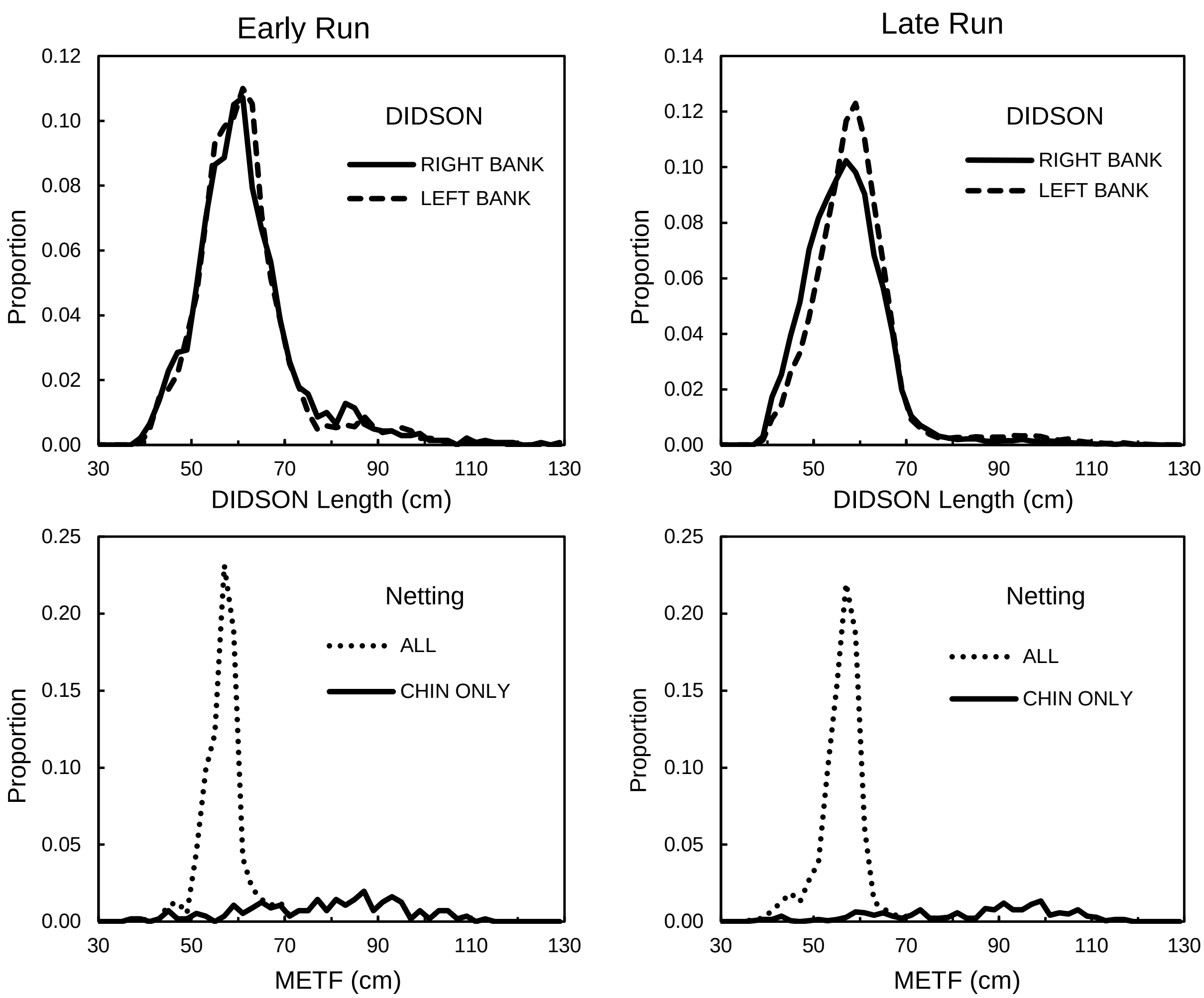

Note: data were not filtered by direction of travel.

Figure 23.–Frequency distributions of fish length as measured by the DIDSON (top, by bank) and mid eye to tail fork measurements from an onsite netting project (bottom, all species vs. Chinook salmon only), Kenai River RM 8.5, early and late runs, 2010.

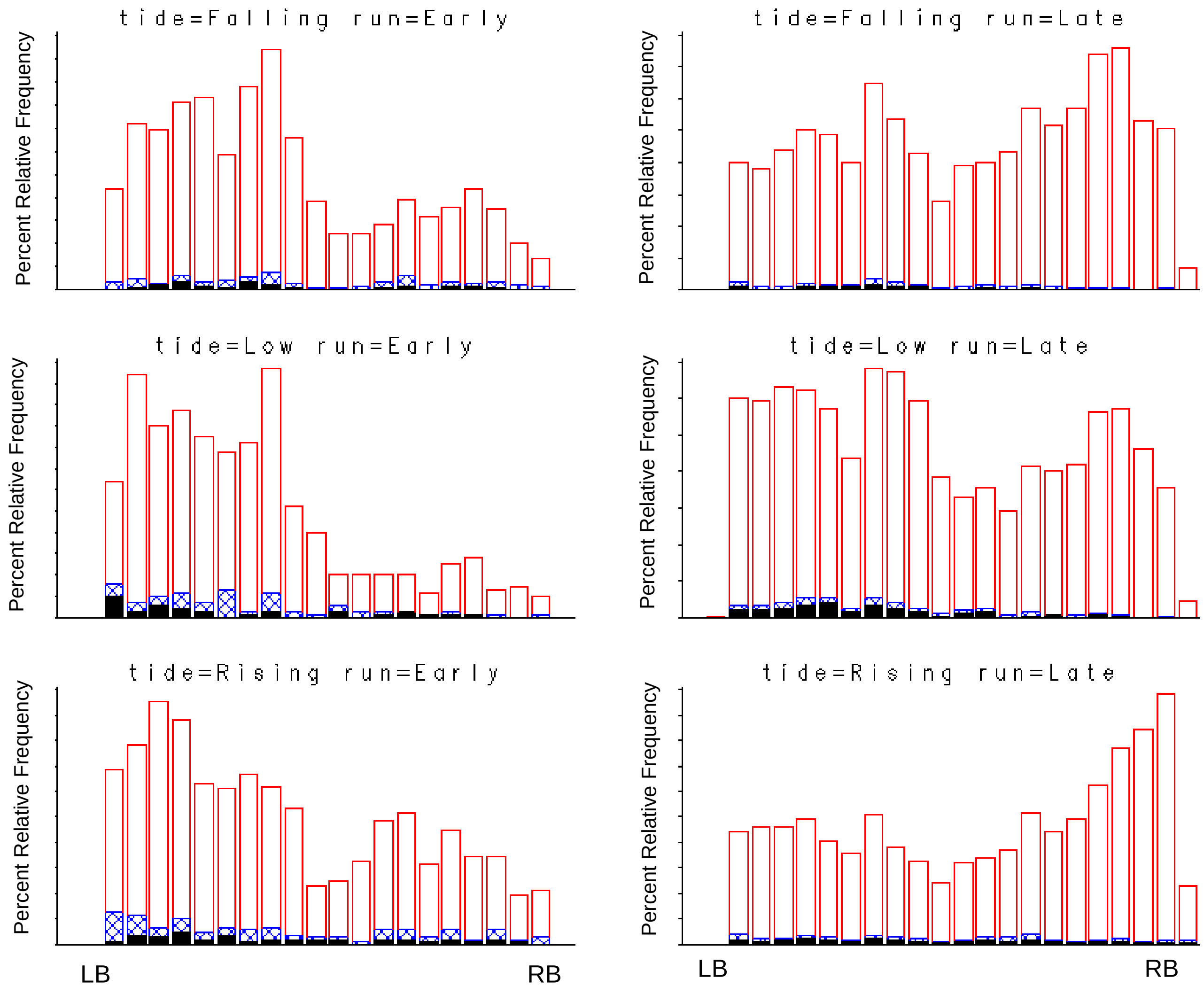

Note: Approximately 60 meters separates the left-bank (LB) and right-bank (RB) transducers.

Figure 24.–Relative frequency distribution of horizontal (cross-river) position of upstream bound fish, by tide stage and DIDSON length class (black solid = $\geq$90 cm, blue hatched = 75–90 cm, red open = <75 cm), Kenai River RM 8.5, early and late runs, 2010.

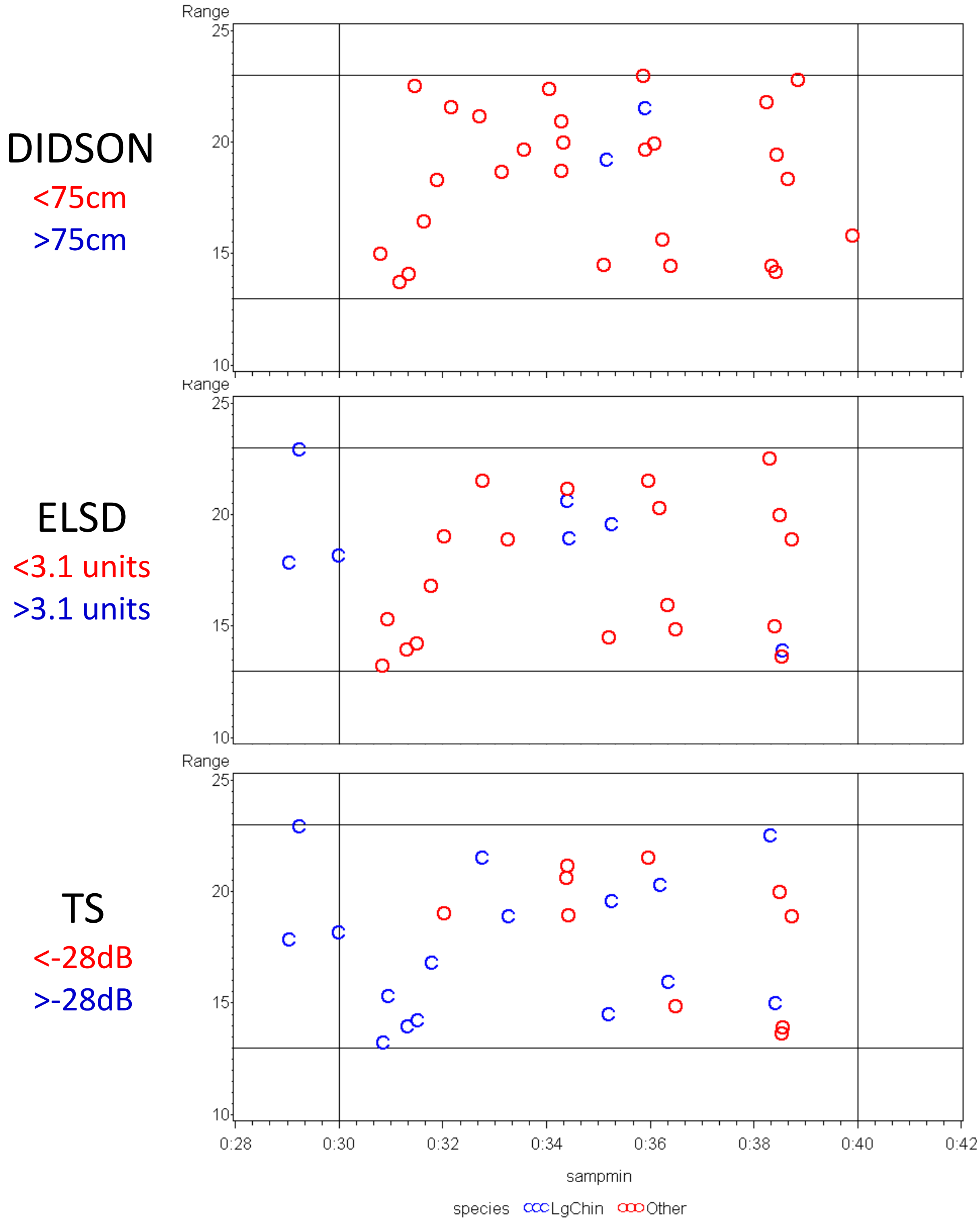

Note: Symbol "C" represents an upstream bound fish classified as a large Chinook salmon, symbol "O" represents an upstream bound fish classified as a small Chinook salmon or other species.

Figure 25.–Typical 10-minute matched sample of DIDSON and split-beam sonar data (20 July, south bank, mid-range stratum, 2330–2340 hours).

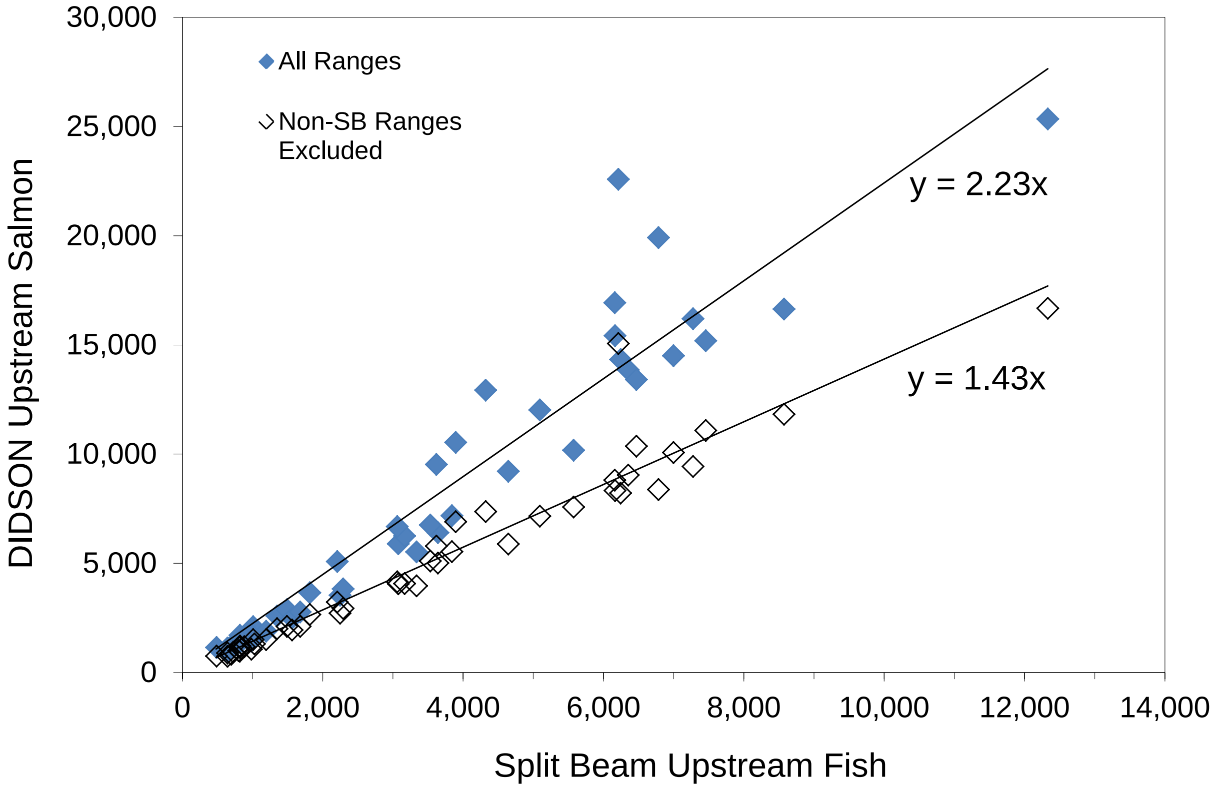

Note: Two versions of DIDSON estimates are shown: with fish at all ranges included, and with fish outside of split-beam ranges excluded.

Figure 26.–Daily midriver upstream salmon passage at RM 8.5 Kenai River as determined by DIDSON versus split-beam sonar, 11 June–4 August 2010.

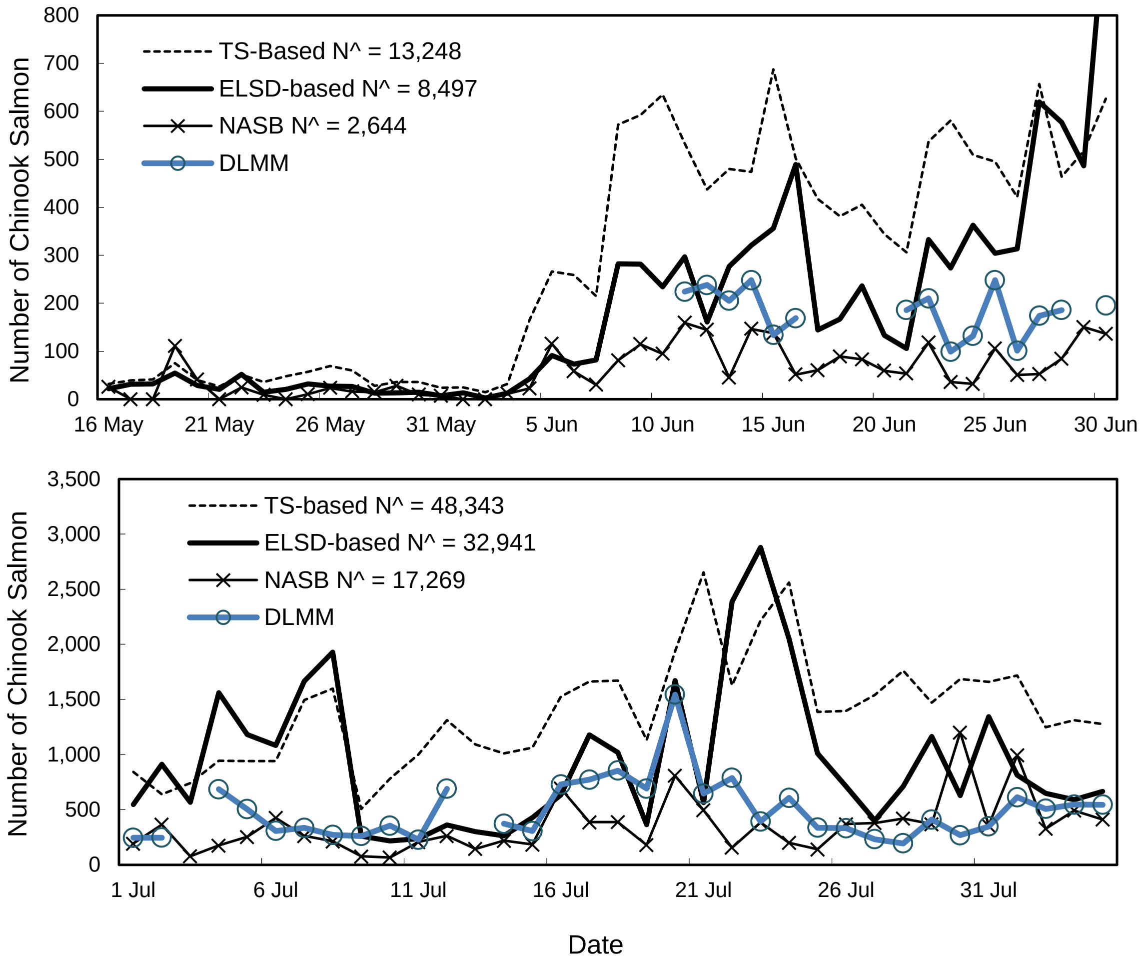

Figure 27.–Estimated upstream bound fish passage based on TS-based split-beam sonar, net-apportioned split-beam sonar (NASB), ELSD-based sonar, and DIDSON-length mixture model (DLMM), for early- (top) and late-run (bottom) Kenai River Chinook salmon, 2010.

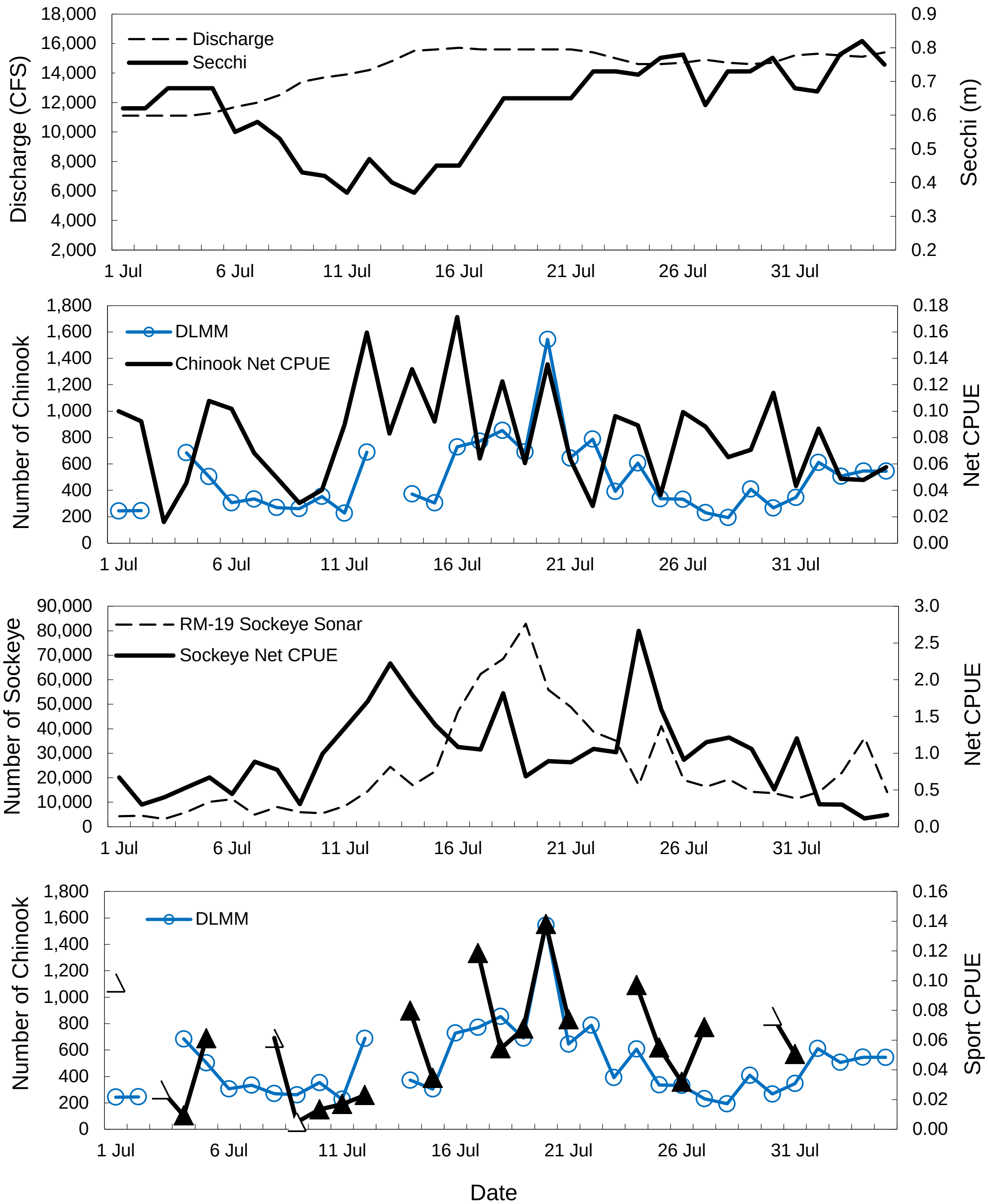

Note: river discharge taken from USGS.[37] Net CPUE and sport fish CPUE taken from Perschbacher (2012). Open triangles represent days on which only unguided anglers were allowed to fish. RM-19 sonar from Westerman and Willette (2011).

Figure 28.–Daily discharge rates collected at the Soldotna Bridge and Secchi disk readings taken at the RM-8.5 sonar site (A), DIDSON-length mixture model (DLMM) estimates of Chinook salmon passage and inriver gillnet Chinook salmon CPUE (B), RM-19 sockeye salmon sonar passage and inriver gillnet sockeye salmon CPUE (C), and DLMM estimates compared to Chinook salmon sport fishery CPUE (D), Kenai River, late run, 2010.

[37] USGS Water resource data, Alaska, water year 2010. Website Daily Streamflow for Alaska, Soldotna gauging station, site #15266300, accessed September 23, 2010. http://water.usgs.gov/ak/nwis/discharge.

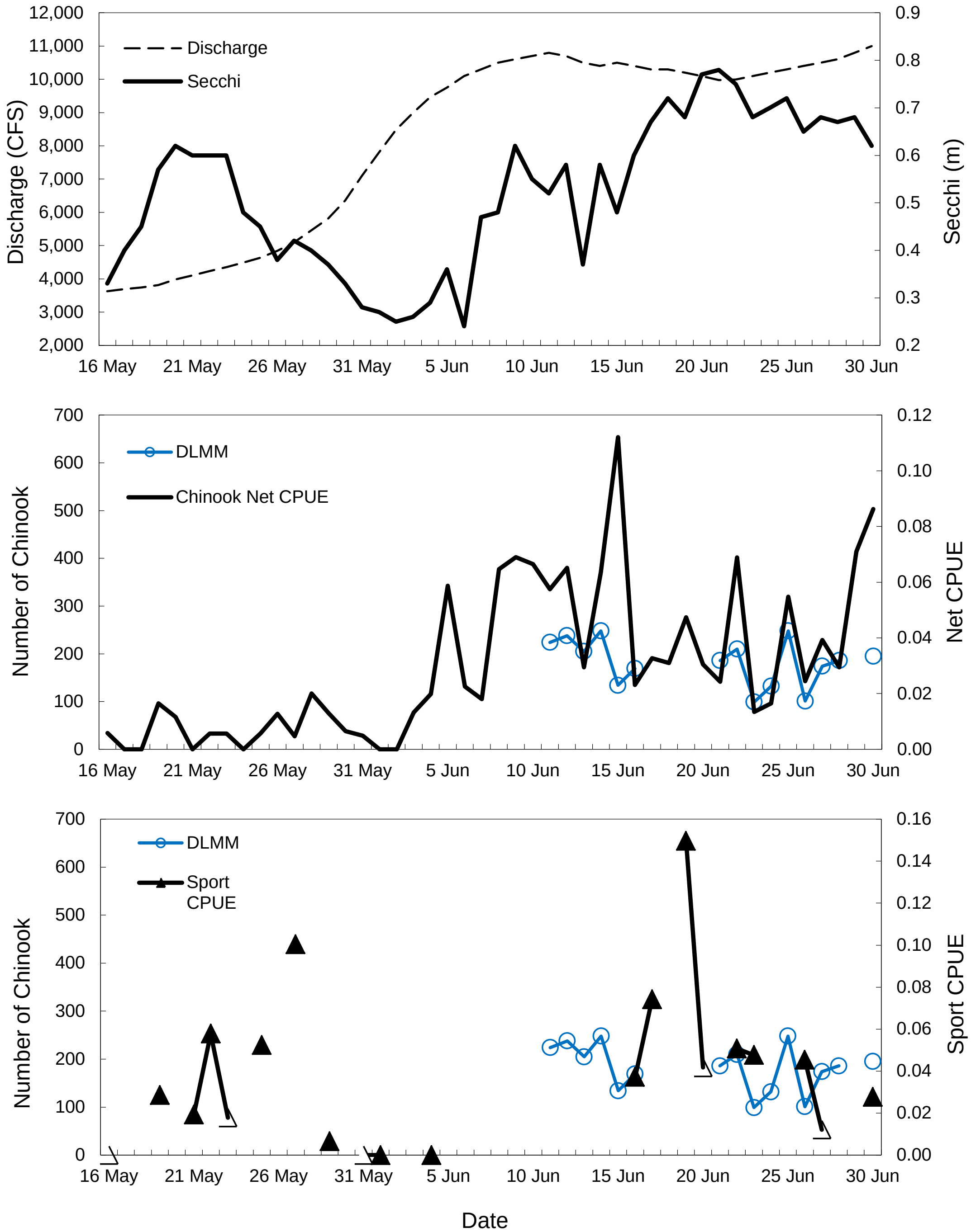

Note: river discharge taken from USGS[38]. Net CPUE and sport fish CPUE taken from Perschbacher (2012). Open triangles represent days on which only unguided anglers were allowed to fish.

Figure 29.–Daily discharge rates collected at the Soldotna Bridge and Secchi disk readings taken from the sonar site (A), DIDSON-length mixture model (DLMM) estimates of Chinook salmon passage and inriver gillnet Chinook salmon CPUE (B), and DLMM estimates compared to Chinook salmon sport fishery CPUE (C), Kenai River, early run, 2010.

[38] USGS Water resource data, Alaska, water year 2010. Website Daily Streamflow for Alaska, Soldotna gauging station, site #15266300, accessed September 23, 2010. http://water.usgs.gov/ak/nwis/discharge.

APPENDIX A: TARGET STRENGTH ESTIMATION

Appendix A1.–The sonar equation used to estimate target strength in decibels with dual- and split-beam applications.

Target strength (TS), in decibels (dB), of an acoustic target located at range R (in meters), θ degrees from the maximum response axis (MRA) in one plane and ϕ degrees from the MRA in the other plane is estimated as follows:

$$TS = 20\log_{10}(V_0) - SL - G_r + 40\log_{10}(R) + 2\alpha R - G_{TVG} - 2B(\theta,\phi)$$

where

V_0	=	voltage of the returned echo, output by the echo sounder,
SL	=	source level of transmitted signal in dB,
G_r	=	receiver gain in dB,
$40\log_{10}(R)$	=	2-way spherical spreading loss in dB,
$2\alpha R$	=	2-way absorption loss in dB,
G_{TVG}	=	time-varied gain correction of the echo sounder, and
$2B(\theta,\phi)$	=	2-way loss due to position of the target off of the MRA.

The source level and gain are measured during calibration and confirmed using *in situ* standard sphere measurements. The time-varied gain correction compensates for spherical spreading loss. Absorption loss ($2\alpha R$) was ignored in this study.

In practice, the location of the target in the beam (θ and ϕ) is not known, so $B(\theta,\phi)$ must be estimated in order to estimate target strength. Dual-beam and split-beam sonars differ in how they estimate $B(\theta,\phi)$, also called the beam pattern factor.

Dual-beam sonar (Ehrenberg 1983) uses one wide and one narrow beam. The system transmits on the narrow beam only and receives on both. The ratio between the voltages of the received signals is used to estimate beam pattern factor:

$$B(\theta,\phi) = 20\log_{10}(V_N/V_W) \times WBDO$$

where V_N is the voltage of the returned echo on the narrow beam, V_W is the voltage of the echo on the wide beam, *WBDO* is the wide beam drop-off correction, specific to each transducer and estimated at calibration.

Split-beam sonar (MacLennan and Simmonds 1992) estimates target location (angles θ and ϕ of the target from the MRA) directly, not just the beam pattern factor ($B[\theta,\phi]$). Split-beam transducers are divided into 4 quadrants, and θ and ϕ are estimated by comparing the phases of signals received by opposing pairs of adjacent quadrants. The beam pattern factor is a function of θ and ϕ, determined during laboratory calibration.

APPENDIX B: SPLIT-BEAM SONAR SYSTEM PARAMETERS

Appendix B1.–Example of system parameters used for data collection on the right bank (transducer 733).

Parameter number	Subfield number[a]	Parameter value	Parameter description
100	-1	1	MUX argument #1 - multiplexer port to activate
101	-1	0	percent - sync pulse switch, ping rate determiner NUS
102	-1	13201	maxp - maximum number of pings in a block NUS
103	-1	32767	maxbott - maximum bottom range in samples NUS
104	-1	13	N_th_layer - number of threshold layers
105	-1	5	max_tbp - maximum time between pings in pings
106	-1	5	min_pings - minimum number of pings per fish
507	-1	FED5	timval - 0xFED5 corresponds to about 20 kHz NUS
108	-1	1	mux_on - means multiplexing enabled on board NUS
109	-1	200	mux_delay - samples delay between sync and switching NUS
110	-1	0	decimate_mask - decimate input samples flag NUS
112	-1	1	echogram_on - flag for DEP echogram enable 0=off, 1=on
113	-1	1	Hourly Sampling flag 1=On 0=Off
118	-1	5	maxmiss - maximum number of missed pings in auto bottom
119	-1	0	bottom-0=fix, 1=man, 2=scope, 3=acq_chan1, 4=acq_chan2, 5=auto_1, 6=auto_chan2
120	-1	0	sb_int_code - sb only=0, sb-int: 40log a bot=1, 20log=2
121	-1	0	sb_int_code2 - sb only=0, sb-int 40log eg=0, 20log=2
122	-1	13	N_int_layers-number of integration strata
123	-1	13	N_int_th_layers - number of integration threshold strata
124	-1	0	int_print - print integrator interval results to printer
125	-1	0	circular element transducer flag for bpf calculation
126	-1	80	grid spacing for Model 404 DCR (in samples, 16 s/m)
127	-1	1	TRIG argument #1 - trigger source
128	-1	0	TRIG argument #2 - digital data routing
130	-1	0	TVG Blank (0=Both Start/End,1=Stop Only,2=Start Only,3=None)
200	-1	20	sigma flag 0.0 = no sigma, else sigma is output
201	-1	221.08	sl - transducer source level
202	-1	-171.1	gn - transducer through system gain at one meter
203	-1	-18	rg - receiver gain used to collect data
204	-1	2.8	narr_ax_bw - vertical nominal beam width
205	-1	10	wide_ax_bw - horizontal axis nominal beam width
206	-1	0	narr_ ax_corr - vertical axis phase correction
207	-1	0	wide_ax_corr - horizontal axis phase correction
208	-1	11.0011	ping_rate - pulses per second
209	-1	0	echogram start range in meters
210	-1	40.5	echogram stop range in meters
211	-1	706	echogram threshold in millivolts
212	-1	13.2	print width in inches
213	-1	0	Chirp Bandwidth (0.0 = CHIRP OFF)
214	-1	20	Sampling within Hour Ending Time (in Decimal Minutes)
215	-1	1500	Speed of Sound (m/s)
216	-1	200	The Transducer's Frequency (kHz)
217	-1	-2.5	min_angoff_v - minimum angle off axis vertical
218	-1	2	max_angoff_v - maximum angle off axis vertical
219	-1	-5	min_angoff_h - minimum angle off axis horiz.

-continued-

Appendix B1.–Part 2 of 3

Parameter number	Subfield number[a]	Parameter value	Parameter description
220	-1	5	max_angoff_ h - maximum angle off axis horiz.
221	-1	-24	max_dB_off - maximum angle off in dB
222	-1	-16.2706	ux - horizontal electrical to mechanical angle ratio
223	-1	-32.7499	uy - vertical electrical to mechanical angle ratio
224	-1	0	ud_coef_a - a coeff. for up-down beam pattern eq.
225	-1	-0.0053	ud_coef_b - b coeff. for up-down beam pattern eq.
226	-1	-2.4245	ud_coef_c - c coeff. for up-down beam pattern eq.
227	-1	0.093	ud_coef_d - d coeff. for up-down beam pattern eq.
228	-1	-0.1658	ud_coef_e - e coeff. for up-down beam pattern eq.
229	-1	0	lr_coef_a - a coeff. for left-rt beam pattern eq.
230	-1	-0.0002	lr_coef_b - b coeff. for left-rt beam pattern eq.
231	-1	-0.2163	lr_coef_c - c coeff . for left-rt beam pattern eq.
232	-1	0.0007	lr_coef_d - d coeff. for left-rt beam pattern eq.
233	-1	-0.0002	lr_coef_e - ecoeff. for left-rt beam pattern eq.
234	-1	4	maximum fish velocity in meters per second
235	-1	1	Echo Scope Bottom Location
236	-1	0.4	maxpw - pulse width search window size
238	-1	38.5	bottom - bottom depth in meters
239	-1	0	init_slope - initial slope for tracking in m/ping
240	-1	0.2	exp_cont - exponent for expanding tracking window
241	-1	0.2	max_ch_rng - maximum change in range in m/ping
242	-1	0.04	pw_criteia->min_pw_6-min -6 dB pulse width
243	-1	10	pw_criteria->max_pw_6-max -6 dB pulse width
244	-1	0.04	pw_criteria->min_pw_12 - min -12 dB pulse width
245	-1	10	pw_criteria->max_pw_12 - max -12 dB pulse width
246	-1	0.04	pw_criteria->min_pw_18 - min -18 dB pulse width
247	-1	10	pw_criteria->max_pw_18 - max -18 dB pulse width
249	-1	10	maximum voltage to allow in .RAW file
250	-1	0.2	TX argument #1 - pulse width in milliseconds
251	-1	25	TX argument #2 - transmit power in dB-watts
252	-1	-12	RX argument #1 - receiver gain
253	-1	90.9	REP argument #1 - ping rate in ms per ping
254	-1	10	REP argument #2 - pulsed cal tone separation
255	-1	1	TVG argument #1 - TVG start range in meters
256	-1	100	TVG argument #2 - TVG end range in meters
257	-1	40	TVG argument #3 - TVG function (XX Log Range)
258	-1	-6	TVG argument #4 - TVG gain
259	-1	0	TVG argument #5 - alpha (spreading loss) in dB/Km
260	-1	0.2	minimum absolute distance fish must travel in x plane
261	-1	0.2	minimum absolute distance fish must travel in y plane
262	-1	0.2	minimum absolute distance fish must travel in z plane
263	-1	2	bottom_window - auto tracking bottom window (m)
264	-1	3	bottom_threshold - auto tracking bottom threshold (V)
265	-1	11.2	TVG argument #7 - 20/40 log crossover (meters)
266	-1	0	rotator - which rotator to aim
267	-1	0	aim_pan - transducer aiming angle in pan (x, lf/rt)
268	-1	0	aim_tilt - transducer aiming angle in tilt (y, u/d)

-continued-

Appendix B1.–Part 3 of 3.

Parameter number	Subfield number[a]	Parameter value	Parameter description
401	0	1	th_layer[0] – bottom of first threshold layer (m)
401	1	5	th_layer[1] – bottom of second threshold layer (m)
401	2	10	th_layer[2] – bottom of third threshold layer (m)
401	3	15	th_layer[3] – bottom of fourth threshold layer (m)
401	4	20	th_layer[4] – bottom of fifth threshold layer (m)
401	5	25	th_layer[5] – bottom of sixth threshold layer (m)
401	6	30	th_layer[6] – bottom of seventh threshold layer (m)
401	7	35	th_layer[7] – bottom of eighth threshold layer (m)
401	8	40	th_layer[8] – bottom of ninth threshold layer (m)
401	9	45	th_layer[9] – bottom of tenth threshold layer (m)
401	10	50	th_layer[10] – bottom of eleventh threshold layer (m)
401	11	55	th_layer[11] – bottom of twelfth threshold layer (m)
401	12	60	th_layer[12] – bottom of thirteenth threshold layer (m)
402	0	706	th_val[0], threshold for 1st layer in millivolts
402	1	706	th_val[1], threshold for 2nd layer in millivolts
402	2	706	th_val[2], threshold for 3rd layer in millivolts
402	3	706	th_val[3], threshold for 4th layer in millivolts
402	4	706	th_val[4], threshold for 5th layer in millivolts
402	5	706	th_val[5], threshold for 6th layer in millivolts
402	6	706	th_val[6], threshold for 7th layer in millivolts
402	7	706	th_val[7], threshold for 8th layer in millivolts
402	8	706	th_val[8], threshold for 9th layer in millivolts
402	9	706	th_val[9], threshold for 10th layer in millivolts
402	10	706	th_val[10], threshold for 11th layer in millivolts
402	11	706	th_val[11], threshold for 12th layer in millivolts
402	12	9999	th_val[12], threshold for 13th layer in millivolts
405	0	100	Integration threshold value for layer 1 (mV)
405	1	100	Integration threshold value for layer 2 (mV)
405	2	100	Integration threshold value for layer 3 (mV)
405	3	100	Integration threshold value for layer 4 (mV)
405	4	100	Integration threshold value for layer 5 (mV)
405	5	100	Integration threshold value for layer 6 (mV)
405	6	100	Integration threshold value for layer 7 (mV)
405	7	100	Integration threshold value for layer 8 (mV)
405	8	100	Integration threshold value for layer 9 (mV)
405	9	100	Integration threshold value for layer 10 (mV)
405	10	100	Integration threshold value for layer 11 (mV)
405	11	100	Integration threshold value for layer 12 (mV)
405	12	9999	Integration threshold value for layer 13 (mV)
602	-1	1017536	Echo sounder serial number
604	-1	306733	Transducer serial number
605	-1	Spd-4	Echogram paper speed
606	-1	9_pin	Echogram resolution
607	-1	Board_Ext	Trigger option
608	-1	LeftToRight	River flow direction

Note: Start processing at Port 1 –FILE_PARAMETERS- Thurs. 1 July 12:00:03 2010.

Note: Data processing parameters used in collecting this file for Port 1.

[a] -1 = unique record or field; other values represent the threshold layer number.

Appendix B2.–Example of system parameters used for data collection on the left bank (transducer 738).

Parameter number	Subfield number[a]	Parameter value	Parameter description
100	-1	2	MUX argument #1 - multiplexer port to activate
101	-1	0	percent - sync pulse switch, ping rate determiner NUS
102	-1	19200	maxp - maximum number of pings in a block NUS
103	-1	32767	maxbott - maximum bottom range in samples NUS
104	-1	293	N_th_layer - number of threshold layers
105	-1	5	max_tbp - maximum time between pings in pings
106	-1	5	min_pings - minimum number of pings per fish
507	-1	FED5	timval - 0xFED5 corresponds to about 20 kHz NUS
108	-1	1	mux_on - means multiplexing enabled on board NUS
109	-1	200	mux_delay - samples delay between sync and switching NUS
110	-1	0	decimate_mask - decimate input samples flag NUS
112	-1	1	echogram_on - flag for DEP echogram enable 0=off, 1=on
113	-1	1	Hourly Sampling flag 1=On 0=Off
118	-1	5	maxmiss - maximum number of missed pings in auto bottom
119	-1	0	bottom-0=fix, 1=man, 2=scope, 3=acq_chan1, 4=acq_chan2, 5=auto_1, 6=auto_chan2
120	-1	0	sb_int_code - sb only=0, sb-int: 40log a bot=1, 20log=2
121	-1	0	sb_int_code2 - sb only=0, sb-int 40log eg=0, 20log=2
122	-1	293	N_int_layers-number of integration strata
123	-1	293	N_int_th_layers - number of integration threshold strata
124	-1	0	int_print - print integrator interval results to printer
125	-1	0	circular element transducer flag for bpf calculation
126	-1	80	grid spacing for Model 404 DCR (in samples, 16 s/m)
127	-1	1	TRIG argument #1 - trigger source
128	-1	0	TRIG argument #2 - digital data routing
130	-1	0	TVG Blank (0=Both Start/End,1=Stop Only,2=Start Only,3=None)
200	-1	20	sigma flag 0.0 = no sigma, else sigma is output
201	-1	219.07	sl - transducer source level
202	-1	-173.39	gn - transducer through system gain at one meter
203	-1	-18	rg - receiver gain used to collect data
204	-1	2.8	narr_ax_bw - vertical nominal beam width
205	-1	10	wide_ax_bw - horizontal axis nominal beam width
206	-1	0	narr_ ax_corr - vertical axis phase correction
207	-1	0	wide_ax_corr - horizontal axis phase correction
208	-1	16	ping_rate - pulses per second
209	-1	0	echogram start range in meters
210	-1	25.5	echogram stop range in meters
211	-1	431	echogram threshold in millivolts
212	-1	13.2	print width in inches
213	-1	0	Chirp Bandwith (0.0 = CHIRP OFF)
214	-1	40	Sampling within Hour Ending Time (in Decimal Minutes)
215	-1	1500	Speed of Sound (m/s)
216	-1	200	The Transducer's Frequency (kHz)
217	-1	-2.5	min_angoff_v - minimum angle off axis vertical
218	-1	2	max_angoff_v - maximum angle off axis vertical
219	-1	-5	min_angoff_h - minimum angle off axis horiz.

-continued-

Appendix B2.–Part 2 of 3.

Parameter number	Subfield number[a]	Parameter value	Parameter description
220	-1	5	max_angoff_ h - maximum angle off axis horiz.
221	-1	-24	max_dB_off - maximum angle off in dB
222	-1	-16.2282	ux - horizontal electrical to mechanical angle ratio
223	-1	-55.4983	uy - vertical electrical to mechanical angle ratio
224	-1	0	ud_coef_a - a coeff. for up-down beam pattern eq.
225	-1	0.0095	ud_coef_b - b coeff. for up-down beam pattern eq.
226	-1	-2.9375	ud_coef_c - c coeff. for up-down beam pattern eq.
227	-1	-0.1411	ud_coef_d - d coeff. for up-down beam pattern eq.
228	-1	-0.1196	ud_coef_e - e coeff. for up-down beam pattern eq.
229	-1	0	lr_coef_a - a coeff. for left-rt beam pattern eq.
230	-1	-0.0045	lr_coef_b - b coeff. for left-rt beam pattern eq.
231	-1	-0.2558	lr_coef_c - c coeff . for left-rt beam pattern eq.
232	-1	0.0009	lr_coef_d - d coeff. for left-rt beam pattern eq.
233	-1	-0.0001	lr_coef_e - ecoeff. for left-rt beam pattern eq.
234	-1	4	maximum fish velocity in meters per second
235	-1	1	Echo Scope Bottom Location
236	-1	0.4	maxpw - pulse width search window size
238	-1	24.5	bottom - bottom depth in meters
239	-1	0	init_slope - initial slope for tracking in m/ping
240	-1	0.2	exp_cont - exponent for expanding tracking window
241	-1	0.2	max_ch_rng - maximum change in range in m/ping
242	-1	0.04	pw_criteria->min_pw_6-min -6 dB pulse width
243	-1	10	pw_criteria->max_pw_6-max -6 dB pulse width
244	-1	0.04	pw_criteria->min_pw_12 - min -12 dB pulse width
245	-1	10	pw_criteria->max_pw_12 - max -12 dB pulse width
246	-1	0.04	pw_criteria->min_pw_18 - min -18 dB pulse width
247	-1	10	pw_criteria->max_pw_18 - max -18 dB pulse width
249	-1	10	maximum voltage to allow in .RAW file
250	-1	0.2	TX argument #1 - pulse width in milliseconds
251	-1	25	TX argument #2 - transmit power in dB-watts
252	-1	-12	RX argument #1 - receiver gain
253	-1	62.5	REP argument #1 - ping rate in ms per ping
254	-1	10	REP argument #2 - pulsed cal tone separation
255	-1	2	TVG argument #1 - TVG start range in meters
256	-1	100	TVG argument #2 - TVG end range in meters
257	-1	40	TVG argument #3 - TVG function (XX Log Range)
258	-1	-6	TVG argument #4 - TVG gain
259	-1	0	TVG argument #5 - alpha (spreading loss) in dB/Km
260	-1	0.2	minimum absolute distance fish must travel in x plane
261	-1	0.2	minimum absolute distance fish must travel in y plane
262	-1	0.2	minimum absolute distance fish must travel in z plane
263	-1	2	bottom_window - auto tracking bottom window (m)
264	-1	3	bottom_threshold - auto tracking bottom threshold (V)
265	-1	11.2	TVG argument #7 - 20/40 log crossover (meters)
266	-1	0	rotator - which rotator to aim
267	-1	0	aim_pan - transducer aiming angle in pan (x, lf/rt)
268	-1	0	aim_tilt - transducer aiming angle in tilt (y, u/d)

-continued-

Appendix B2.–Part 3 of 3.

Parameter number	Subfield number[a]	Parameter value	Parameter description
401	0-292	1-30.2	th_layer[0-292], bottom of 1st threshold layer – bottom of 293rd threshold layer (i.e. 293 threshold layers in 0.1 m increments and numbered 0 through 292)
402	0-291	431	th_val[0-291], threshold for 1st through 292nd layer in millivolts
402	292	9999	th_val[292], threshold for 293rd layer in millivolts
405	0-291	100	Integration threshold value for layer 1-292 (mV)
405	292	9999	Integration threshold value for layer 293 (mV)
602	-1	1017536	Echo sounder serial number
604	-1	306738	Transducer serial number
605	-1	Spd-4	Echogram paper speed
606	-1	9_pin	Echogram resolution
607	-1	Board_Ext	Trigger option
608	-1	LeftToRight	River flow direction

Note: Start processing at Port 2 –FILE_PARAMETERS- Thurs. 1 July 12:20:03 2010.

Note: Data processing parameters used in collecting this file for Port 2.

[a] -1 = unique record or field; other values represent the threshold layer number.

APPENDIX C: SPLIT-BEAM SONAR DATA FLOW

Appendix C1.–Data flow diagram for the Kenai River Chinook salmon sonar project, 2010.

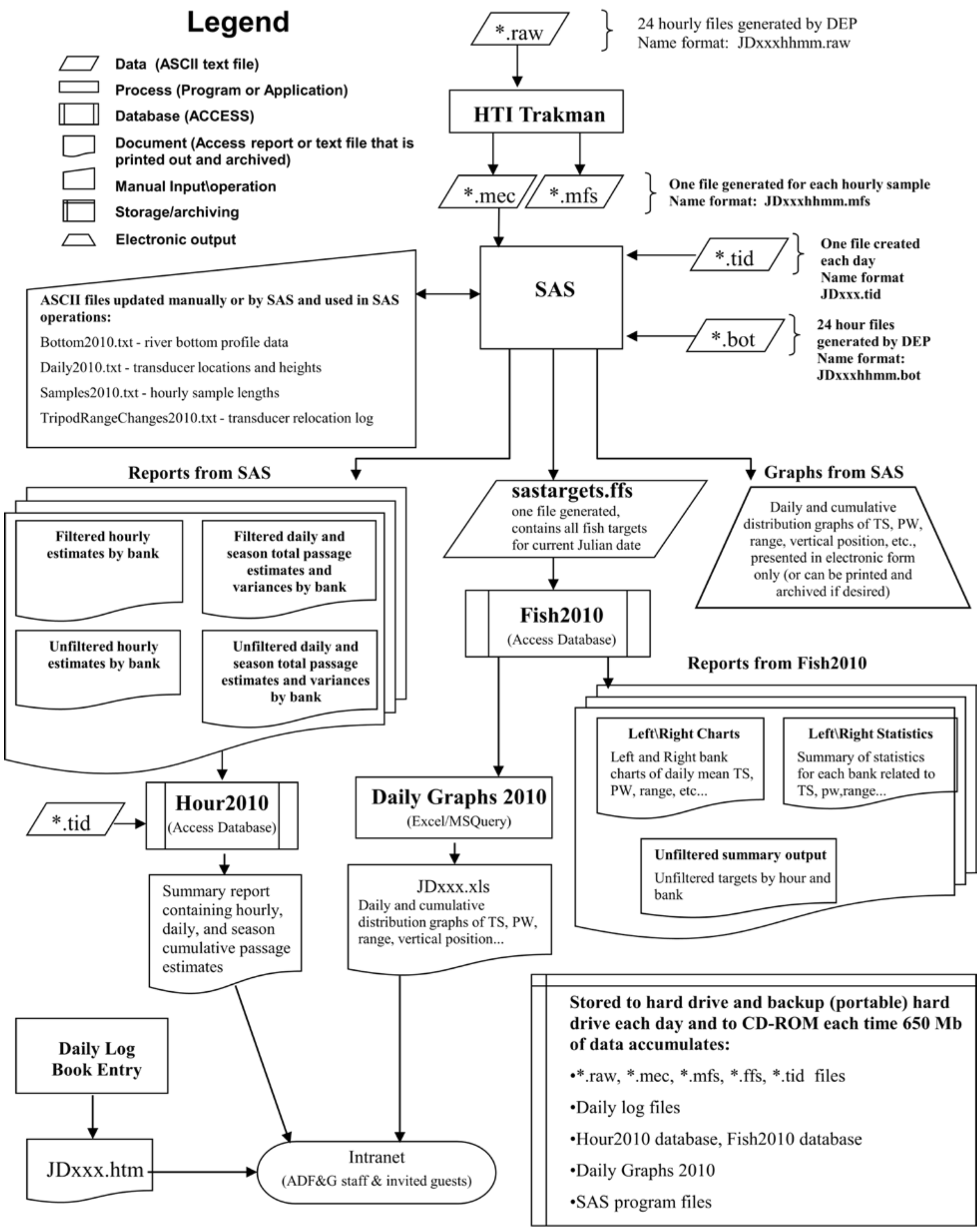

APPENDIX D: SPLIT-BEAM SONAR EXCLUDED HOURLY SAMPLES

Appendix D1.–Hourly samples excluded from calculation of daily Chinook salmon passage estimates using split-beam sonar, Kenai River RM 8.5, 2010.

		Excluded sample hours[a]	
Run	Date	Left bank	Right bank
Early run			
	8 Jun	1520, 1720–1920	1500, 1700, 1900
	10 Jun	1720	–
	11 Jun	1820–1920	1900
	12 Jun	1020, 1920	1900
	13 Jun	1920, 2020	0600, 0900
	14 Jun	1020–1120, 2020–2120	1000–1100, 2100
	15 Jun	1420–1520	1500
	16 Jun	1820–1920	1800–1900
	17 Jun	620	–
	18 Jun	0720–0820	0700–0800, 1100
	19 Jun	2120	1000–1100, 1900
	20 Jun	920	–
	21 Jun	1620, 2320	1600–1700, 2300
	22 Jun	1720	1700
	23 Jun	520	0500–0700, 1600–1700
	24 Jun	–	1400, 1800
	25 Jun	–	1800, 2000
	27 Jun	2100	–
	30 Jun	0920, 1820, 2120	1000, 1800, 2100
Late run			
	2 Jul	520	0700, 1900, 2000
	3 Jul	0720–0820, 1920–2020	0700–0800, 1900–2000, 2200
	4 Jul	0920, 2020–2120	0900–1200, 2000, 2200
	5 Jul	0320–0420, 2220	0300–0400, 2200
	6 Jul	1120, 2120–2220	1100–1200, 2100–2200
	7 Jul	1320, 1720, 2220-2320	1200–1300, 1700, 2200–2300
	8 Jul	0020, 1320–1420	1300–1500
	10 Jul	0720, 2120	0700, 2000–2100
	11 Jul	0820–1020, 1920–2120	0700–1000, 1900–2100
	12 Jul	920	0200, 0800–1000, 1900, 2200
	13 Jul	–	0800–1100
	14 Jul	1000–1100	1020–1120
	15 Jul	0920–1120	1500, 2100

-continued-

Appendix D1. Part 2 of 2.

Run	Date	Excluded sample hours[a] Left bank	Right bank
Late run	16 Jul	0020, 1020–1320, 1820	0000–0100, 0600, 1000–1100
	17 Jul	0820, 1320–1420, 1920–2020, 2220–2320	0700–0800, 1200–1400, 2000–2300
	18 Jul	0820–1020, 1420–1520	0800–1100, 1300–1600, 2200
	19 Jul	1120, 1420	0200, 1100–1200, 1400
	20 Jul	0720, 1120–1220, 1420–1520, 1720–1820, 2220–2320	0200, 0700, 0900, 1100–1500, 1700–1800, 2200–2300
	21 Jul	0020–0420, 1320, 1520, 1820, 2320	0000–0800, 1000, 1300–1600, 1800–1900, 2300
	22 Jul	0020–0320, 0720–0820, 1420–1620, 1920	0000–0300, 0500, 0700–0800, 1400–1700, 1900–2000
	23 Jul	0120–0220, 0820, 1420	0100–0300, 0800, 1400–1500, 1900–2100
	24 Jul	0220–0420, 1220, 1520, 1720, 2220	0200–0500,1500–1800
	25 Jul	0220–0420, 0620–1120, 1620, 2020–2220	0000, 0200–0400, 0600–1100, 1600, 2000–2200
	26 Jul	0720–1020, 2120–2220	0700–1000, 2100–2200
	27 Jul	0920–1020, 1720–1820, 2120–2320	0900–1100, 1700–2320
	28 Jul	0620–0720, 0920–1320, 1720–1920, 2120–2220	0400–0700, 0900–1400, 1700–2300
	29 Jul	0620, 0820–1420, 1720–1820, 2020–2320	0000, 0600–1500, 1700–1800, 2000–2300
	30 Jul	0620–0820, 1020–1420, 1820–2320	0600–1400, 1800–2300
	31 Jul	0020–0120, 0620–1520, 1820–2020, 2320	0000–0100, 0600–1500, 1800–2000, 2300
	1 Aug	0020–0220, 0720–0920, 1220–1320,1720–2020	0000–0200, 0800–1000, 1200–1600, 1800–2000
	2 Aug	0120, 1420, 1620–1720, 1920–2120	0100–0200, 1500, 1700, 2000–2100
	3 Aug	0120–0220, 0620–0820, 1020, 1220, 2120–2220	0100–0200, 0600–0800, 1100–1200, 1700, 2100–2200
	4 Aug	0420–0520, 0720, 0920–1320, 1720–2320	0100, 0400–0500, 0900–1300, 1800–2300

[a] Dash indicates there were no samples excluded for that date and bank.

APPENDIX E: WINBUGS CODE

Appendix E1.-WinBUGS code for hierarchical age-composition model for development of prior distributions for ELSD mixture model.

```
# Age Mixture.odc  version 6a:

model {
 #Overall means and std deviations
 for (  a in 1:A)  {
  sigma[a] ~ dnorm(  0,1.0E-4)  I(  0,)
  tau[a] <- 1 / sigma[a] / sigma[a]
  mu[a] ~ dnorm(  0,1.0E-12)  I(  0,)
  }
 #Dirichlet distributed age proportions across years within weeks
 D.scale ~ dunif(  0,1)
 D.sum <- 1 / (  D.scale * D.scale)
 for (  w in 1:W)  {
  pi[w,1] ~ dbeta(  0.2,0.4)
  pi.2p[w] ~ dbeta(  0.2,0.2)
  pi[w,2] <- pi.2p[w] * (  1 - pi[w,1])
  pi[w,3] <- 1 - pi[w,1] - pi[w,2]
  for (  y in 1:Y)  {
   for (  a in 1:A)  {
    D[w,y,a] <- D.sum * pi[w,a]
    g[w,y,a] ~ dgamma(  D[w,y,a],1)
    pi.wy[w,y,a] <- g[w,y,a]/sum(  g[w,y,])
    }
   }
  }
 for (  i in 1:nfish)  {
  age[i] ~ dcat(  pi.wy[week[i],year[i],1:A])
  length[i] ~ dnorm(  mu[age[i]],tau[age[i]])
  }
}
```

Appendix E2.–WinBUGS code for ELSD mixture model fit to 2010 Kenai River Chinook salmon sonar, gillnetting, and tethered fish data.

```
# ELSD 07 version 4:
# fish with neighbors < 1m in range excluded,
model{
 beta0 ~ dnorm(0,1.0E-4)
 beta1 ~ dnorm(0,1.0E-4)
 gamma ~ dnorm(0,1.0E-4)
 sigma.elsd ~ dunif(0,2)
 sigma.beta0 ~ dunif(0,2)
 tau.elsd  <- 1 / sigma.elsd / sigma.elsd
 tau.beta0 <- 1 / sigma.beta0 / sigma.beta0
 ps[1:2] ~ ddirch(D.species[])
 pa[1,1] ~ dbeta(B1,B2)
 theta1 ~ dbeta(B3,B4)
 pa[1,2] <- theta1 * (1 - pa[1,1])
 pa[1,3] <- 1 - pa[1,1] - pa[1,2]
 pa[2,1] ~ dbeta(0.5,0.5)
 theta2 ~ dbeta(0.5,0.5)
 pa[2,2] <- theta2 * (1 - pa[2,1])
 pa[2,3] <- 1 - pa[2,1] - pa[2,2]

 p.chin <- ps[1] * p_n * p_i
 Lsig[1] <- 75
 Lsig[2] <- 25   #CHANGED FROM 34 in 2006, BASED ON AGE MIXTURE.ODC V5D SOCKEYE
 Ltau[1] <- 1 / Lsig[1] / Lsig[1]
 Ltau[2] <- 1 / Lsig[2] / Lsig[2]
 mu[1,1] ~ dnorm(636,0.0006)
 mu[1,2] ~ dnorm(816,0.0070)
 mu[1,3] ~ dnorm(1032,0.0006)
 mu[2,1] ~ dnorm(380,0.003)
 mu[2,2] ~ dnorm(500,0.006)
 mu[2,3] ~ dnorm(580,0.006)
 D.age.sockeye[1] <- 0.01
 D.age.sockeye[2] <- 0.5
 D.age.sockeye[3] <- 3.5
 for (a in 1:3)  {
  pa.effective[1,a] <- pa[1,a] * q1.a[a] /  inprod(pa[1,],q1.a[])
  pa.effective[2,a] <- pa[2,a]
  }

 for (y in 1:3) {
  beta0.y[y] ~ dnorm(beta0,tau.beta0)
  }
 beta0.predict ~ dnorm(beta0,tau.beta0)
 for (k in 1:141) {
  elsd1[k] ~ dnorm(mu.elsd1[k],tau.elsd)
  mu.elsd1[k] <- beta0.y[year[k]] + beta1 * cm75[k] + gamma * sock.indic[k]
  }
```

-continued-

```
for (i in 1:nfish) {
 age[i] ~ dcat(pa.effective[species[i],1:3])
 mefl[i] ~ dnorm(mu[species[i],age[i]],Ltau[species[i]])
 }
for (j in 1:ntgts) {
 species2[j] ~ dcat(ps[])
 age2[j] ~ dcat(pa[species2[j],1:3])
 mefl2[j] ~ dnorm(mu[species2[j],age2[j]],Ltau[species2[j]])
 elsd2[j] ~ dt(mu.elsd2[j],tau.elsd,8)
 cm75t[j] <- (mefl2[j] / 10) - 75;
 sock.indic2[j] <- species2[j] - 1;
 mu.elsd2[j] <- beta0.predict + gamma*sock.indic2[j] + beta1 * cm75t[j]
 } }
```

Note: Prior distributions in green font, likelihoods in blue.

Appendix E3.–WinBUGS code for DIDSON-length mixture model.

```
model{
 beta0 ~ dnorm(75,0.0025)
 beta1 ~ dnorm(0.8,25)
 sigma.DL ~ dunif(0,20)
 tau.DL  <- 1 / sigma.DL / sigma.DL
 ps[1:2] ~ ddirch(D.species[])
 pa[1,1] ~ dbeta(0.5,0.5)
 theta1 ~ dbeta(0.5,0.5)
 pa[1,2] <- theta1 * (1 - pa[1,1])
 pa[1,3] <- 1 - pa[1,1] - pa[1,2]
 pa[2,1] ~ dbeta(0.5,0.5)
 theta2 ~ dbeta(0.5,0.5)
 pa[2,2] <- theta2 * (1 - pa[2,1])
 pa[2,3] <- 1 - pa[2,1] - pa[2,2]
 n.chin <- ps[1] * ntgts
 p.large <- ps[1] * (1 - pa[1,1])
 n.large <- p.large * ntgts
  Lsig[1,1] <- 78
 Lsig[1,2] <- 70
 Lsig[1,3] <- 74
 Lsig[2,1] <- 25
 Lsig[2,2] <- 25
 Lsig[2,3] <- 25
 for (s in 1:2)  {for (a in 1:3)  {Ltau[s,a] <- 1 / Lsig[s,a] / Lsig[s,a] } }
 mu[1,1] ~ dnorm(621,0.0076)
 mu[1,2] ~ dnorm(825,0.0021)
 mu[1,3] ~ dnorm(1020,0.0047)
 mu[2,1] ~ dnorm(380,0.0004)
 mu[2,2] ~ dnorm(500,0.0004)
 mu[2,3] ~ dnorm(580,0.0004)
 for (a in 1:3)  {
   pa.effective[1,a] <- pa[1,a] * q1.a[a] /  inprod(pa[1,],q1.a[])
   pa.effective[2,a] <- pa[2,a]
   }
 for (k in 1:5) {
   TL.cm.75[k] <- TL.cm[k] - 75
   mu.DL1[k] <- beta0 + beta1 * TL.cm.75[k]
   DL1[k] ~ dnorm(mu.DL1[k],tau.DL)
   }
 for (i in 1:nfish) {
   age[i] ~ dcat(pa.effective[species[i],1:3])
   mefl.mm[i] ~ dnorm(mu[species[i],age[i]],Ltau[species[i],age[i]])
   }
 for (j in 1:ntgts) {
   species2[j] ~ dcat(ps[])
   age2[j] ~ dcat(pa[species2[j],1:3])
   mefl.mm.2[j] ~ dnorm(mu[species2[j],age2[j]],Ltau[species2[j],age2[j]])
   TL2.cm.75[j] <- (1.1*mefl.mm.2[j] + 2) / 10 - 75     # CONVERT TO TL -NUSHAGAK 2001 DATA
   mu.DL2[j] <- beta0 + beta1 * TL2.cm.75[j]
   DL2[j] ~ dnorm(mu.DL2[j],tau.DL)
   }
 }
```

Note: Prior distributions in green font, likelihoods in blue.

APPENDIX F: DIDSON CONFIGURATION FOR KENAI RIVER CHINOOK SONAR STUDY, 2010

Selection of the appropriate DIDSON hardware configuration and operating parameters is primarily determined by the range and resolution needs of a specific application. Because resolution generally decreases as the insonified range increases, the need to balance and optimize these parameters determined the configuration used at the Kenai River RM-8.5 site.

Frequency

DIDSON sonars operate at 2 frequencies: a higher frequency that produces higher resolution images and a lower frequency that can detect targets at farther ranges but at a reduced image resolution. Two DIDSON models are currently available based on different operating frequencies (Appendix F2). The short-range or standard model (DIDSON-S) operates at 1.8 MHz to approximately 15 m and 1.1 MHz to approximately 30 m and produces higher resolution images than the long-range model. The long-range model (DIDSON-LR) operates at 1.2 MHz to approximately 30 m and 0.7 MHz to ranges exceeding 100 m, but produces images with approximately half the resolution of the DIDSON-S (see explanation below). A long-range model (DIDSON-LR) was used in this study to insonify the required range and was operated in high frequency mode (1.2 MHz) to achieve maximum image resolution.

Beam Dimensions and Lens Selection

The DIDSON-LR used in this study was fitted with a high-resolution lens to further enhance the image resolution of the DIDSON-LR system (DIDSON-LR+HRL).The high-resolution lens has a larger aperture that increases the image resolution by approximately a factor of 2 over the standard lens by reducing the width of the individual beams and spreading them across a narrower field of view (Appendices F2 and F3). Overall nominal beam dimensions for a DIDSON-LR with a standard lens are approximately 29° in the horizontal axis and 14° in the vertical axis. Operating at 1.2 MHz, the 29° horizontal axis is a radial array of 48 beams that are nominally 0.54° wide and spaced across the array at approximately 0.60° intervals. With the addition of the high-resolution lens, the overall nominal beam dimensions of the DIDSON-LR are reduced to approximately 15° in the horizontal axis and 3° in the vertical axis and the 48 individual beams are reduced to approximately 0.3° wide and spaced across the array at approximately 0.3° intervals. The combined concentration of horizontal and vertical beam widths also increases the returned signal from a given target by 10 dB, which increases the range capability of the DIDSON-LR from 25 m to at least 30 m (Appendix F2). After adding the high resolution lens, the DIDSON-LR has equivalent resolution and twice the range capabilities as the DIDSON-S. However, the reduction in beam dimensions could potentially reduce detection capabilities, particularly at very close range (e.g., at ranges less than 5 m).

-continued-

Resolution

The resolution of a DIDSON image is defined in terms of down-range and cross-range resolution where cross-range resolution refers to the width and down-range resolution refers to the height of the individual pixels that make up the DIDSON image (Appendix F4). Each image pixel in a DIDSON frame has (x, y) rectangular coordinates that are mapped back to a beam and sample number defined by polar coordinates. The pixel height defines the down-range resolution and the pixel width defines the cross-range resolution of the image. Appendix F4 shows that image pixels are sometimes broken down into smaller screen pixels (e.g., pixels immediately to the right of the enlarged pixels), which are an artifact of conversions between rectangular and polar coordinates.

"Window length" is the range interval sampled by the sonar, and it controls the down-range resolution of the DIDSON image. Because the DIDSON image is composed of 512 samples (pixels) in range, images with shorter window lengths are better resolved (i.e., down-range resolution = window length/512). Window length can be set to 2.5, 5.0, 10.0, or 20.0 m for the DIDSON-LR+HRL at 1.2 MHz. Shorter window lengths have higher resolution, but require more individual strata to cover the desired range. However, dividing the total range covered into too many discrete strata increases the data-processing time. For this study, a window length of 10 m was used for each of 3 range strata sampled, a compromise which allowed a relatively high resolution while allowing a reasonable distance to be covered by each stratum. The down-range resolution (or pixel height) for a 10 m window length is 2 cm (1,000 cm/512).

The cross-range resolution is primarily determined by the individual beam spacing and beam width, both of which are approximately 0.3° for the DIDSON LR+HRL at 1.2 MHz (Appendix F2). Targets at closer range are better resolved because the individual beam widths and corresponding image pixels increase with range following the formula below:

$$X = 2R\tan\left(\theta/2\right) \tag{F1}$$

where

X = width of the individual beam or "image pixel" in meters,

R = range of interest in meters, and

θ = individual beam angle in degrees (approximately 0.3°).

Other Settings

The transmit power of the DIDSON sonar is fixed but the receiver gain is user-configurable. The maximum receiver gain (−40 dB) was used during all data collection. The autofocus feature was enabled so that the sonar automatically set the lens focus to the midrange of the selected display window (e.g., for a window length of 10 m that started at 5 m, the focus range would be 15 m – (5 m/2).

Appendix F2.–Summary of manufacturer specifications for maximum range, individual beam dimensions, and spacing for a DIDSON-S and a DIDSON-LR with and without the addition of a high resolution lens (specifications from Sound Metrics Corporation).

System	Maximum range (m)[a]	Horizontal beam width	Vertical beam width	Number of beams	Individual beam width[b,c]	Individual beam spacing[b,c]
DIDSON-S (1.8 MHz)	15	29°	14°	96	0.30°	0.30°
DIDSON-S (1.1 MHz)	30	29°	14°	48	0.40°	0.60°
DIDSON-S (1.8 MHz) +HRL	20	15°	3°	96	0.17°	0.15°
DIDSON-S (1.1 MHz) +HRL	40	15°	3°	48	0.22°	0.30°
DIDSON-LR (1.2 MHz)	25	29°	14°	48	0.40°	0.60°
DIDSON-LR (0.7 MHz)	80	29°	14°	48	0.60°	0.60°
DIDSON-LR (1.2 MHz) +HRL	30	15°	3°	48	0.27°	0.30°
DIDSON-LR (0.7 MHz) +HRL	100	15°	3°	48	0.33°	0.60°

[a] Actual range will vary depending on site and water characteristics.

[b] Beam width values are for 2-way transmission at the −3 dB points.

[c] Values for beam spacing and beam width are approximate. Beam widths are slightly wider near the edges of the beam and the beam spacing is slightly narrower. Conversely, beams are slightly narrower near the center of the beam, and the beam spacing is slightly wider (e.g., the center beam spacing is closer to 0.34°, and the beam width is 0.27 for a DIDSON-S at 1.8 MHz (Bill Hanot, Sound Metrics Corporation, personal communication). Nonlinear corrections are applied by the manufacturer in software to correct for these effects in the standard (but not large) lens.

Appendix F3.–Diagram showing the horizontal plane of a DIDSON-LR sonar with a high resolution lens (DIDSON-LR+HRL).

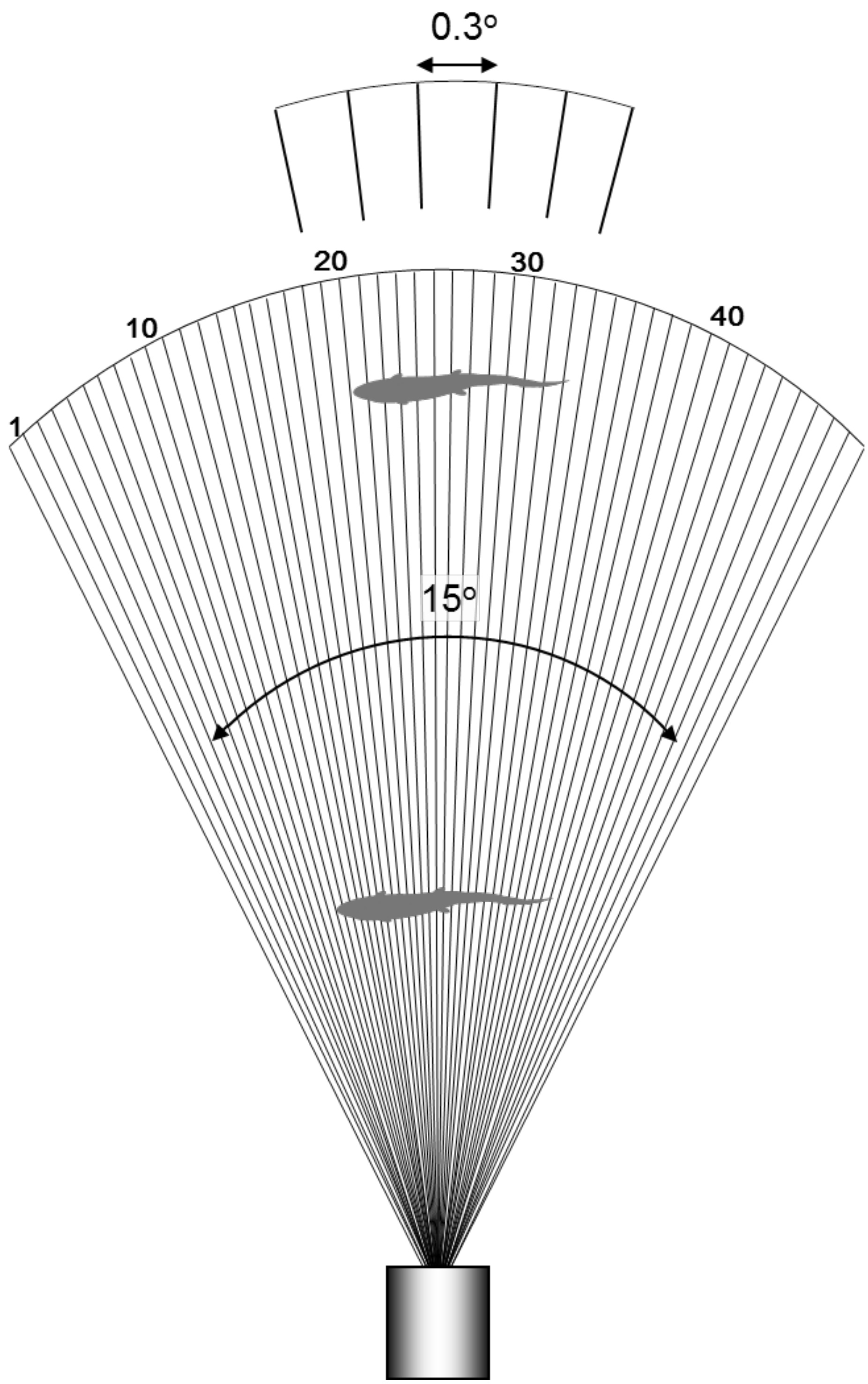

Source: adapted from Burwen et al. 2007.

Note: The overall horizontal beam width of 15° is comprised of 48 sub-beams with approximately 0.3° beam widths. Because the beam widths grow wider with range, fish at close range are better resolved than fish at far range.

Appendix F4.–An enlargement of a tethered Chinook salmon showing the individual pixels that comprise the image.

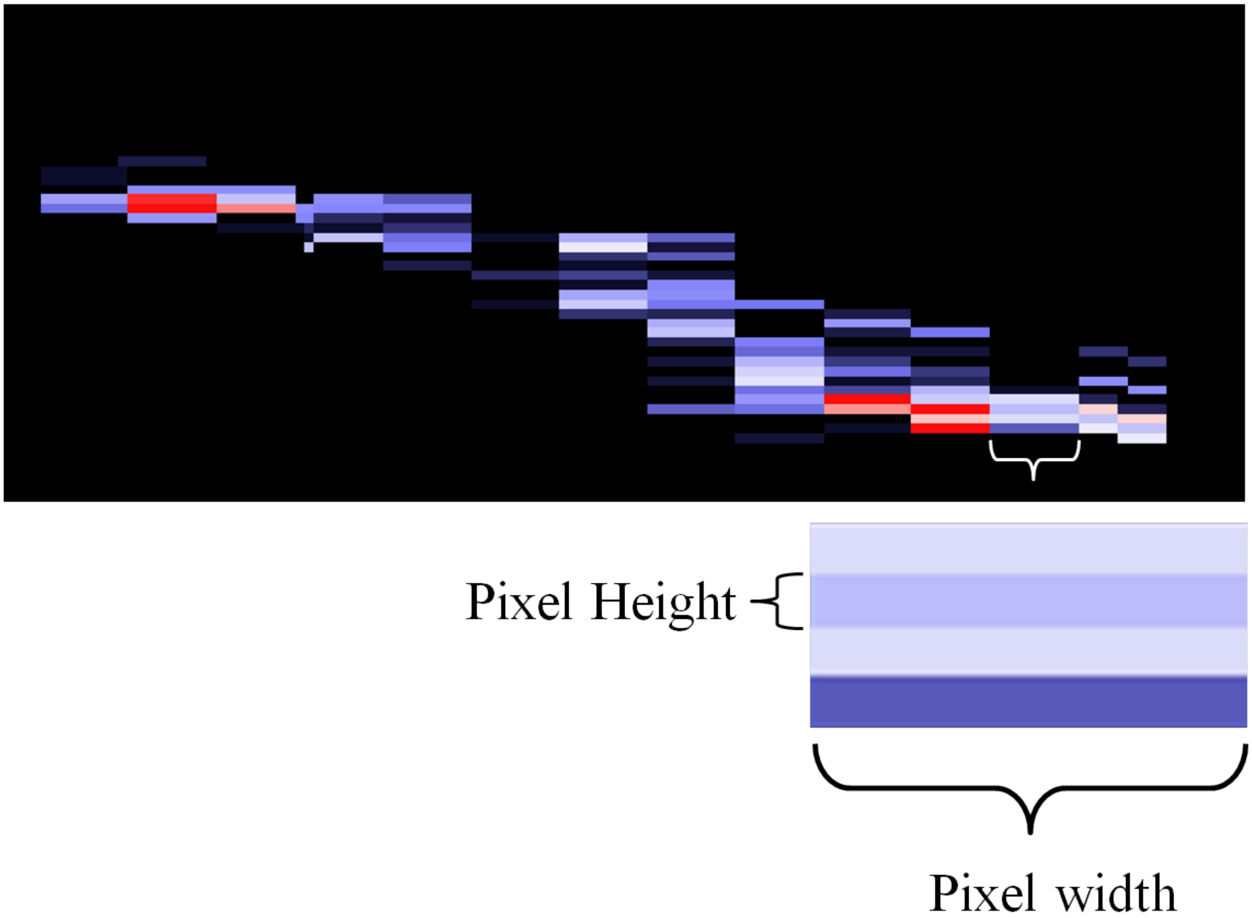

Source: adapted from Burwen et al. 2010

Note: Each image pixel in a DIDSON frame has (x, y) rectangular coordinates that are mapped back to a beam and sample number defined by polar coordinates range.

Appendix F5.–Instructions and settings used for manual length measurements from DIDSON images in 2010 using Sound Metrics Software Version 5.25.28.

Parameter setup prior to beginning measurements

Step 1. Set the number of frames displayed (i.e., when right-clicking on a fish in echogram mode to display in movie mode) from the default of plus-minus one second to plus-minus any number of frames:

1) Select **<image><playback><set endpoints>**
2) [√] Loop on still for +/- N frames
3) Enter the number of frames (I suggest 20–30)

Step 2. Select **<Processing><Echogram><Use Cluster Data>** to use ALL the beams when creating the echogram (we generally do). Use fewer beams by unchecking this option and selecting the number of beams.

Step 3. Set up **processing parameters** (last Icon on right) for **<u>File Creation</u>** as follows:

1) Auto Countfile Name
2) Binary CountFile (.dat)
3) New Countfile on Open
4) Echogram File (.ech)

Step 4. Echogram counts can be reloaded to finish or review at a later time if the Echogram file has been checked as follows:

1) Select **<File><Open> then Files of type .ech** from drop-down menu
2) Open desired file
3) The Echogram file should reload showing previous measurements

Or this option will work as long as the .dat file has been saved (as shown above)

1) Open the file and bring up the echogram (follow instructions below)
2) Select **<Processing><Echogram><Import Echogram Counts>**
3) Select the **.dat** file with saved counts. The file should reload, showing previous measurements (the filename for the .dat file will begin with **FC_**)

Step 5. Make sure **<Image><Configure><Auto Threshold/Intensity>** is UNCHECKED. This will keep the threshold and intensity settings from changing when switching between Echogram and Movie mode.

Step 6. Uncheck the 'Display Raw Data' toolbar icon (first button on left in Combined toolbar). (If you are in Movie mode and it is displaying the raw image data, it is because 'Display Raw Data' is enabled by default).

Instructions for manual echogram-based length measurements

***Note that these settings may already be active because some of them have "memory" and are saved until changed.**

1) Select **<BS>** (for background subtraction) from toolbar or under **<Processing><Background><Background Subtraction>**
2) Select **<Processing><Background><Fixed Background>**
3) Select threshold and range settings given in Table 1. To adjust these settings, use the slider bars under Display Controls to the left of the echogram.
4) Select the threshold and intensity settings for each range stratum as indicated below. To adjust these settings, use slider bars under the Display Controls to the left side of the Echogram or Movie window.

	3–13 m	**13–23 m**	**23–33 m**
Threshold	11	10	9
Intensity	50	45	40

-continued-

5) Select **<EG>** (for view echogram) from toolbar or under **<Processing><Echogram><View echogram**>
6) **<left click>** on the echogram near or on the fish trace of interest to "mark it." A white circle should be visible.
7) **<right click>** INSIDE the white circle to switch to Movie mode (Movie mode will play the 16 frames encompassing this circle continuously)
8) Press **<space bar>** to pause the movie.
9) Step through the movie frames using the right or left arrows until finding a frame that displays the entire length of the fish well (see section below for selecting optimal images).
10) **<right mouse click drag>** will magnify the area in the rectangle.
11) **<left click>** on the FISH SNOUT and continue to <left click> along the body to create a "segmented measurement." ***The segments should follow the midline of the body of the fish*** ending with the tail. Try not to use more than 3 or 4 segments to define the fish (see section below for selecting optimal images).
12) **<double left click>** or select **<f>** key to add measurement to file.
13) **<right click>** to unzoom.
14) **<right click>** to return to the echogram.

Hot keys

1) **<e>** to "save" all echogram measurements to file
2) **<f>** to "fish it" (to accept the measurement and display it on the echogram)
3) **<u>** to "undo" the last segment
4) **<d>** to "delete" the all segments
5) **<space bar>** to pause in Movie mode (if this doesn't work, click in the black area of the display)
6) **<right arrow>** forward direction when selecting play or advances frame one at a time if the pause button is on (pause button = blue square on the toolbar)
7) **<left arrow>** opposite of above
8) **Left Click Drag** to show movie over the selected time
9) **Right Click Drag** zooms the selected area

Selecting optimal images to measure

Measurements should be taken from frames where contrast between the fish image and background are high and where the fish displays its full length (e.g., Panels a, d, and f in Appendix F6). In general, the best images are obtained when the fish is sinusoidal in shape, rather than straight and perpendicular to the beam axis (e.g., Panel c in Appendix F6) because the head and tail appear most visible when there is curvature to the fish body (e.g., Appendices F6 and F7). Appendix F7 demonstrates the process of measuring a fish using the manual measuring tool. The user pauses the DIDSON movie (top), zooms in on the fish of interest (middle), and measures the fish length with a segmented line created by mouse clicks along the center axis of the fish (bottom). The user selects the leading pixel edge of the snout to start the measurement (yellow start pixel extends beyond snout), and clicks just before the trailing edge of the pixel(s) defining the tail so such that the "yellow measurement line" is flush with the trailing pixel edge.

Appendix F6.–Panels a–f show the variability in length measurements from DIDSON images of a tethered Chinook salmon during one full tail-beat cycle.

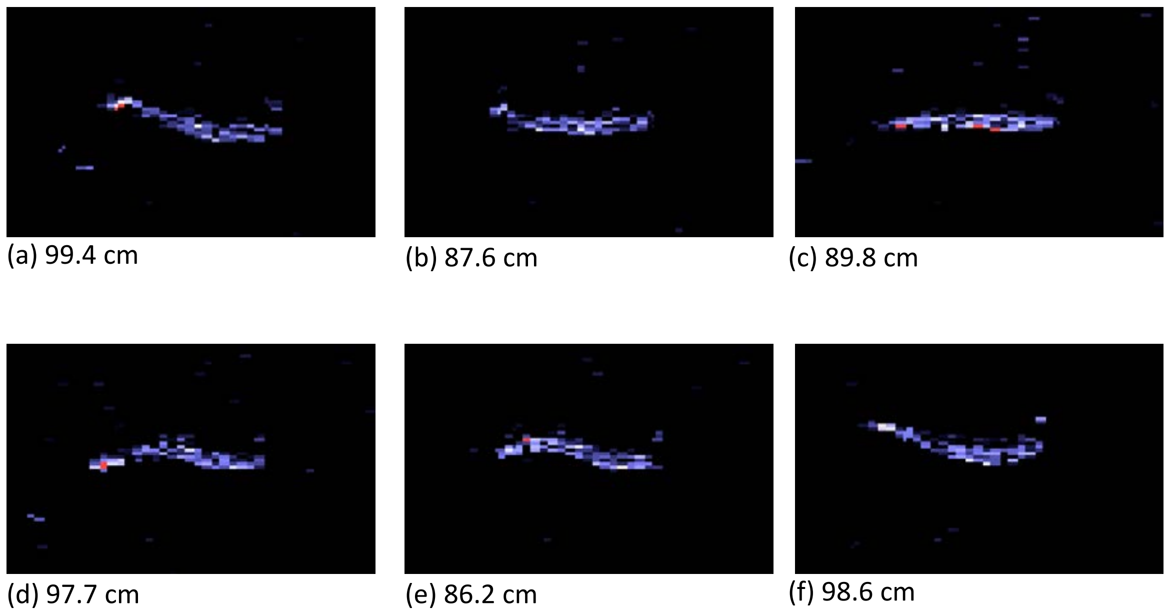

Source: adapted from Burwen et al. 2010.

Appendix F7.–DIDSON images from a tethered Chinook salmon showing the original DIDSON image (top), the zoomed image (middle), and the segmented lines that result when the observer clicks along the length of the fish to mark its length (bottom).

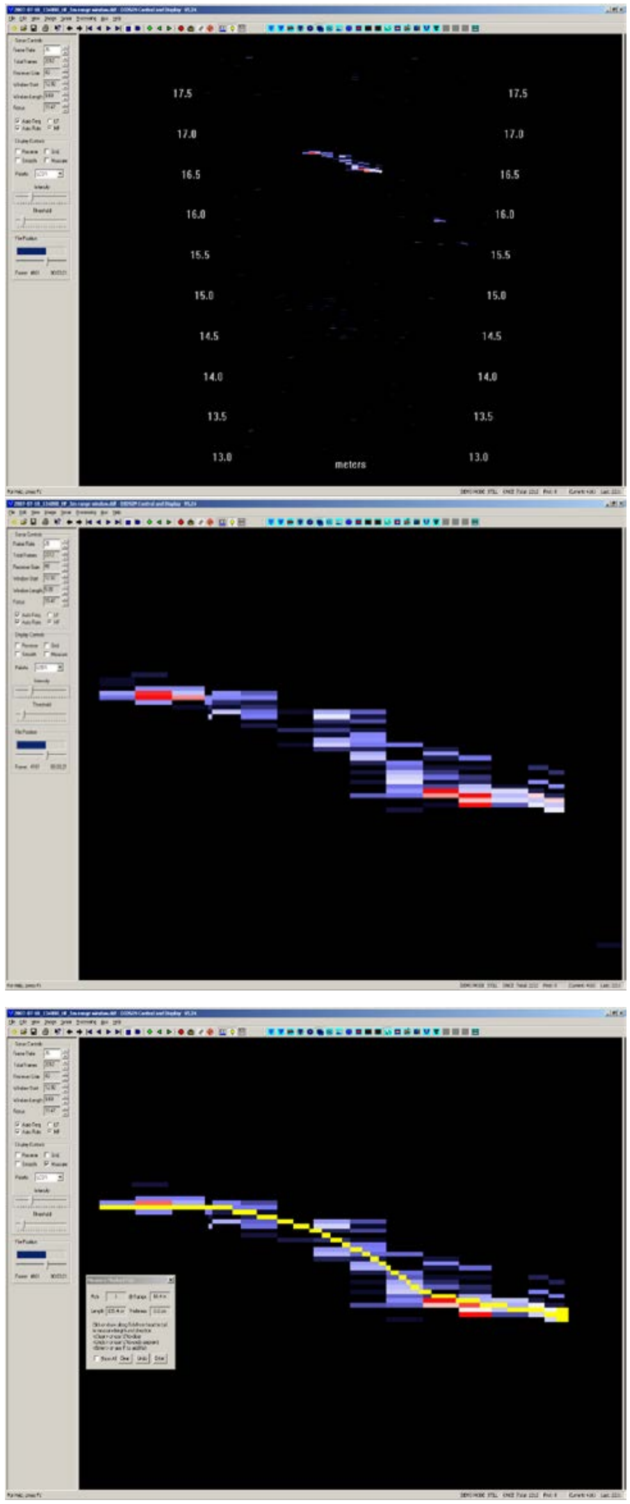

Source: adapted from Burwen et al. 2010.

APPENDIX G: DIRECTION OF TRAVEL OF SPLIT-BEAM TARGETS, KENAI RIVER, 2010

Appendix G1.–Daily proportion of upstream and downstream moving filtered targets for the early run, Kenai River RM 8.5, 2010.

Date	Downstream count	Upstream count	Daily total	% Downstream	% Upstream
16 May	3	32	35	9%	91%
17 May	3	39	42	7%	93%
18 May	9	41	50	18%	82%
19 May	23	75	98	23%	77%
20 May	12	40	52	23%	77%
21 May	9	27	36	25%	75%
22 May	3	51	54	6%	94%
23 May	6	36	42	14%	86%
24 May	0	48	48	0%	100%
25 May	0	57	57	0%	100%
26 May	6	69	75	8%	92%
27 May	9	60	69	13%	87%
28 May	4	28	32	13%	88%
29 May	0	36	36	0%	100%
30 May	0	36	36	0%	100%
31 May	6	24	30	20%	80%
1 June	0	25	25	0%	100%
2 June	0	15	15	0%	100%
3 June	0	32	32	0%	100%
4 June	6	165	171	4%	96%
5 June	6	266	272	2%	98%
6 June	3	259	262	1%	99%
7 June	0	215	215	0%	100%
8 June	10	572	582	2%	98%
9 June	3	592	595	1%	99%
10 June	0	635	635	0%	100%
11 June	5	533	538	1%	99%
12 June	8	437	445	2%	98%
13 June	14	480	494	3%	97%
14 June	0	474	474	0%	100%
15 June	18	687	705	3%	97%
16 June	3	502	505	1%	99%
17 June	11	417	428	3%	97%
18 June	2	381	383	1%	99%
19 June	14	405	419	3%	97%
20 June	6	344	350	2%	98%
21 June	3	306	309	1%	99%
22 June	6	537	543	1%	99%
23 June	2	581	583	0%	100%
24 June	0	509	509	0%	100%
25 June	13	495	508	3%	97%
26 June	6	421	427	1%	99%
27 June	0	657	657	0%	100%
28 June	9	464	473	2%	98%
29 June	6	517	523	1%	99%
30 June	9	626	635	1%	99%
Total	256	13,248	13,504	2%	98%

Appendix G2.–Daily proportion of upstream and downstream moving filtered targets for the late run, Kenai River RM 8.5, 2010.

Date	Downstream count	Upstream count	Daily total	% Downstream	% Upstream
1 July	0	843	843	0%	100%
2 July	0	639	639	0%	100%
3 July	2	740	742	0%	100%
4 July	3	943	946	0%	100%
5 July	0	940	940	0%	100%
6 July	2	942	944	0%	100%
7 July	3	1,495	1,498	0%	100%
8 July	3	1,600	1,603	0%	100%
9 July	6	505	511	1%	99%
10 July	7	781	788	1%	99%
11 July	0	1,002	1,002	0%	100%
12 July	4	1,311	1,315	0%	100%
13 July	2	1,090	1,092	0%	100%
14 July	10	1,009	1,019	1%	99%
15 July	9	1,062	1,071	1%	99%
16 July	7	1,525	1,532	0%	100%
17 July	18	1,661	1,679	1%	99%
18 July	23	1,672	1,695	1%	99%
19 July	12	1,131	1,143	1%	99%
20 July	28	1,937	1,965	1%	99%
21 July	22	2,654	2,676	1%	99%
22 July	20	1,627	1,647	1%	99%
23 July	6	2,216	2,222	0%	100%
24 July	23	2,562	2,585	1%	99%
25 July	13	1,388	1,401	1%	99%
26 July	3	1,396	1,399	0%	100%
27 July	13	1,542	1,555	1%	99%
28 July	7	1,761	1,768	0%	100%
29 July	23	1,470	1,493	2%	98%
30 July	32	1,686	1,718	2%	98%
31 July	14	1,659	1,673	1%	99%
1 August	33	1,716	1,749	2%	98%
2 August	53	1,249	1,302	4%	96%
3 August	38	1,312	1,350	3%	97%
4 August	137	1,277	1,414	10%	90%
Total	576	48,343	48,919	1%	99%

APPENDIX H: AVERAGE VERTICAL ANGLE OF FILTERED TARGETS BY TIDE STAGE, RUN, BANK, AND DIRECTION OF TRAVEL (UPSTREAM OR DOWNSTREAM) USING SPLIT-BEAM SONAR FOR THE EARLY AND LATE RUNS, KENAI RIVER, 2010

Appendix H1.–Average vertical angle of split-beam sonar filtered targets by tide stage and direction of travel (upstream or downstream) for the early run, Kenai River RM 8.5, 2010.

Bank	Tide stage	Fish orientation	Average vertical angle	Standard deviation	Sample size
Left bank					
	Falling				
		Downstream	0.28	0.48	14
		Upstream	−0.17	0.25	1,834
		Total	−0.17	0.26	1,848
	Low				
		Downstream	−0.18	0.17	9
		Upstream	−0.19	0.26	551
		Total	−0.19	0.26	560
	Rising				
		Downstream	0.17	0.53	5
		Upstream	0.04	0.50	430
		Total	0.04	0.50	435
		Left bank total	−0.14	0.31	2,843
Right bank					
	Falling				
		Downstream	−0.15	0.49	39
		Upstream	−0.25	0.34	1,488
		Total	−0.24	0.34	1,527
	Low				
		Downstream	−0.39	0.66	12
		Upstream	−0.27	0.32	285
		Total	−0.27	0.34	297
	Rising				
		Downstream	-0.21	0.52	14
		Upstream	−0.09	0.52	441
		Total	−0.10	0.52	455
		Right bank total	−0.22	0.39	2,279

Appendix H2.–Average vertical angle of split-beam sonar filtered targets by tide stage and direction of travel (upstream or downstream) for the late run, Kenai River RM 8.5, 2010.

Bank	Tide stage	Fish Orientation	Average vertical angle	Standard deviation	Sample size
Left bank					
	Falling				
		Downstream	0.01	0.32	66
		Upstream	−0.04	0.25	6,325
		Total	−0.04	0.26	6,391
	Low				
		Downstream	0.09	0.26	25
		Upstream	−0.09	0.22	1,862
		Total	−0.09	0.22	1,887
	Rising				
		Downstream	−0.19	0.28	39
		Upstream	0.00	0.34	3,546
		Total	−0.00	0.34	3,585
		Left bank total	−0.04	0.28	11,863
Right bank					
	Falling				
		Downstream	0.05	0.29	125
		Upstream	−0.01	0.25	10,404
		Total	−0.00	0.20	10,529
	Low				
		Downstream	0.07	0.27	44
		Upstream	−0.03	0.22	1,881
		Total	−0.03	0.22	1,925
	Rising				
		Downstream	0.02	0.32	58
		Upstream	−0.01	0.24	6,456
		Total	−0.01	0.24	6,514
		Right bank total	−0.01	0.25	18,968

APPENDIX I. DAILY TARGET-STRENGTH-BASED SPLIT-BEAM SONAR PASSAGE ESTIMATES OF CHINOOK SALMON ABUNDANCE, 1987–2010

Appendix I1.–Target-strength-based split-beam sonar passage estimates for RM 8.5, Kenai River early-run Chinook salmon, 1987–2010.

Date	1987[a]	1988	1989	**1990**	**1991**	**1992**	1993	1994	1995	1996	**1997**	**1998** [b,c]
7 May												6
8 May												18
9 May												3
10 May												3
11 May												12
12 May												12
13 May												27
14 May												43
15 May												63
16 May		188	180	78	30	54	64	238	98	60	114	48
17 May		415	319	57	12	48	85	342	99	91	99	45
18 May		259	264	93	65	88	91	260	78	63	93	57
19 May		260	180	136	55	40	66	302	149	96	165	36
20 May		406	147	93	68	78	69	369	228	177	84	54
21 May		184	245	69	51	90	165	327	465	165	129	33
22 May		182	164	75	111	108	117	246	265	156	114	15
23 May		231	186	63	66	150	160	212	286	159	162	12
24 May		288	279	51	66	126	141	303	265	159	138	33
25 May		351	300	76	57	79	150	170	198	153	165	81
26 May		393	270	70	81	93	168	150	189	240	220	43
27 May		387	419	87	81	66	150	267	165	204	325	60
28 May		483	357	61	78	78	361	258	159	330	317	63
29 May		713	269	221	51	45	538	347	222	512	288	63
30 May		333	164	154	51	111	388	321	351	348	350	129
31 May		501	157	175	69	114	266	369	282	474	318	93

-continued-

Appendix I1.–Part 2 of 5.

Date	1987[a]	1988	1989	**1990**	**1991**	**1992**	1993	1994	1995	1996	**1997**	**1998** [b,c]
1 Jun		556	258	153	150	106	187	321	357	603	213	111
2 Jun		545	194	294	240	107	412	266	369	741	241	189
3 Jun		598	233	225	362	232	324	298	549	873	376	192
4 Jun	1,059	755	246	178	177	190	255	304	693	1,051	324	186
5 Jun	552	782	280	192	316	166	276	351	429	943	427	**162**
6 Jun	1,495	493	384	156	**296**	319	327	198	807	741	327	**150**
7 Jun	1,145	506	545	**304**	**215**	515	198	384	843	773	591	**283**
8 Jun	602	771	890	**414**	**243**	375	297	306	999	918	441	**300**
9 Jun	1,024	569	912	**339**	**444**	**486**	378	462	789	1,140	391	**234**
10 Jun	985	333	913	**272**	**275**	**264**	453	432	876	684	527	**327**
11 Jun	1,004	320	710	**453**	**334**	**234**	549	423	774	882	512	**600**
12 Jun	1,044	302	577	**568**	**400**	**394**	600	329	417	864	537	**1,168**
13 Jun	2,168	188	599	**445**	**369**	**236**	951	376	492	1,071	681	**719**
14 Jun	1,297	289	458	**330**	**268**	**174**	811	514	691	1,111	424	**912**
15 Jun	975	510	335	**658**	**441**	**312**	407	306	636	1,116	318	**951**
16 Jun	786	808	397	**485**	**615**	**239**	616	453	648	420	348	**770**
17 Jun	612	535	514	**267**	**330**	**339**	567	315	750	495	**405**	**675**
18 Jun	783	533	464	**238**	**493**	**320**	606	435	808	697	**315**	**498**
19 Jun	771	200	295	**331**	**437**	**390**	422	636	419	657	**399**	**510**
20 Jun	682	175	498	**369**	**314**	**548**	504	402	594	315	**408**	**351**
21 Jun	517	373	520	**257**	**457**	**372**	621	570	438	351	**252**	**309**
22 Jun	487	312	614	**267**	**433**	**297**	399	366	375	396	**390**	**273**
23 Jun	529	375	547	**240**	**396**	**213**	607	550	178	401	**225**	**294**
24 Jun	303	674	564	**322**	**251**	**337**	720	696	450	573	**285**	**288**
25 Jun	564	582	374	**258**	**235**	**362**	808	734	429	684	**332**	**228**
26 Jun	731	436	369	**322**	**261**	**330**	1,051	597	334	504	**381**	**219**
27 Jun	452	549	309	**231**	**340**	**291**	1,158	639	946	228	**363**	**207**
28 Jun	587	827	425	**240**	**327**	**253**	798	681	696	303	**297**	**308**
29 Jun	371	495	376	**208**	**258**	**121**	728	929	984	234	**570**	**363**
30 Jun	388	915	292	**193**	**270**	**197**	660	649	615	351	**582**	**276**
May–Jun Total	21,913[a]	20,880	17,992	**10,768**	**10,939**	**10,087**	19,669	18,403	21,884	23,505	**14,963**	**13,103**

-continued-

Appendix I1.–Part 3 of 5.

Date	1999[c]	**2000[c]**	2001[c]	**2002[c]**	2003[c]	2004[c]	2005[c]	2006[c]	2007[c]	2008[c]	2009[c]	**2010[c]**
7 May												
8 May												
9 May												
10 May												
11 May												
12 May												
13 May												
14 May												
15 May												
16 May	33	18	62	24	35	24	54	40	62[d]	33	69	32
17 May	63	49	111	21	35	30	51	30	75[d]	52	15	39
18 May	66	54	117	54	63	31	27	39	84[d]	60	39	41
19 May	39	84	133	60	81	57	21	66	92[d]	42	39	75
20 May	116	64	156	66	123	48	66	57	18	39	72	40
21 May	186	84	101	42	162	84	108	48	66	69	57	27
22 May	192	123	128	36	174	61	78	72	60	114	21	51
23 May	243	132	81	36	237	153	96	51	51	147	45	36
24 May	159	147	147	33	168	129	76	69	91	154	36	48
25 May	141	234	175	48	129	138	93	96	88	135	45	57
26 May	330	186	278	65	195	240	75	81	72	207	72	69
27 May	342	177	314	75	192	324	97	152	81	270	140	60
28 May	402	84	291	103	180	452	140	135	117	353	272	28
29 May	378	204	323	57	248	233	203	242	144	287	353	36
30 May	273	105	440	90	183	156	195	401	164	267	245	36
31 May	459	117	276	85	225	128	244	469	252	361	239	24

-continued-

Appendix I1.–Part 4 of 5.

Date	1999[c]	**2000[c]**	2001[c]	**2002[c]**	2003[c]	2004[c]	2005[c]	2006[c]	2007[c]	2008[c]	2009[c]	**2010[c]**
1 Jun	633	192	259	210	294	148	342	820	225	213	153	25
2 Jun	444	250	316	216	195	91	335	702	186	210	205	15
3 Jun	540	282	328	119	389	72	255	334	277	288	159	32
4 Jun	924	266	255	144	435	143	551	326	303	343	266	165
5 Jun	876	139	519	120	381	301	671	231	519	423	344	**266**
6 Jun	807	186	432	165	464	239	908	297	605	563	466	**259**
7 Jun	672	237	427	140	422	474	784	343	996	373	371	**215**
8 Jun	609	108	486	202	615	665	1,063	357	1,146	363	305	**572**
9 Jun	504	135	591	466	605	730	969	495	731	374	533	**592**
10 Jun	439	207	639	246	395	784	861	684	647	601	445	**635**
11 Jun	596	315	575	211	446	754	1,135	832	488	975	603	**533**
12 Jun	723	165	1,357	118	284	525	939	727	724	1,047	452	**437**
13 Jun	393	**337**	939	**142**	153	438	587	835	716	824	514	**480**
14 Jun	610	**309**	647	**118**	292	282	712	688	666	956	357	**474**
15 Jun	436	**571**	600	**138**	291	446	548	1,196	698	610	116	687
16 Jun	696	**441**	499	**110**	204	440	594	1,099	494	302	290	502
17 Jun	807	**765**	364	**251**	205	422	443	1,730	470	288	298	417
18 Jun	742	**591**	607	**243**	137	383	636	1,167	270	212	136	381
19 Jun	771	**348**	559	**201**	313	581	597	901	486	284	156	405
20 Jun	1,247	**319**	418	**187**	365	461	661	1,046	282	267	193	344
21 Jun	1,192	**522**	417	**228**	474	461	394	612	283	196	238	306
22 Jun	819	**456**	345	**213**	428	532	440	797	320	273	355	537
23 Jun	935	**462**	272	**153**	386	552	344	657	485	144	285	581
24 Jun	1,151	**408**	240	**193**	522	666	344	763	276	245	453	509
25 Jun	1,292	**186**	213	**330**	450	520	557	562	195	288	443	495
26 Jun	731	**359**	203	**381**	414	240	479	369	250	303	488	421
27 Jun	678	615	220	**310**	237	255	380	553	320	328	276	657
28 Jun	537	489	224	**186**	231	426	459	578	641	343	277	464
29 Jun	753	516	191	**231**	362	530	687	873	434	632	201	517
30 Jun	687	441	403	**295**	506	649	1,151	704	567	497	197	626
May–Jun Total	25,666	**12,479**	16,676	**7,162**	13,325	15,498	20,450	23,326	16,217	15,355	11,334	**13,248**

-continued-

Appendix I1. Part 5 of 5.

Note: Bold and outlined numbers represent the dates that the Chinook salmon fishery was restricted due to low inriver run.

[a] Sonar operations did not begin until 4 June, so the early run total passage estimate for 1987 is incomplete.

[b] Sonar operations began early (7 May) to determine the proportion of early run fish that may pass the site prior to the normal start date (16 May).

[c] Only upstream moving fish reported.

[d] Extreme tides and debris prevented sampling 16–19 May 2007. Values for 16–19 May were inferred from previous years.

Appendix I2.–Target-strength-based split-beam sonar passage estimates for RM 8.5, Kenai River late-run Chinook salmon, 1987–2010.

Date	1987	1988	1989	**1990**	1991	**1992**	1993[a]	1994[a]	1995	1996	1997	**1998**[b]
1 Jul	507	526	769	578	267	364	619	663	350	341	486	491
2 Jul	429	404	489	305	300	297	525	342	398	240	642	597
3 Jul	405	398	353	486	333	320	404	625	353	303	600	480
4 Jul	628	292	566	436	519	198	468	858	439	393	633	450
5 Jul	596	482	1,106	853	316	225	429	705	667	1,067	657	606
6 Jul	523	654	879	795	242	331	996	975	720	879	627	612
7 Jul	769	379	680	929	186	247	1,746	1,050	931	780	1,158	660
8 Jul	483	725	776	432	139	170	2,142	655	417	867	1,221	462
9 Jul	384	471	1,404	309	393	205	2,078	744	519	768	1,618	480
10 Jul	314	1,732	560	359	481	221	955	1,289	450	1,023	3,486	450
11 Jul	340	1,507	2,010	778	403	143	1,402	509	325	1,146	5,649	171
12 Jul	751	1,087	2,763	557	330	1,027	671	828	276	714	4,497	192
13 Jul	747	2,251	910	1,175	308	605	3,572	1,072	570	1,128	5,373	262
14 Jul	761	2,370	2,284	1,481	572	689	3,425	1,332	714	4,437	2,031	368
15 Jul	913	2,405	1,111	1,149	542	745	2,353	2,221	750	3,222	4,042	1,118
16 Jul	1,466	1,259	1,344	1,011	1,029	703	2,421	3,802	1,962	3,494	3,420	1,416
17 Jul	1,353	1,520	963	2,395	2,052	570	2,098	4,692	1,128	2,253	4,584	1,424
18 Jul	841	2,180	1,382	2,113	3,114	853	1,472	2,157	3,942	2,820	2,334	1,638
19 Jul	2,071	1,724	425	1,363	1,999	1,128	714	3,504	4,692	2,236	1,146	1,146
20 Jul	3,709	2,670	820	1,499	1,422	1,144	1,383	2,328	4,779	2,609	1,578	741
21 Jul	3,737	3,170	916	787	1,030	799	959	1,695	3,132	3,435	894	1,608
22 Jul	1,835	1,302	583	573	1,050	619	1,140	1,386	3,465	2,250	1,840	1,411
23 Jul	1,700	1,502	756	642	2,632	1,449	1,146	1,050	2,421	3,050	1,441	808
24 Jul	2,998	1,386	783	1,106	2,204	**711**	1,376	1,320	831	3,634	1,080	933
25 Jul	1,915	999	495	810	1,306	**1,713**	2,253	1,444	840	3,240	532	542
26 Jul	1,968	924	432	671	1,216	**1,296**	1,421	1,432	1,683	2,319	519	723
27 Jul	1,523	960	618	755	1,195	**1,561**	1,945	1,289	1,806	1,782	438	807
28 Jul	2,101	1,398	538	**603**	1,901	**1,957**	1,906	2,226	789	861	333	**954**
29 Jul	1,923	1,400	441	**546**	1,146	**1,533**	1,400	1,333	558	474	401	**1,255**
30 Jul	2,595	1,158	391	**382**	791	**1,198**	1,680	1,769	510	621	450	**1,556**
31 Jul	2,372	910	383	**316**	974	**951**	873	1,808	480	1,548	420	**1,344**

-continued-

Appendix I2.–Part 2 of 4.

Date	1987	1988	1989	**1990**	1991	**1992**	1993[a]	1994[a]	1995	1996	1997	**1998[b]**
1 Aug	470	925	351	**393**	897	**921**	776	1,037	474		247	**909**
2 Aug	314	781	201	**388**	867	**1,018**	626	1,223	369		291	**1,512**
3 Aug	263	989	132	**533**	392	**837**	350	1,078	447		213	**1,006**
4 Aug	835	1,524	142	**717**	331	**862**	467	658	519			**1,131**
5 Aug	904	1,091	107	**723**	174	**861**	711	536	404			**1,094**
6 Aug	648	1,333	107	**552**	343	**654**	1,076	1,042	408			**864**
7 Aug	694	1,186	65	**516**	618	**558**	655	797	279			**843**
8 Aug	658	1,449		**682**	600	**217**	682		267			**750**
9 Aug	368	1,132		**679**		**165**	424		272			**570**
10 Aug	312	755		**678**		**249**	252					**496**
11 Aug		698		**547**								
12 Aug				**362**								
13 Aug				**221**								
14 Aug				**139**								
15 Aug				**150**								
Jul–Aug Total	48,123	52,008	29,035[c]	**33,474**	34,614	**30,314**	51,991	53,474[d]	44,336[e]	53,934[f]	54,881[g]	**34,878**

-continued-

Appendix I2.–Part 3 of 4.

Date	1999[b]	2000[b]	2001[b]	2002[b]	2003[b]	2004[b]	2005[b]	2006[b]	2007[b]	2008[b]	2009[b]	2010[b]
1 Jul	453	461	697	563	727	1,167	1,283	580	609	527	631	843
2 Jul	612	373	766	1,596	735	1,125	1,109	343	401	520	755	639
3 Jul	486	370	1,075	2,456	982	1,053	1,204	269	450	461	956	740
4 Jul	396	488	714	1,855	1,212	715	778	844	501	257	751	943
5 Jul	369	787	676	1,949	1,684	842	1,454	953	506	221	656	940
6 Jul	683	778	645	1,205	1,462	1,231	1,020	718	510	188	419	942
7 Jul	936	1,020	887	1,241	1,322	1,932	863	828	578	242	751	1,495
8 Jul	1,030	1,713	751	1,069	1,666	1,287	882	1,269	1,051	260	666	1,600
9 Jul	1,047	1,632	568	1,618	1,183	815	1,687	814	601	718	610	505
10 Jul	717	1,461	908	1,533	1,880	757	1,616	446	500	899	674	781
11 Jul	1,059	1,038	858	1,369	1,693	1,061	1,475	310	927	482	1,091	1,002
12 Jul	560	1,506	575	1,245	1,289	1,208	2,557	431	710	892	1,114	1,311
13 Jul	401	2,327	1,148	1,288	1,227	2,567	1,643	376	527	632	822	1,090
14 Jul	969	2,709	1,448	1,034	697	2,577	1,203	644	1,037	414	1,400	1,009
15 Jul	636	2,808	1,338	450	1,212	1,943	1,427	1,925	1,282	1,636	1,099	1,062
16 Jul	927	2,264	1,201	1,253	1,107	2,718	1,811	2,266	667	1,297	1,136	1,525
17 Jul	3,558	1,915	2,415	1,481	1,482	2,262	1,710	1,116	776	1,349	1,249	1,661
18 Jul	2,784	2,154	2,065	1,001	1,731	2,008	1,142	1,207	1,729	829	924	1,672
19 Jul	1,869	1,919	1,568	915	1,773	1,753	1,786	1,307	1,754	791	1,149	1,131
20 Jul	3,471	1,155	994	964	1,384	1,566	1,091	1,575	2,153	809	1,009	1,937
21 Jul	3,354	933	786	970	1,153	1,757	847	1,259	1,677	1,257	914	2,654
22 Jul	1,998	702	497	845	2,159	1,401	752	1,017	2,751	1,292	1,052	1,627
23 Jul	1,875	760	526	1,637	1,693	1,812	712	933	1,901	1,160	826	2,216
24 Jul	1,748	1,868	529	1,175	1,774	2,044	662	639	3,008	1,081	527	2,562
25 Jul	1,937	1,761	676	974	1,525	1,107	782	958	3,490	876	579	1,388
26 Jul	1,098	1,034	667	930	1,149	941	1,050	874	2,659	1,035	959	1,396
27 Jul	3,066	992	775	591	1,449	2,277	985	1,073	3,357	1,577	390	1,542
28 Jul	1,358	999	1,070	707	909	1,540	814	1,291	1,779	1,395	441	1,761
29 Jul	1,185	1,029	928	406	808	1,724	989	1,602	859	1,277	452	1,470
30 Jul	969	577	508	571	691	1,523	1,059	1,225	922	1,408	432	1,686
31 Jul	1,308	549	883	540	751	1,480	819	762	1,340	1,586	344	1,659

-continued-

Appendix I2.–Part 4 of 4.

Date	1999[b]	2000[b]	2001[b]	2002[b]	2003[b]	2004[b]	2005[b]	2006[b]	2007[b]	2008[b]	2009[b]	2010[b]
1 Aug	591	695	455	642	377	1,078	689	669	866	1,385	216	1,716
2 Aug	468	421	459	553	394	688	682	605	330	1,177	194	1,249
3 Aug	642	294	504	752	379	722	660	576	397	1,009	156	1,312
4 Aug	444	453	840	995		754	587	769	374	682[h]	344	1,277
5 Aug	436	489	581	575		940	464	1,632		643[h]		
6 Aug	654	504	417	754[i]		1,009[i]	776[i]	912		621[h]		
7 Aug	678	366	618	676[i]		905[i]	696[i]	880		554[h]		
8 Aug	804	417	467	636[i]		854[i]	657[i]	1,095		537[h]		
9 Aug	328	399	232	456[i]		611[i]	470[i]	444[j]		382[h]		
10 Aug	165	397	200	337[i]		451[i]	347[i]	307[j]		282[h]		
11 Aug												
12 Aug												
13 Aug												
14 Aug												
15 Aug												
Jul–Aug Total	48,069	44,517	33,916	41,807	41,659[k]	56,205	43,240	37,743	42,979[l]	34,631	25,688[l]	48,343[m]

Note: Bold and outlined numbers represent dates when the Chinook salmon fishery was restricted because of low inriver run.

[a] Late run daily and total passage estimates for the years 1993 and 1994 were incorrectly reported in historical tables presented in previous reports (i.e., Bosch and Burwen 2000; Miller et al. 2002; Miller and Burwen 2002; and Miller et al. 2003). Estimates presented in this table are correct and were originally reported by Burwen and Bosch (1995a-b).

[b] Only upstream moving fish reported.

[c] Sampling was terminated on 7 August 1989 following several consecutive days of passage less than 1% of the cumulative passage.

[d] Sampling was terminated on 7 August 1994 due to pink salmon spawning in the insonified area.

[e] Sampling was terminated on 9 August 1995 following several consecutive days of passage less than 1% of the cumulative passage.

[f] Sampling was terminated on 31 July 1996 due to pink salmon spawning in the insonified area.

[g] Sampling was terminated on 3 August 1997 following several consecutive days of passage less than 1% of the cumulative passage.

[h] Sampling was terminated on 3 August 2008 due to fish holding in the sonar beam. Values for 4–10 August were inferred from previous years.

[i] Sampling was terminated on 5 August 2002, 2004, and 2005 due to budget constraints. Values for 6–10 August were inferred from previous years.

[j] Sampling was terminated on 8 August 2006 due to fish holding in the sonar beam. Values for 9–10 August were inferred from previous years.

[k] Sampling was terminated on 3 August 2003 following 3 consecutive days of passage less than 1% of the cumulative passage.

[l] Sampling was terminated on 4 August 2007 and 2009 following 3 consecutive days of passage less than 1% of the cumulative passage.

[m] Sampling was terminated on 4 August due to fish holding in the sonar beam.

APPENDIX J: DIRECTION OF TRAVEL OF LARGE FISH DETECTED BY DIDSON, RM 8.5 KENAI RIVER, 2010.

Appendix J1.–Daily proportion of upstream and downstream moving fish greater than or equal to 75 cm DIDSON length for the early run, RM 8.5 Kenai River, 2010.

Date	Number downstream	Number upstream	Total fish sampled	Percent downstream	Percent upstream
16 May			0		
17 May	0	2	2	0%	100%
18 May	0	1	1	0%	100%
19 May	1	2	3	33%	67%
20 May			0		
21 May			0		
22 May	0	3	3	0%	100%
23 May			0		
24 May			0		
25 May			0		
26 May	0	1	1	0%	100%
27 May	0	2	2	0%	100%
28 May	0	1	1	0%	100%
29 May	0	1	1	0%	100%
30 May			0		
31 May			0		
1 Jun	0	1	1	0%	100%
2 Jun			0		
3 Jun			0		
4 Jun	0	2	2	0%	100%
5 Jun			0		
6 Jun	0	3	3	0%	100%
7 Jun	0	3	3	0%	100%
8 Jun	0	6	6	0%	100%
9 Jun	0	16	16	0%	100%
10 Jun	0	11	11	0%	100%
11 Jun	1	21	22	5%	96%
12 Jun	0	24	24	0%	100%
13 Jun	2	17	19	11%	90%
14 Jun	1	30	31	3%	97%
15 Jun	0	16	16	0%	100%
16 Jun	0	16	16	0%	100%
17 Jun	0	16	16	0%	100%
18 Jun	0	15	15	0%	100%
19 Jun	0	6	6	0%	100%
20 Jun	0	7	7	0%	100%
21 Jun	0	25	25	0%	100%
22 Jun	0	28	28	0%	100%
23 Jun	0	13	13	0%	100%
24 Jun	0	16	16	0%	100%
25 Jun	2	22	24	8%	92%
26 Jun	2	8	10	20%	80%
27 Jun	0	12	12	0%	100%
28 Jun	1	16	17	6%	94%
29 Jun			0		
30 Jun	0	13	13	0%	100%
Total	10	376	386	2.6%	97.4%

Appendix J2.–Daily proportion of upstream and downstream moving fish greater than or equal to 75 cm DIDSON length for the late run, RM 8.5 Kenai River, 2010.

Date	Number downstream	Upstream	Total fish sampled	Percent downstream	Percent upstream
1 Jul	0	18	18	0%	100%
2 Jul	2	14	16	13%	88%
3 Jul	0	10	10	0%	100%
4 Jul	0	44	44	0%	100%
5 Jul	3	35	38	8%	92%
6 Jul	1	24	25	4%	96%
7 Jul	1	27	28	4%	96%
8 Jul	0	26	26	0%	100%
9 Jul	0	23	23	0%	100%
10 Jul	0	22	22	0%	100%
11 Jul	0	21	21	0%	100%
12 Jul	1	80	81	1%	99%
13 Jul	0	31	31	0%	100%
14 Jul	0	37	37	0%	100%
15 Jul	0	35	35	0%	100%
16 Jul	2	83	85	2%	98%
17 Jul	2	102	104	2%	98%
18 Jul	1	64	65	2%	99%
19 Jul	0	82	82	0%	100%
20 Jul	2	191	193	1%	99%
21 Jul	1	73	74	1%	99%
22 Jul	1	95	96	1%	99%
23 Jul	1	51	52	2%	98%
24 Jul	3	81	84	4%	96%
25 Jul	1	47	48	2%	98%
26 Jul	2	49	51	4%	96%
27 Jul	2	30	32	6%	94%
28 Jul	0	35	35	0%	100%
29 Jul	1	62	63	2%	98%
30 Jul	2	43	45	4%	96%
31 Jul	0	105	105	0%	100%
1 Aug	1	88	89	1%	99%
2 Aug	1	78	79	1%	99%
3 Aug	1	86	87	1%	99%
4 Aug	1	77	78	1%	99%
5 Aug	3	98	101	3%	97%
6 Aug	1	55	56	2%	98%
7 Aug	2	39	41	5%	95%
8 Aug	0	36	36	0%	100%
9 Aug	5	20	25	20%	80%
10 Aug	2	26	28	21%	79%
Total	35	2165	2200	1.6%	98.4%

APPENDIX K: SPATIAL AND TEMPORAL DISTRIBUTION OF FISH BY SIZE AS MEASURED BY DIDSON, RM 8.5 KENAI RIVER, 2010

Appendix K1.–Spatial and temporal distribution of small (DIDSON length DL < 75 cm; small red symbols), medium (75 cm ≤ DL < 90 cm; larger blue squares), and large fish (DL ≥ 90 cm; large black symbols), RM 8.5 Kenai River, 6–19 June 2010.

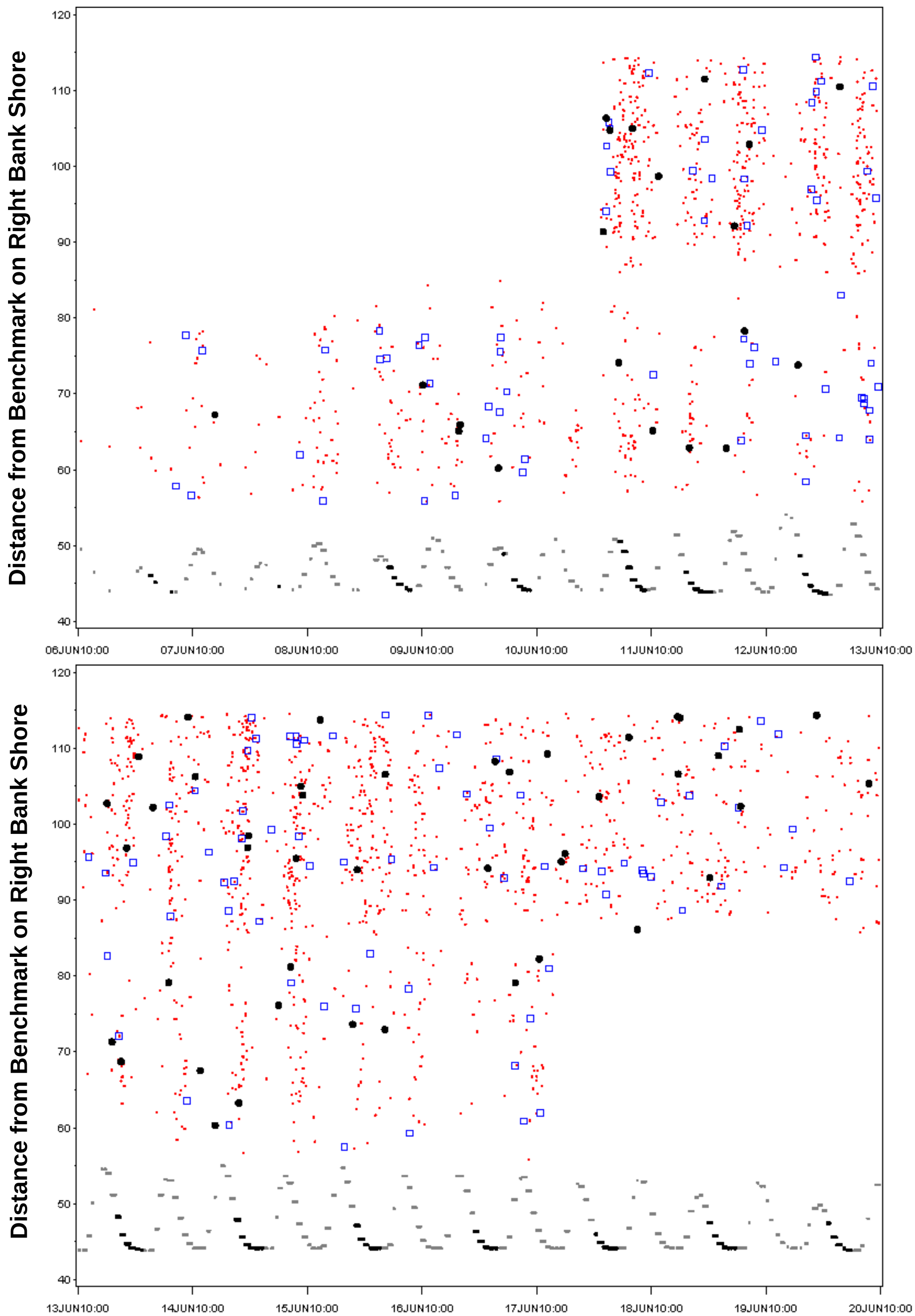

Note: Relative water level is plotted at bottom (small grey symbols), with netting periods in black.

Appendix K2.– Spatial and temporal distribution of small (DIDSON length DL < 75 cm; small red symbols), medium (75 cm ≤ DL < 90 cm; larger blue squares), and large fish (DL ≥ 90 cm; large black symbols), RM 8.5 Kenai River, 20 June–3 July 2010.

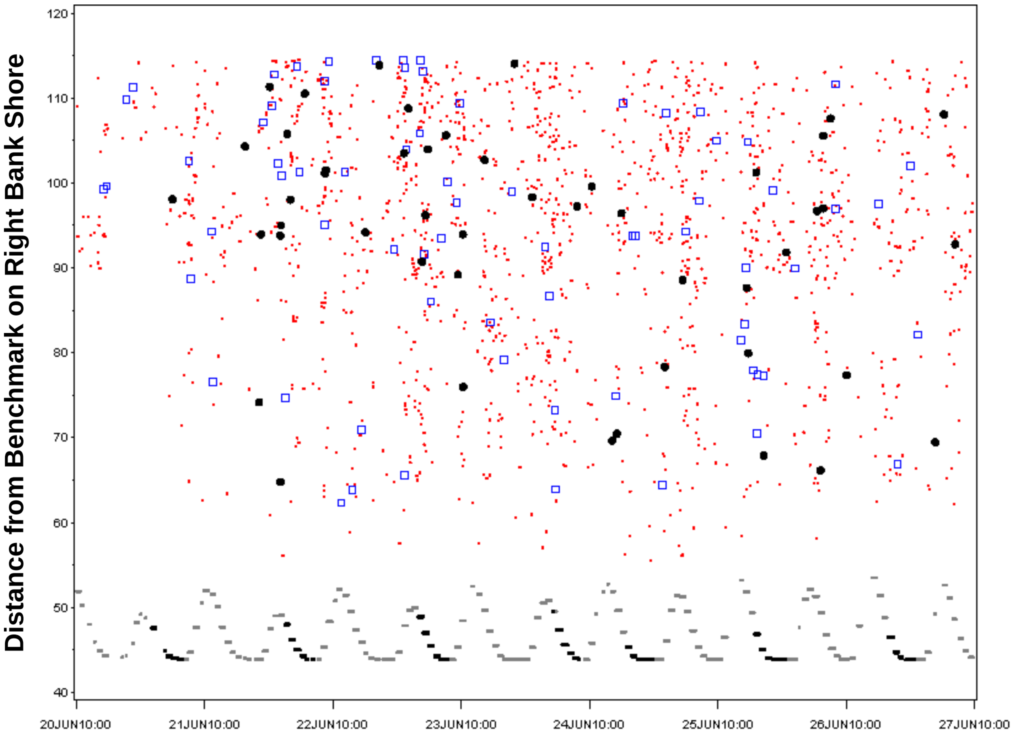

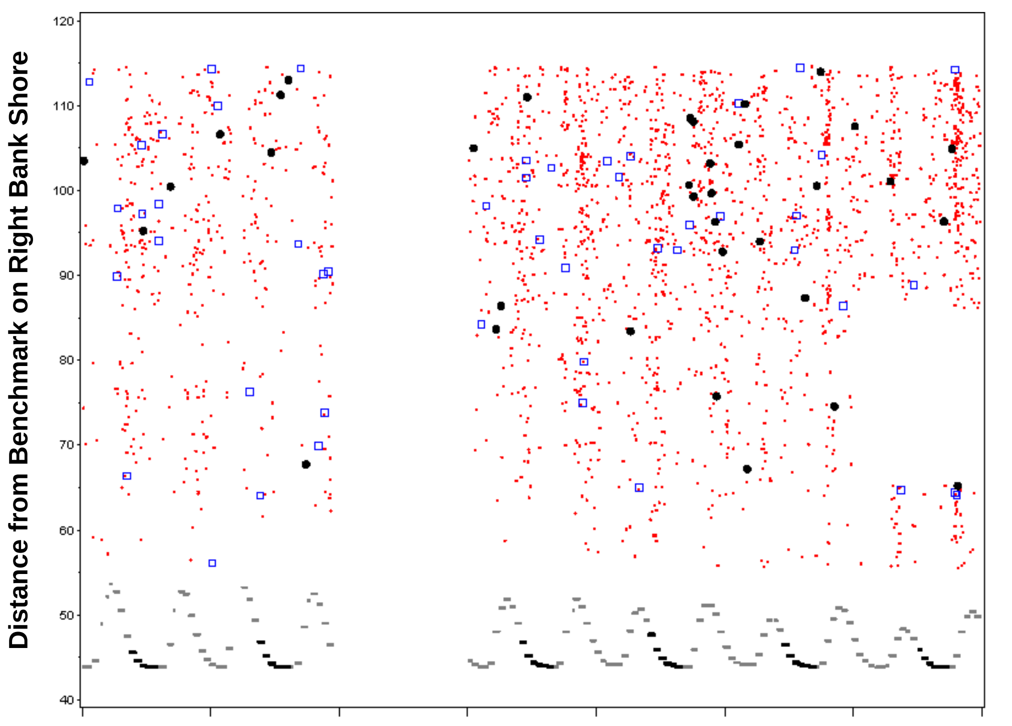

Note: Relative water level is plotted at bottom (small grey symbols), with netting periods in black.

Appendix K3.– Spatial and temporal distribution of small (DIDSON length DL < 75 cm; small red symbols), medium (75 cm ≤ DL < 90 cm; larger blue squares), and large fish (DL ≥ 90 cm; large black symbols), RM 8.5 Kenai River, 4–17 July 2010.

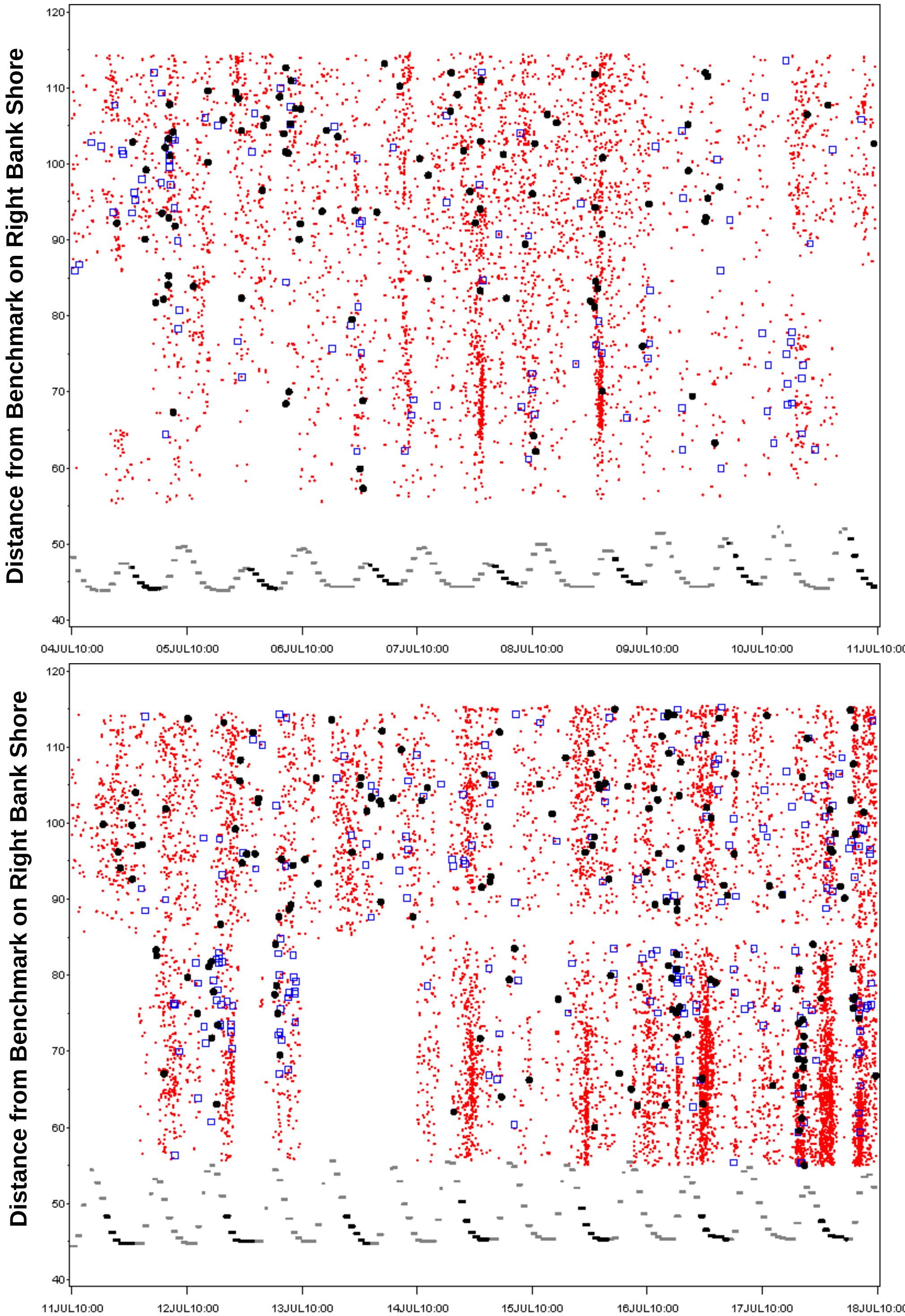

Note: Relative water level is plotted at bottom (small grey symbols), with netting periods in black.

Appendix K4.– Spatial and temporal distribution of small (DIDSON length DL < 75 cm; small red symbols), medium (75 cm ≤ DL < 90 cm; larger blue squares), and large fish (DL ≥ 90 cm; large black symbols), RM 8.5 Kenai River, 18–31 July 2010.

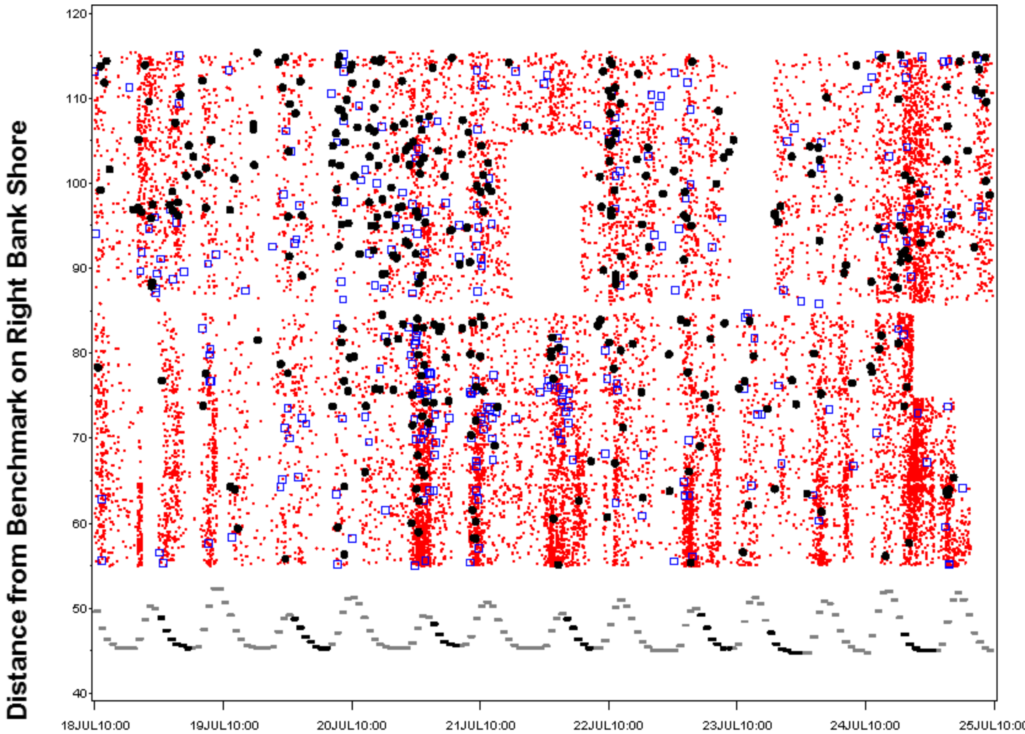

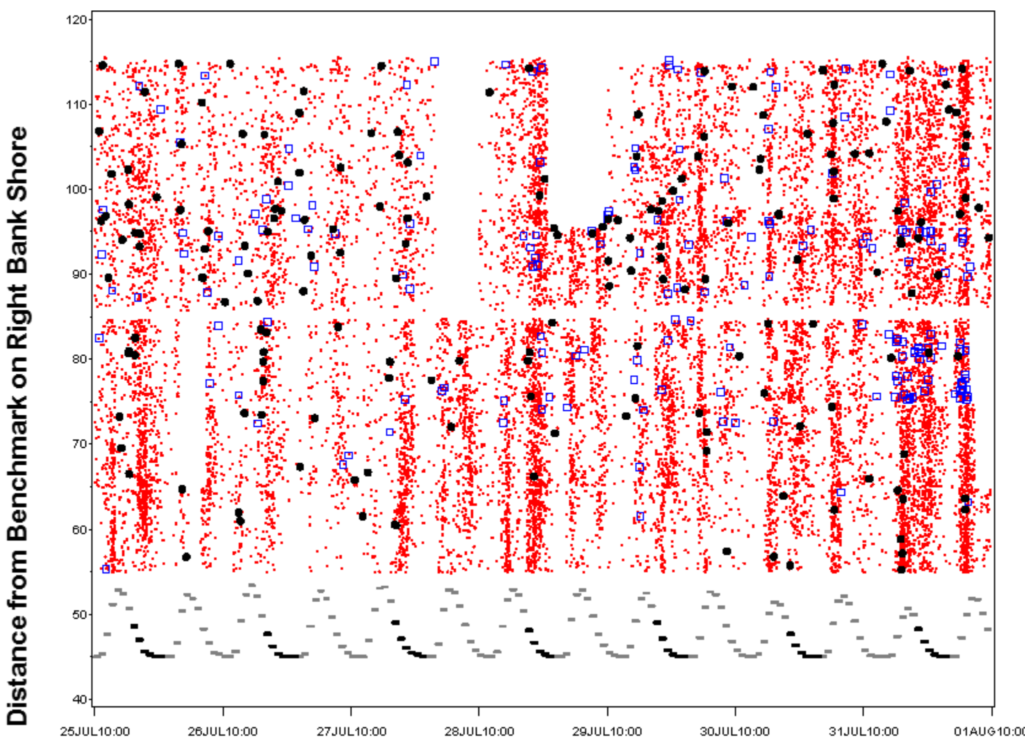

Note: Relative water level is plotted at bottom (small grey symbols), with netting periods in black.

Appendix K5.– Spatial and temporal distribution of small (DIDSON length DL < 75 cm; small red symbols), medium (75 cm ≤ DL < 90 cm; larger blue squares), and large fish (DL ≥ 90 cm; large black symbols), RM 8.5 Kenai River, 1–10 August 2010.

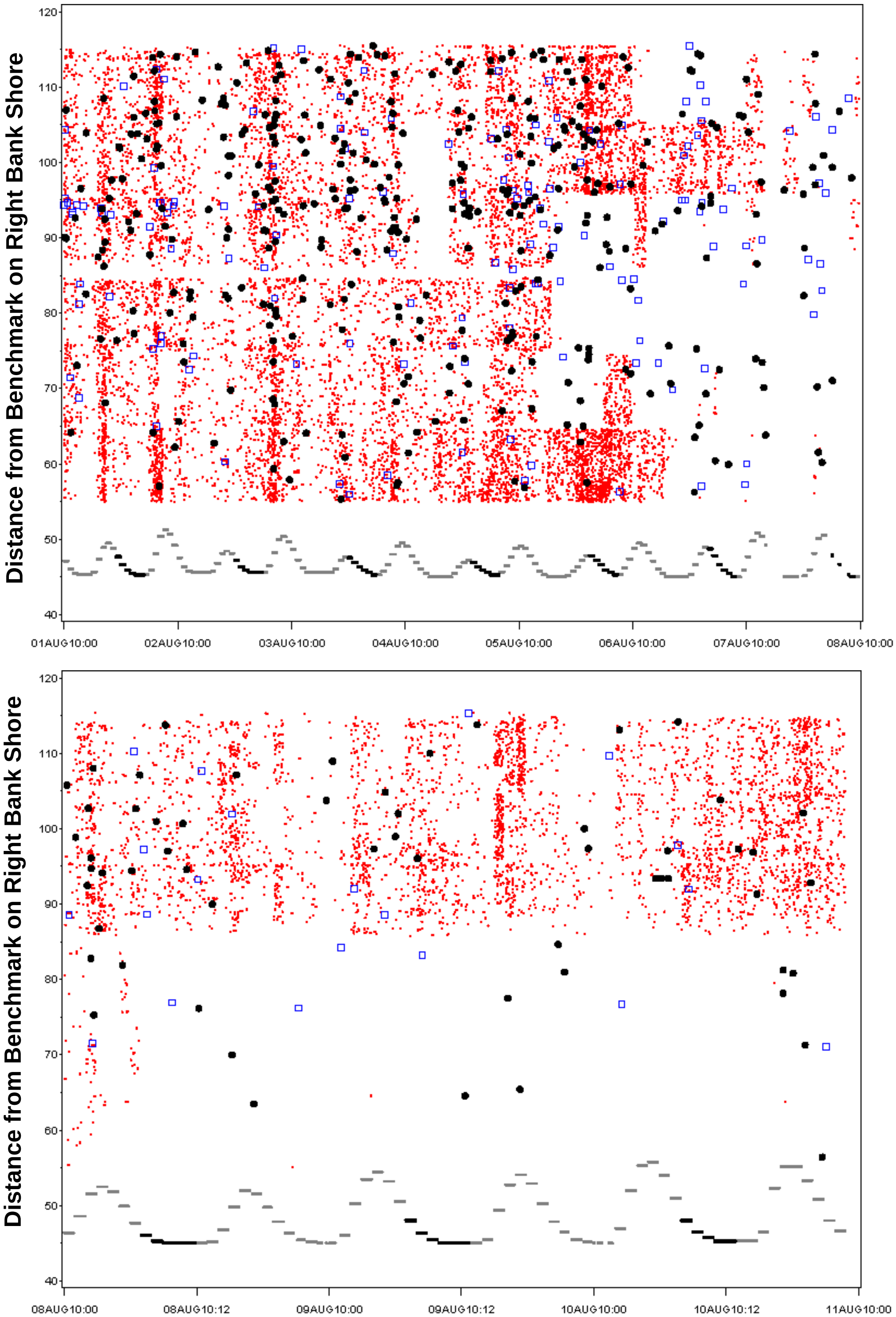

Note: Relative water level is plotted at bottom (small grey symbols), with netting periods in black. Beginning on 5 August, only medium and large fish were measured in some samples.

APPENDIX L: COMPARISON OF DIDSON LENGTH, ELSD, AND TS FISH SIZE CRITERIA APPLIED TO MATCHING SAMPLES OF DIDSON AND SPLIT-BEAM SONAR DATA, KENAI RIVER 2010

Appendix L1.–Number of upstream bound fish detected and classified as large Chinook salmon using DIDSON length, ELSD, and TS criteria applied to matching left-bank mid-range (13–23 m) samples of DIDSON and split-beam sonar data, RM 8.5 Kenai River, early run, 2010.

	Upstream fish detected		Number of "large" fish		
Date	DIDSON	Split-beam sonar	DL > 75 cm	ELSD > 3.1 units	TS > −28 dB
10 Jun	59	48	2	2	36
11 Jun	70	59	6	12	46
12 Jun	77	61	4	3	43
13 Jun	68	56	7	5	34
14 Jun	83	71	10	11	56
15 Jun	70	57	2	7	41
16 Jun	54	43	3	0	34
17 Jun	47	37	4	7	31
18 Jun	45	30	4	2	28
19 Jun	26	19	1	5	14
20 Jun	28	15	3	3	13
21 Jun	47	26	9	9	21
22 Jun	63	48	7	8	32
23 Jun	69	55	4	12	35
24 Jun	65	49	3	9	29
25 Jun	73	51	5	7	33
26 Jun	36	29	2	6	25
27 Jun	65	50	6	4	38
28 Jun	41	34	1	7	23
30 Jun	119	99	4	23	68
Early run	1,205	937	87	142	680

Appendix L2.–Number of upstream bound fish detected and classified as large Chinook salmon using DIDSON length, ELSD, and TS criteria applied to matching left-bank mid-range (13–23 m) samples of DIDSON and split-beam sonar data, RM 8.5 Kenai River, late run, 2010.

	Upstream fish detected		Number of "large" fish		
Date	DIDSON	Split-beam sonar	DL > 75 cm	ELSD > 3.1 units	TS > -28 dB
1 Jul	127	90	10	22	56
2 Jul	112	88	3	20	57
5 Jul	126	99	7	19	66
6 Jul	147	127	4	26	91
7 Jul	234	184	9	35	131
8 Jul	220	163	5	32	106
9 Jul	75	50	8	8	29
10 Jul	106	79	2	13	45
11 Jul	207	140	8	14	83
12 Jul	195	152	11	19	82
13 Jul	197	61	14	11	41
14 Jul	204	158	10	14	74
15 Jul	191	188	13	22	95
16 Jul	241	189	13	21	117
17 Jul	268	186	25	25	107
18 Jul	322	212	23	34	123
19 Jul	119	73	18	20	48
20 Jul	326	226	37	41	131
21 Jul	144	108	10	12	77
22 Jul	339	249	29	40	167
23 Jul	149	109	12	16	64
24 Jul	585	166	17	21	100
25 Jul	342	201	10	19	132
26 Jul	231	163	13	17	113
27 Jul	128	83	7	4	47
28 Jul	286	164	3	19	107
29 Jul	446	244	21	35	125
30 Jul	415	215	11	21	98
31 Jul	681	423	11	33	175
1 Aug	381	251	17	36	95
2 Aug	273	135	16	29	57
3 Aug	220	128	23	23	61
4 Aug	234	95	18	14	44
5 Aug	555	306	32	40	116
Late Run	8,826	5,505	470	775	3,060

APPENDIX M: DIDSON-LENGTH THRESHOLD ESTIMATES OF LARGE CHINOOK SALMON, RM 8.5 KENAI RIVER, 2010

Appendix M1.–Daily DIDSON length (DL) threshold estimates of large Chinook salmon passage (DL ≥ X cm) at RM 8.5 in the Kenai River, early run 2010.

	DL ≥ 75 cm		DL ≥ 80 cm		DL ≥ 90 cm	
Date	Passage	SE	Passage	SE	Passage	SE
16 May						
17 May						
18 May						
19 May						
20 May						
21 May						
22 May						
23 May						
24 May						
25 May						
26 May						
27 May						
28 May						
29 May						
30 May						
31 May						
1 Jun						
2 Jun						
3 Jun						
4 Jun						
5 Jun						
6 Jun						
7 Jun						
8 Jun						
9 Jun						
10 Jun						
11 Jun	127	23	108	21	48	12
12 Jun	145	23	96	19	12	7
13 Jun	103	17	90	14	48	12
14 Jun	169	21	133	17	66	14
15 Jun	100	24	68	19	30	12
16 Jun	96	14	84	13	24	9
17 Jun						
18 Jun						
19 Jun						
20 Jun						
21 Jun	151	26	133	28	72	21
22 Jun	169	34	127	29	54	14
23 Jun	78	15	66	14	36	12
24 Jun	96	20	78	16	36	9
25 Jun	134	30	104	26	60	19
26 Jun	48	13	48	13	24	9
27 Jun	72	21	72	21	18	8
28 Jun	101	17	57	12	31	11
29 Jun						
30 Jun	82	22	63	19	25	8

Note: all estimates are of upstream bound fish in midriver between and less than 3 m from the transducers.

Appendix M2.–Daily DIDSON length (DL) threshold estimates of large Chinook salmon passage (DL ≥ X cm) at RM 8.5 in the Kenai River, late run 2010.

	DL ≥ 75 cm		DL ≥ 80 cm		DL ≥ 90 cm	
Date	Passage	SE	Passage	SE	Passage	SE
1 Jul	109	21	84	17	60	14
2 Jul	84	17	72	17	48	11
3 Jul						
4 Jul	292	44	199	34	111	25
5 Jul	211	29	181	26	145	25
6 Jul	145	27	115	23	66	17
7 Jul	163	38	151	37	96	25
8 Jul	157	38	139	34	102	26
9 Jul	139	35	127	32	66	27
10 Jul	147	27	88	20	22	10
11 Jul	156	31	135	27	87	21
12 Jul	601	80	429	62	205	31
13 Jul						
14 Jul	211	38	169	30	84	15
15 Jul	211	25	181	25	133	18
16 Jul	500	64	446	57	235	34
17 Jul	615	77	470	74	259	55
18 Jul	551	116	451	95	283	71
19 Jul	495	70	440	60	308	42
20 Jul	1,151	96	971	89	669	67
21 Jul	593	62	489	65	244	57
22 Jul	659	79	608	75	416	61
23 Jul	435	56	345	56	256	38
24 Jul	508	68	470	61	326	45
25 Jul	299	52	294	53	193	34
26 Jul	295	35	289	36	199	32
27 Jul	241	45	177	33	145	33
28 Jul	263	48	165	34	81	22
29 Jul	384	52	323	49	175	37
30 Jul	260	46	223	42	157	38
31 Jul	649	78	354	51	210	38
1 Aug	550	53	435	47	339	47
2 Aug	471	95	459	95	399	74
3 Aug	519	58	519	58	423	49
4 Aug	514	62	490	60	403	48
5 Aug	592	61	586	60	429	46
6 Aug	332	25	290	20	175	17
7 Aug	252	39	252	39	173	33
8 Aug	217	43	205	41	157	35
9 Aug	121	19	121	19	91	16
10 Aug	164	26	158	25	120	25

Note: all estimates are of upstream bound fish in midriver between and less than 3 m from the transducers.

APPENDIX N: DAILY ABUNDANCE MODEL FITTED TO KENAI RIVER CHINOOK SALMON DATA, 2010

Appendix N1.–OpenBUGS code for daily abundance model fit to 2010 Kenai River Chinook salmon sonar and gillnetting data.

```
model{
q.ncpu ~ dnorm(0,1.0E-6)I(0,1)
tau.log.ncpu ~ dgamma(0.001,0.001)
phi.ncpu ~ dnorm(0,1.0E-4)I(-1,1)
log.resid.ncpu.0 ~ dnorm(0,4)I(-3,3)
sigma.ncpu <- 1 / sqrt(tau.log.ncpu)
q.nasb ~ dnorm(0,1.0E-6)I(0,10)
tau.log.nasb ~ dgamma(0.001,0.001)
phi.nasb ~ dnorm(0,1.0E-4)I(-1,1)
log.resid.nasb.0 ~ dnorm(0,4)I(-3,3)
sigma.nasb <- 1 / sqrt(tau.log.nasb)
q.gt80 ~ dnorm(0,1.0E-6)I(0,1)
tau.log.gt80 ~ dgamma(0.001,0.001)
phi.gt80 ~ dnorm(0,1.0E-4)I(-1,1)
log.resid.gt80.0 ~ dnorm(0,4)I(-3,3)
sigma.gt80 <- 1 / sqrt(tau.log.gt80)

N.early <- sum(N[1:46])
N.late <- sum(N[47:87])
N.dseqe <- sum(N[1:26]) + sum(N[33:36]) + N[45]
N.dseql <- N[49] + N[59] + sum(N[82:87])
for (d in 1:87) {
 log.N[d] ~ dnorm(0,1.0E-12)I(0,)
 DID[d] ~ dlnorm(log.N[d],tau.log.DID[d])
 nasb[d] ~ dlnorm(log.q1Nmean2[d],tau.log.nasb)
 ncpu[d] ~ dlnorm(log.q2Nmean2[d],tau.log.ncpu)
 gt80[d] ~ dlnorm(log.q3Nmean2[d],tau.log.gt80)
 N[d] <- exp(log.N[d])
 tau.log.DID[d] <- 1 / log(cv.DID[d]*cv.DID[d] + 1)
 log.q1Nmean1[d] <- log(q.nasb * N[d])
 log.resid.nasb[d] <- log(nasb[d]) - log.q1Nmean1[d]
 log.q2Nmean1[d] <- log(q.ncpu * N[d])
 log.resid.ncpu[d] <- log(ncpu[d]) - log.q2Nmean1[d]
 log.q3Nmean1[d] <- log(q.gt80 * N[d])
 log.resid.gt80[d] <- log(gt80[d]) - log.q3Nmean1[d]
 Npred.nasb[d] <- exp(log.q1Nmean2[d]) / q.nasb
 Npred.ncpu[d] <- exp(log.q2Nmean2[d]) / q.ncpu
 Npred.gt80[d] <- exp(log.q3Nmean2[d]) / q.gt80
 }
log.q1Nmean2[1] <- log.q1Nmean1[1] + phi.nasb * log.resid.nasb.0
log.q2Nmean2[1] <- log.q2Nmean1[1] + phi.ncpu * log.resid.ncpu.0
log.q3Nmean2[1] <- log.q3Nmean1[1] + phi.gt80 * log.resid.gt80.0
for (d in 2:87) {
 log.q1Nmean2[d] <- log.q1Nmean1[d] + phi.nasb * log.resid.nasb[d-1]
 log.q2Nmean2[d] <- log.q2Nmean1[d] + phi.ncpu * log.resid.ncpu[d-1]
 log.q3Nmean2[d] <- log.q3Nmean1[d] + phi.gt80 * log.resid.gt80[d-1]
 }}
```

Note: Prior distributions are in green font, likelihoods in blue. Block updaters were disabled prior to compiling. Posterior distribution for node "N" is the basis for DIDSON-equivalent estimates described in report text.

Appendix N2.–OpenBUGS output with posterior statistics for key quantities from daily abundance model fit to 2010 Kenai River Chinook salmon sonar and gillnetting data.

	mean	sd	MC_error	val2.5pc	median	val97.5pc	start	sample
phi.gt80	0.9355	0.05449	0.0011	0.7957	0.9491	0.9969	501	68943
phi.nasb	0.3863	0.1386	0.003166	0.1119	0.3878	0.6554	501	68943
phi.ncpu	0.3828	0.1335	0.002967	0.1184	0.3832	0.641	501	68943
q.gt80	0.6203	0.1506	0.003222	0.3145	0.6105	0.9405	501	68943
q.nasb	0.5592	0.077	0.001423	0.4203	0.5554	0.7215	501	68943
q.ncpu	2.02E-04	2.65E-05	5.80E-07	1.58E-04	2.00E-04	2.61E-04	501	68943
sigma.gt80	0.1215	0.03758	0.001011	0.06436	0.1159	0.2105	501	68943
sigma.nasb	0.5829	0.05593	8.18E-04	0.4831	0.5794	0.7029	501	68943
sigma.ncpu	0.5574	0.05242	8.68E-04	0.4633	0.5545	0.6692	501	68943
N[1]	39.8	18.1	0.5	16.0	36.1	84.6	501	68943
N[2]	6.6	4.1	0.1	1.8	5.6	17.0	501	68943
N[3]	7.0	4.5	0.1	1.9	6.0	18.3	501	68943
N[4]	134.4	63.3	1.9	49.3	122.3	288.9	501	68943
N[5]	73.0	33.6	0.9	27.2	66.5	156.7	501	68943
N[6]	6.5	4.0	0.1	1.8	5.6	16.8	501	68943
N[7]	39.9	18.5	0.6	15.4	35.9	87.2	501	68943
N[8]	24.4	11.9	0.4	9.0	22.0	53.0	501	68943
N[9]	3.4	1.6	0.0	1.3	3.1	7.4	501	68943
N[10]	26.9	12.5	0.4	9.9	24.5	58.4	501	68943
N[11]	59.1	28.6	0.9	21.4	53.2	127.7	501	68943
N[12]	29.8	14.9	0.4	10.5	26.5	67.5	501	68943
N[13]	60.1	30.7	0.9	21.0	53.5	138.1	501	68943
N[14]	64.8	33.1	1.1	21.9	57.8	148.3	501	68943
N[15]	24.8	12.5	0.4	8.8	22.2	57.3	501	68943
N[16]	27.2	14.1	0.5	9.8	24.1	62.2	501	68943
N[17]	3.4	1.8	0.1	1.3	3.0	8.0	501	68943
N[18]	3.5	1.8	0.1	1.3	3.1	8.2	501	68943
N[19]	43.8	22.6	0.7	15.1	38.8	100.0	501	68943
N[20]	93.3	47.9	1.6	31.9	83.1	212.7	501	68943
N[21]	284.9	147.0	5.1	99.3	252.0	667.2	501	68943
N[22]	123.6	61.3	1.9	43.7	110.5	278.7	501	68943
N[23]	77.5	38.9	1.2	27.6	69.7	177.3	501	68943
N[24]	240.5	115.6	3.7	86.0	218.0	536.0	501	68943
N[25]	286.3	131.8	4.0	107.0	260.6	613.8	501	68943
N[26]	247.4	111.8	3.0	97.3	226.3	525.2	501	68943
N[33]	174.1	73.7	2.0	73.5	159.9	359.0	501	68943
N[34]	190.9	86.3	2.6	74.2	173.9	405.3	501	68943
N[35]	235.4	107.7	3.2	88.5	214.3	505.7	501	68943
N[36]	182.4	76.2	2.1	74.0	169.4	367.8	501	68943
N[45]	310.0	125.5	3.1	132.4	287.3	618.5	501	68943
N[46]	178.7	27.7	0.4	133.4	175.6	241.6	501	68943
N[49]	104.0	42.3	1.0	45.4	96.2	209.1	501	68943
N[59]	330.6	138.5	3.5	141.0	305.9	667.9	501	68943
N[82]	623.1	96.0	1.3	442.9	619.4	825.0	501	68943
N[83]	323.5	59.9	0.9	220.1	318.3	456.3	501	68943
N[84]	282.8	58.3	1.0	183.7	277.5	413.3	501	68943
N[85]	241.8	54.2	1.0	153.2	235.4	365.6	501	68943
N[86]	149.0	36.3	0.6	91.8	144.3	232.8	501	68943
N[87]	201.8	53.1	0.9	120.3	194.5	326.4	501	68943
N.early	5824	639.5	23.12	4737	5767	7230	501	68943
N.late	18250	692.1	10.52	16940	18230	19650	501	68943
N.dseqe	3124	564.1	21.6	2193	3062	4392	501	68943
N.dseql	2257	325.3	6.458	1689	2230	2964	501	68943

Appendix N3.–"DIDSON-equivalent" (DSEQ) estimates of 2010 Kenai River Chinook salmon abundance predicted with a time series term as reconstructed from DIDSON-length mixture model (DLMM) estimates and 3 indices of relative abundance: DIDSON-length threshold (DL > 80) estimates, gillnetting catch rate at RM 8.5 (Net CPUE), and net-apportioned split beam sonar (NASB) estimates.

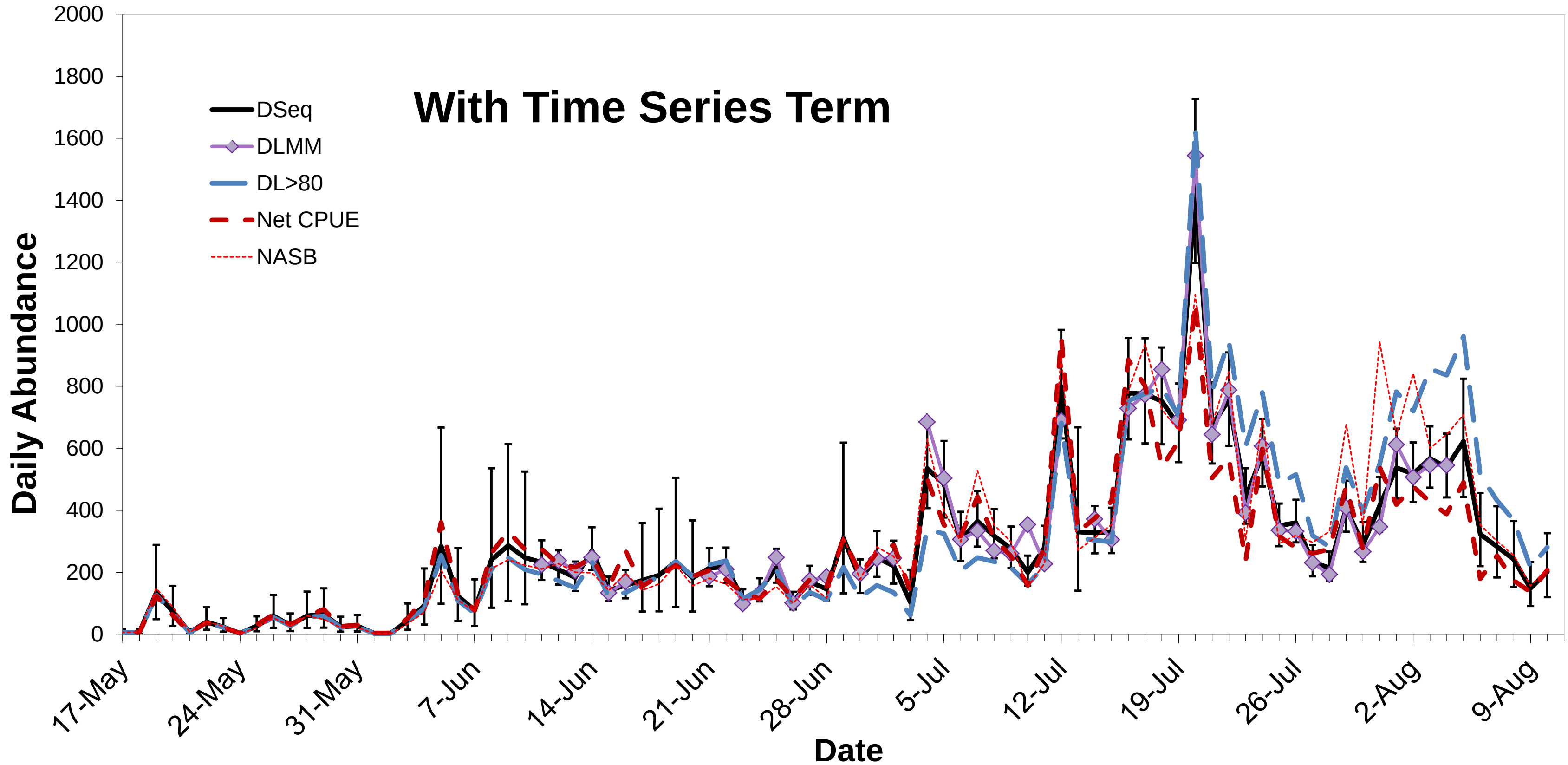

Note: daily predictions of abundance specific to each individual index are plotted with an AR(1) time series term in the model (see Methods). DSEQ estimates (black solid lines with error bars) were used to estimate abundance on those days that lacked DLMM estimates (solid line with diamond symbols).

Appendix N4.–"DIDSON-equivalent" (DSEQ) estimates of 2010 Kenai River Chinook salmon abundance predicted without a time series term as reconstructed from DIDSON-length mixture model (DLMM) estimates and 3 indices of relative abundance: DIDSON-length threshold (DL > 80) estimates, gillnetting catch rate at RM 8.5 (Net CPUE), and net-apportioned split beam sonar (NASB) estimates.

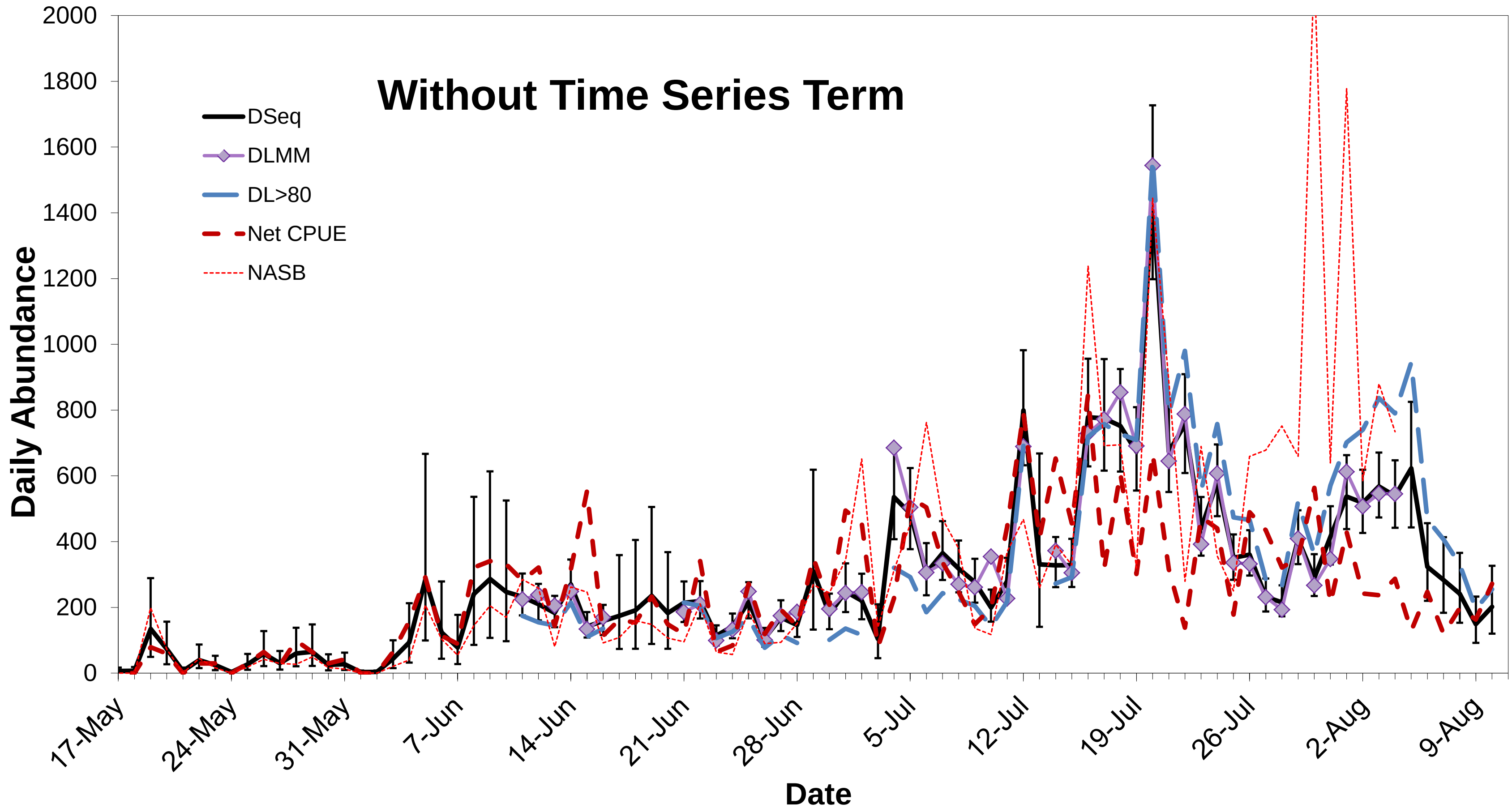

Note: daily predictions of abundance specific to each individual index are plotted without an AR(1) time series term in the model (see Methods). DSEQ estimates (black solid lines with error bars) were used to estimate abundance on those days that lacked DLMM estimates (solid line with diamond symbols).